Distribution Agreement

In presenting this thesis or dissertation as a partial fulfillment of the requirements for an advanced degree from Emory University, I hereby grant to Emory University and its agents the non-exclusive license to archive, make accessible, and display my thesis or dissertation in whole or in part in all forms of media, now or hereafter known, including display on the world wide web. I understand that I may select some access restrictions as part of the online submission of this thesis or dissertation. I retain all ownership rights to the copyright of the thesis or dissertation. I also retain the right to use in future works (such as articles or books) all or part of this thesis or dissertation.

Signature:

_____ _____

John M. Lattier **Date**

Pigment epithelium-derived factor (PEDF) inhibits progression of liver metastasis in a mouse model of uveal melanoma

By
John M. Lattier
B.S., Georgia State University, 2007
Doctor of Philosophy candidate

Graduate Division of Biological and Biomedical Sciences
Biochemistry, Cell and Developmental Biology

_____
Advisor: Hans E. Grossniklaus, M.D., M.B.A.

_____
Committee Member: P. Michael Iuvone, Ph.D.

_____
Committee Member: Michael Koval, Ph.D.

_____
Committee Member: Andrew P. Kowalczyk, Ph.D.

_____
Committee Member: Keith D. Wilkinson, Ph.D.

Accepted:

_____
Lisa A. Tedesco, Ph.D.
Dean of the James T. Laney School of Graduate Studies

_____
Date

Pigment epithelium-derived factor (PEDF) inhibits progression of liver metastasis in a mouse model of uveal melanoma

By
John Lattier
B.S., Georgia State University, 2007

Advisor: Hans E. Grossniklaus, M.D., M.B.A.

An abstract of
A dissertation submitted to the Faculty of the James T. Laney School of Graduate Studies of Emory University in a partial fulfillment of the requirements for the degree of Doctor of Philosophy in the Graduate Division of Biological and Biomedical Sciences in Biochemistry, Cell and Developmental Biology, 2014

Abstract

Pigment epithelium-derived factor (PEDF) inhibits progression of liver metastasis in a mouse model of uveal melanoma

By John M. Lattier

Uveal melanoma is the most common form of adult eye cancer in the United States, forming in the middle layer of the eye and originating in pigmented melanocytes. While the primary eye tumor is treatable with high success, patients often succumb to liver metastasis within 2 to 5 years. Metastatic progression is highly dependent on angiogenesis, or the formation of new blood vessels, to nourish the growing tumor with oxygen and nutrients. Pigment epithelium-derived factor (PEDF) is one of the most potent inhibitors of angiogenesis, and it is naturally produced by liver hepatocytes. I hypothesized that PEDF inhibits metastatic progression via a mechanism involving angiogenesis. I used PEDF null mice, injected melanoma cells into the posterior compartment of the eye, and measured liver metastasis after 4 weeks. PEDF null mice exhibited a 34.6-fold increase in liver metastasis area and a much greater population of macrometastases (>200μm diameter) when compared to controls. Vascular density was also significantly increased in these metastases, and various other characteristics were measured such as stromagenic factors and the effects of fatty liver. I concluded that PEDF is protective against metastatic progression of ocular melanoma in the liver. These findings may prove useful for future therapies.

Pigment epithelium-derived factor (PEDF) inhibits progression of liver metastasis in a mouse model of uveal melanoma

By
John Lattier
B.S., Georgia State University, 2007

Advisor: Hans E. Grossniklaus, M.D., M.B.A.

A dissertation submitted to the Faculty of the James T. Laney School of Graduate Studies of Emory University in partial fulfillment of the requirements for the degree of Doctor of Philosophy in the Graduate Division of Biological and Biomedical Sciences in Biochemistry, Cell and Developmental Biology, 2014

Acknowledgements

I owe Dr. Hans Grossniklaus an immeasurable amount of gratitude for his vision, his wisdom, his patience, and his belief in me. Three years into graduate school, I was without a lab, without an advisor, and Dr. G took me under his wing. I can honestly say I have never met another individual in my life like him – he has a seemingly endless breadth of knowledge, coupled with an unbreakable optimism. Thank you, Dr. G, for everything.

My labmate Dr. Hua Yang has contributed greatly to this work, including training me on the surgical procedures and supplying me with reagents such as primary cells and histological slides. I would also like to thank Dr. Shin Kang and Dr. Qing Zhang for their assistance over the years, Pingbo Liu and Xiaoqun Mao for swiftly and efficiently processing hundreds upon hundreds of tissue sections, Dr. Martina Herwig and Alison Ziesel for keeping me sane, Micah Chrenek for having a calm solution to every problem, Chris and Chuck for their academic input, and all of the fifth floor researchers that have been so very supportive. I also owe my gratitude to my collaborators, Drs. Sue Crawford, Pat Becerra, and Manuela Bartoli and their students and scientists.

I'd like to give a huge thank you to my committee and the BCDB program, including certain special faculty members and staff who have set aside their time to help me and my peers through the biggest challenge of our lives.

And lastly I want to thank a few people whose emotional support I could not have survived without: Mom, Dad and Jill, my brother Chris, and my friends Tara, Paul, and Wes. I also want to thank some of my dearest loved ones whom I lost during my time here, Aunt Sharon, Nana, and Mary. Your memories give me strength. I am thankful for all of your support.

Table of Contents

List of Figures

Chapter 1—Introduction to Uveal Melanoma and PEDF

Chapter 2—Host Pigment Epithelium-Derived Factor (PEDF) Prevents Progression of Liver Metastasis in a Mouse Model of Uveal Melanoma

Chapter 3—Further Investigation of Angiogenesis in our Mouse Model of Uveal Melanoma

Chapter 4—Effects of Fatty Liver on Metastasis Progression

Chapter 5—Summary and Conclusions

Abbreviations used in this document:

ANOVA ..... Analysis of variance, a statistical test

ATGL ..... Adipose triglyceride lipase, a PEDF receptor

B16-LS9 ..... Mouse cutaneous melanoma cell line

BAP1 ..... Breast cancer antigen-associated protein 1

C57BL/6 ..... A common laboratory mouse strain

CD105 ..... Cluster of differentiation 105, Endoglin

CD31 ..... Cluster of differentiation 31, PECAM-1

CHOP ..... CCAAT/enhancer-binding homologous protein 1

c-Met ..... A surface receptor expressed by melanoma

CNV ..... Choroidal neovascularization

Ctrl ..... Control

CXCR4 ..... A chemokine receptor expressed by melanoma

DNA ..... Deoxyribonucleic acid

ECM ..... Extracellular matrix

EMT ..... Epithelial-to-mesenchymal transition

FAS ..... A receptor involved in apoptosis

FASL ..... A ligand involved in apoptosis

FGF ..... Fibroblast growth factor

GNA11 ..... A protein mutated in uveal melanoma

GNAQ ..... A protein mutated in uveal melanoma

H&E ..... Hematoxylin and eosin, a type of stain

HCFC1..... Host cell factor C1

Het ..... Heterozygote

HGF ..... Hepatocyte growth factor

HIF..... Hypoxia-inducible factor

HNF4 ..... Hepatocyte nuclear factor 4

HPF..... High powered field, a magnification term

HSC..... Hepatic stellate cell

IGF..... Insulin-like growth factor

IHC ..... Immunohistochemistry

IRES-LacZ-Neo ..... A gene-targeting cassette

kDa..... Kilodalton, a measurement of protein size

MAPK ..... Mitogen-activated protein kinase

Met..... Metastasis

MHC ..... Major histocompatibility complex, surface antigen

MMP ..... Matrix metalloproteinase

MVD..... Mean vascular density

NK..... Natural killer cells, a type of lymphocyte

PECAM-1 ..... Platelet endothelial cell adhesion molecule 1

PEDF..... Pigment epithelium-derived factor

PEDF-R..... A receptor for PEDF, also called ATGL

PI3K..... Phosphoinositide 3-kinase

PPAR-gamma ..... Peroxisome proliferator-activated receptor gamma

ROS..... Reactive oxygen species

RPE..... Retinal pigment epithelium

RTK..... Receptor tyrosine kinase

SDF ..... Stromal derived factor

SMA ..... Smooth muscle actin

TGF ..... Transforming growth factor

TIMP..... Tissue inhibitors of metalloproteinases

UM ..... Uveal melanoma

USF ..... Upstream stimulator factor

UV ..... Ultraviolet

VEGF ..... Vascular endothelial growth factor

VEGF-R ..... A family of receptors for VEGF

Wt ..... Wild type

Chapter 1:

Introduction to Uveal Melanoma and PEDF

Key questions to be addressed in this section:

1. What are the characteristics of uveal melanoma?
2. How and why does uveal melanoma metastasize to the liver?
3. Once in the liver, how do the metastases grow?
4. What types of liver cells interact with metastases?
5. What factors regulate metastatic progression?
6. What is angiogenesis, and how do metastases become vascularized?
7. What is stromagenesis, and how do hepatic stellate cells promote cancer cell and endothelial cell growth?
8. What are some factors that regulate angiogenesis and stromagenesis?
9. What is pigment epithelium-derived factor (PEDF), and where is it produced?
10. How does PEDF regulate angiogenesis and stromagenesis?
11. Are there other mechanisms by which PEDF may regulate metastatic progression, such as via lipid metabolism?

1.1—PURPOSE AND CENTRAL HYPOTHESIS

My purpose with this work is to determine the role of a protein, called pigment epithelium-derived factor (PEDF), in metastatic progression. I am specifically interested in the disease uveal melanoma, which is the most common adult eye cancer. This cancer is often fatal due to liver metastasis. After melanoma cells leave the primary tumor, they often spread into the liver, where they lodge and slowly grow to form metastases that can be life-threatening. In the interest of slowing the progression of metastasis, I examined mechanisms that favor metastatic growth. This includes angiogenesis, or the formation of new blood vessels, and stromagenesis, or the formation of structural proteins and cytokines. PEDF, a protein secreted by hepatocytes in the liver, inhibits both angiogenesis and stromagenesis. Another function of PEDF is to promote hydrolysis of triglycerides within the lipid droplets of hepatocytes, but the role of this mechanism in metastatic progression is unknown. Exogenous or transfected PEDF are known to inhibit growth of melanoma, but host-derived PEDF has not been examined. To address whether host-derived PEDF can inhibit metastatic progression through mechanisms involving angiogenesis, stromagenesis, or lipid hydrolysis, we utilized control C57BL/6 mice or mice lacking one or both copies of the PEDF gene. These mice were injected with melanoma cells into their right eyes, allowed to metastasize over several weeks, and analyzed for key features of metastatic progression.

PEDF null mouse eyes or wild type C57BL/6 eyes were injected with melanoma, and cells were allowed to metastasize as a method to investigate the role of PEDF in progression of melanoma metastasis in the liver.

My purpose is to determine if host-derived PEDF is protective against metastatic progression in the liver, and if so, whether it functions through a mechanism involving angiogenesis, stromagenesis, or lipid metabolism.

I hypothesize that host-produced PEDF inhibits the progression of liver metastasis in our mouse model of uveal melanoma through a mechanism involving angiogenesis, stromagenesis, or lipid metabolism.

1.2—UVEAL MELANOMA

1.2.1—Biology of the Primary Uveal Melanoma Tumor

Uveal melanoma forms in uveal melanocytes, a type of pigmented cell found in the choroid, iris, and ciliary body (Eagle 2013). The *choroid* is the heavily vascularized middle layer of the eye located between the white outer sclera and the inner photo-sensing retina (**Figure 1**). The *iris* is the pigmented structure responsible for adjusting pupil diameter, and the *ciliary body* consists mostly of muscle tissue and epithelium adjacent to the iris. These three tissues make up the uveal layer. The melanocytes in this layer are of a neural crest origin similar to cutaneous melanoma, in contrast with the nearby retinal pigment epithelium of neural ectoderm origin (Hu *et al.* 2008). The normal function of these cells is to scavenge excess photons and reactive oxygen species (ROS) (Tolleson 2005, Hu *et al.* 2008). After they acquire mutations to genes such as GNAQ and GNA11, which encode guanine nucleotide binding proteins, they can proliferate and de-differentiate into a more stem cell-like phenotype (Chang *et al.* 2008, Van Raamsdonk *et al.* 2009, Van Raamsdonk *et al.* 2010, Eagle 2013). The tumor initially appears as a dome-shaped, variably pigmented mass under the retina (Lee *et al.* 2001, Jovanovic *et al.* 2013). The tumor grows, becomes hypoxic and vascularized, and can eventually invade inward towards the retina, forming a mushroom-like protrusion, or outward through the sclera (Albert 1998, el Filali *et al.* 2010, Eagle 2013). About 80% of uveal melanomas are located in the choroid, and about 20% are found in either the iris or ciliary body (Singh *et al.* 2011). The choroid, a highly vascularized tissue, provides the developing tumor with ample supplies of oxygen and nutrients

(Pina *et al.* 2009). These growing tumors co-opt this preexistent mature vasculature found at the base of the tumor, while the remainder of the tumor is filled with immature neovessels (Pina *et al.* 2009). The primary route of metastasizing cancer cells out of the choroid is via the tumor vasculature (Woll *et al.* 1999, Bakalian *et al.* 2008, Nakao *et al.* 2012).

The primary uveal melanoma tumor is a variably pigmented mass consisting of proliferating melanocytes and a mixture of various other cell types including mature and immature vascular endothelial cells.

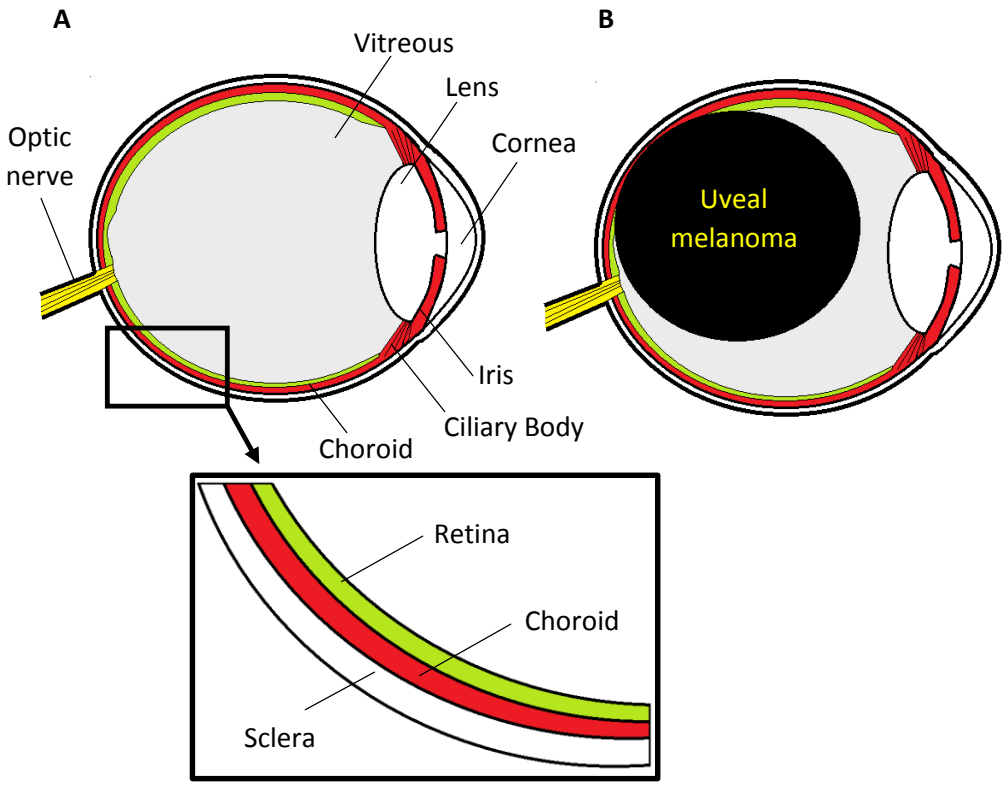

Figure 1 **Uveal melanoma in the eye. A)** The uveal layer of the eye (red) is comprised of the choroid (red, inset), the ciliary body, and the iris. External to the uveal layer is the sclera (white, inset). Internal to the uveal layer is the retina (green, inset), consisting of retinal pigment epithelium, photoreceptors, ganglion cells, and other support cells. A healthy eye also contains an inner fluid compartment called the vitreous (gray). The oval-shaped lens is seen in the anterior part of the eye, along with the dome-shaped cornea. The posterior compartment of the eye also includes the optic nerve (yellow) which relays signals to the brain. **B)** A tumor bearing eye is depicted here with a large black uveal melanoma tumor arising from the melanocytes that normally reside in the choroid.

1.2.2—Diagnosis, Treatment, and Prognosis

The majority of uveal melanoma patients initially complain of blurred vision or vision loss, among other symptoms, but up to 30% are asymptomatic during routine checkups (Damato 2011, Damato *et al.* 2012, Jovanovic *et al.* 2013). Diagnosis takes place by use of ophthalmoscopy, ultrasonography, fluorescein angiography, and optical coherence tomography (Lee *et al.* 2001, Jovanovic *et al.* 2013). Malignant uveal melanoma tumors are clinically distinguished from benign choroidal nevi by size, location, and accumulation of subretinal fluids, and histologically by cellular morphology, mitotic activity, and vascularization, among other features (Lee *et al.* 2001, Landreville *et al.* 2008, Miyamoto *et al.* 2012). The most common treatments are: 1) plaque brachytherapy (35%), which involves temporarily attaching a radioactive plaque to the sclera near the site of the tumor, 2) enucleation (30%), which is the removal of the entire eye, and 3) proton beam radiotherapy (25%), which irradiates the tumor with protons or helium ions (Damato *et al.* 2012, Pereira *et al.* 2013). Enucleation is not a preferred treatment due to the risk of spreading tumor cells, however it is still a common procedure for very large uveal melanoma tumors (Damato 2011, Singh *et al.* 2011). The 5-year survival rate of 81.6% has remained stable from 1973-2008 (Singh *et al.* 2011). Death is commonly attributed to liver metastasis, after the primary tumor has been treated (Landreville *et al.* 2008, Singh *et al.* 2011). Surviving patients often experience vision loss in the irradiated eye (Landreville *et al.* 2008).

After biopsy, patient survival can be estimated by the loss of one copy of chromosome 3, referred to as monosomy 3 (Damato 2011, Abdel-Rahman *et al.* 2012). In one case study, 57% of patients with monosomy 3 developed metastatic disease that often leads to death, compared to 0% of patients with disomy 3 (Prescher *et al.* 1996). A more recent method of prognosis is genetic profiling to determine class 1 versus class 2 tumors. Class 1 tumors are defined as low-grade tumors that are less aggressive and much less likely to metastasize, while class 2 tumors are aggressive and highly metastatic (Onken *et al.* 2004). These two classes have very different genetic signatures, and a 15-gene panel has been developed that can test whether a tumor exhibits a class 1 or class 2 profile, allowing for prediction of metastatic disease (Harbour 2014). Once liver metastasis has been confirmed, median survival is 4 to 6 months (Pereira *et al.* 2013). Another prognostic marker is a mutation in the breast cancer antigen associated protein 1 (BAP1) gene. Somatic mutations were found in BAP1 in 84% of metastasizing uveal melanoma tumors, but only 4% of non-metastasizing tumors (Harbour *et al.* 2010). One function of this tumor suppressor is to remove ubiquitin from host cell factor C1 (HCFC1), which regulates cell proliferation (Harbour *et al.* 2010). Ubiquitin is a small protein that binds to other proteins as a post-translational modification, and in this case, ubiquitin removal promotes HCFC1 activity and regulates proper cell proliferation. BAP1 also interacts with O-linked N-acetylglucosamine transferase (OGT), which is involved in DNA repair, and the polycomb proteins additional sex comb like 1 and 2 (ASXL1 and ASXL2) which are involved in chromatin remodeling (Dey *et al.* 2012). BAP1 is located on chromosome 3, and it has recently been

suggested that loss of BAP1 may be responsible for the increased metastatic potential in tumors with monosomy 3 (Abdel-Rahman *et al.* 2012).

Once a patient has been diagnosed with uveal melanoma, they are usually treated by radiation therapy or surgical excision, and their prognosis for metastatic disease and death can be estimated by genetic profiling of the primary tumor.

1.2.3—Epidemiology of Uveal Melanoma

According to a 36-year study, from 1973 to 2008, uveal melanoma is the most common adult eye cancer in the United States with a rate of 5.1 cases per million (Singh *et al.* 2011). The overall incidence of uveal melanoma remained remarkably steady over this period. Meanwhile, over the same time frame, the incidence of retinoblastoma, the most common eye cancer in children, has remained steady at 11.8 cases per million American children ages 0-4 (Broaddus *et al.* 2009). In contrast, the incidence of cutaneous melanoma in the United States has risen sharply from 230 cases per million in 1992 to about 300 cases per million in 2006 (Jemal *et al.* 2011). Despite a lower incidence, the 5-year mortality rate of uveal melanoma is 18%, whereas retinoblastoma is 3% and cutaneous melanoma is 10% (Singh *et al.* 2003, Broaddus *et al.* 2009, Pollack *et al.* 2011). Males experience a significantly higher rate of uveal melanoma than females, with 5.8 cases per million in males versus 4.4 in females (Singh *et al.* 2011). Males also have a significantly faster rate of formation of metastatic disease which has been

attributed to behavioral patterns leading to later diagnosis in males than in females (Zloto *et al.* 2013). The vast majority of uveal melanoma cases in the United States are among the Caucasian population, at 98% of reported incidences, although this is due in part to the large Caucasian population (Singh *et al.* 2011). The incidence per million by race in the US is as follows: Caucasian 6.02, Hispanic 1.67, Asian 0.38, African American 0.31 (Hu *et al.* 2005). The median age of diagnosis is around 60 years (Damato 2011, Singh *et al.* 2011, Jovanovic *et al.* 2013).

Uveal melanoma is the most common eye cancer in adults in the United States, and it predominantly affects older white individuals.

1.2.4—Etiology and Risk Factors

The cause of uveal melanoma remains debatable, but there are several potential risk factors. The environmental risk factor most commonly focused upon is ultraviolet light (UV), due to its causative relationship to cutaneous melanoma and its ability to induce genetic mutations (Mallet *et al.* 2013). Several studies have asked patients to comment on their daily activity habits and found that increased sunlight exposure correlated with increased incidence of uveal melanoma (Tucker *et al.* 1985, Holly *et al.* 1990, Seddon *et al.* 1990, Vajdic *et al.* 2002). Artificial tanning beds and artificial radiation from welding are risk factors for uveal melanoma (Holly *et al.* 1990, Seddon *et al.* 1990, Guenel *et al.* 2001, Weis *et al.* 2006). Additionally, the inherited risk factors of fair skin, light colored eyes and hair, and the presence of moles, suggest UV may be a factor (Holly *et al.* 1990,

Seddon *et al.* 1990, Weis *et al.* 2006, Mallet *et al.* 2013). However, a separate study found that the inferior choroid, a layer of the eye that receives the majority of ultraviolet rays shining down from the sun, displays no significant increase in melanoma distribution compared with other areas of the choroid, suggesting ultraviolet light may not be a risk factor (Schwartz *et al.* 1997). Other correlative studies have also found no relationship between daily sunlight exposure and uveal melanoma (Gallagher *et al.* 1985, Pane *et al.* 2000). Only a small fraction of UV-B, the primary form of UV responsible for direct DNA damage, can traverse the lens and reach the choroid, suggesting UV may not be as major a factor in uveal melanoma as it is in cutaneous melanoma (Hu *et al.* 2008, Mallet *et al.* 2013).

Familial uveal melanoma is extremely rare (Singh *et al.* 2005). However, 83% of uveal melanoma tumors were found to harbor somatic mutations in two related guanine nucleotide alpha subunit proteins, GNAQ and GNA11, suggesting these mutations are an early step in the formation of uveal melanoma (Van Raamsdonk *et al.* 2009, Van Raamsdonk *et al.* 2010). The mutations occur at either R183 or Q209 in GNAQ, as well as R183 or Q209 in GNA11, and when mutated, the proteins are constitutively active (Van Raamsdonk *et al.* 2010). GNAQ and GNA11 are responsible for activating phospholipase C, a protein that cleaves phospholipids and regulates several signal transduction cascades (Dong *et al.* 1995). However, the relationship between these mutations and the formation of uveal melanoma has not been fully elucidated.

Risk factors include light-colored eyes and complexion, the presence of moles, and mutations in G-alpha-q subunit proteins, while ultraviolet light exposure as a risk factor is currently debated.

1.3—METASTASIS OF UVEAL MELANOMA

1.3.1—Epidemiology of Uveal Melanoma Metastasis

Metastatic disease is the primary cause of death for patients with uveal melanoma (Kujala *et al.* 2003). At the time of initial diagnosis of uveal melanoma, patients undergo tests such as a liver ultrasonogram to determine whether they have detectable metastasis, and around 2%-4% of patients show evidence of metastasis (Singh *et al.* 2005, Jovanovic *et al.* 2013). However, 50% of patients eventually form metastasis, suggesting the metastases are present at initial diagnosis but too small to be imaged (Kujala *et al.* 2003). The average doubling time of metastatic uveal melanoma cells in the liver has been calculated to be 63 days (Eskelin *et al.* 2000). However, metastatic growth is not linear; rather there are long periods of dormancy followed by rapid proliferation of activated colonies (Eskelin *et al.* 2000). What triggers this activation is currently unknown, although exponential growth is often associated with angiogenesis (Folkman 1990). Risk factors signaling a greater risk of metastasis include the previously mentioned monosomy 3, mutations in BAP1, and the presence of aggressive class 2 primary tumors (Prescher *et al.* 1996, Onken *et al.* 2004, Harbour 2014). Class 1 tumor cells are prone to differentiating into a melanocyte-like cell, reducing the probability that they metastasize (Landreville *et al.* 2008).

Metastasis occurs in about 50% of patients with uveal melanoma and is the leading cause of death in this disease. Unfortunately, metastasis is rarely detectable at the time of initial diagnosis.

1.3.2—Dissemination of Tumor Cells to the Liver

As choroidal tumors grow and become vascularized, melanoma cells may hematogenously metastasize (**Figure 2**) (Grossniklaus 1998, Zbytek *et al.* 2008). An unknown trigger causes epithelial-to-mesenchymal transformation to occur in these uveal melanoma cells, leading to loss of E-cadherin and upregulation of proteases, causing the cells to become migratory and particularly invasive (Lu *et al.* 2010, van Zijl *et al.* 2011). These cells produce cytokines and proteinases that allow the cell to adhere to and degrade smooth muscle and blood vessel walls (van Zijl *et al.* 2011, Zlotnik *et al.* 2011). This allows the melanoma cells to invade into the circulation in a process known as intravasation. Emerging evidence suggests that these invasive uveal melanoma cells may come from a primitive stem-cell-like population among the heterogenous tumor, determined by comparing the genetic profile of metastasizing and non-metastasizing uveal melanoma cells with primitive neural ectodermal stem cells from which melanocytes differentiate (Onken *et al.* 2006, Chang *et al.* 2008).

Once the cells leave the vasculature of the eye, they spread via the ophthalmic vein to the superior vena cava, the right side of the heart, and then to the lung (Bakalian *et al.* 2008). Melanoma cells pass through the lungs, the left side of the heart, the aorta, and then reach the liver via the hepatic artery. It is the liver, not the lung, that accounts for the vast majority of cases of metastasis of uveal melanoma, between 70%-90%, and in most cases it is the sole end organ of metastasis (Albert *et al.* 1996, Singh *et al.* 2005). The lung accounts for 20%, bone 16%, subcutaneous

tissue 12%, and brain 4% (Albert *et al.* 1996). There are several hypotheses regarding the mechanism of this preferential uveal melanoma metastatic distribution to the liver. The seed-and-soil hypothesis suggests that tumor cells only successfully survive and expand in an end organ environment that is similar to their original environment (Paget 1889). Hepatocytes and retinal pigment epithelium both secrete proteins such as hepatocyte growth factor that may promote melanoma growth in both locations. This seed-and-soil hypothesis may explain why uveal melanoma cells do not thrive in the lung as readily as the liver. Another hypothesis is based on the physical properties of a tumor cell's path. While the lung presents relatively fewer hurdles, the liver poses an arduous journey in which a cancer cell's progression becomes inevitably hindered within the complex branching hepatic sinusoids (Vidal-Vanaclocha 2008). Recent discoveries have demonstrated that the liver secretes gradients of cytokines into the bloodstream that are detected by a specific pattern of surface receptors unique to the uveal melanoma cell (Bakalian *et al.* 2008). For example, uveal melanoma cells express high levels of c-met, the receptor for hepatocyte growth factor (HGF), a ligand produced by the liver and released into the blood stream (Hendrix *et al.* 1998, Mallikarjuna *et al.* 2007). Uveal melanoma cells also respond to HGF gradients *in vitro*, upregulating both migration and invasion, suggesting that a similar process may be happening *in vivo* (Woodward *et al.* 2002).

The end organ in metastatic uveal melanoma is most often solely the liver. This may be due to mechanical factors, a receptor-ligand gradient, or both.

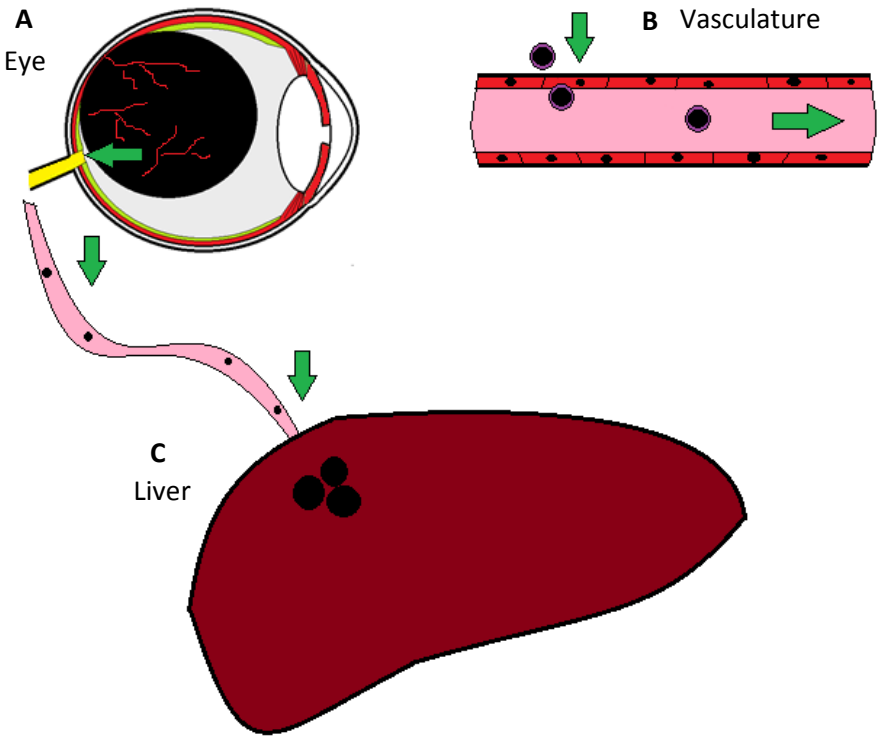

Figure 2 **Metastasis of uveal melanoma from the eye to the liver. A)** The primary uveal melanoma (black) may become vascularized, allowing a pathway for melanoma cells to escape. **B)** Melanoma cells (black) invade tumor vasculature and escape the primary tumor, a process called intravasation. **C)** Melanoma cells that have intravasated travel through the body's circulation and reach the liver where they extravasate to form metastatic colonies

1.3.3—Progression from Micro to Macrometastases

The majority of metastasized uveal melanoma cells that have extravasated, or escaped the vasculature and entered the liver, are solitary and temporarily dormant (Luzzi *et al.* 1998). About one in forty extravasated tumor cells will form a small colony called a micrometastasis, also referred to as a micromet or a stage 1 metastasis, consisting of about 4 to 16 cells which form a spheroidal structure that measures up to 50 μm in diameter (**Figure 3a**) (Luzzi *et al.* 1998, Grossniklaus 2013). A small subset of these micromets will continue to proliferate to form intermediate metastases, also referred to as stage 2 metastases, of about 50 to 500 μm in diameter (Grossniklaus 2013). Only about one in one hundred of these colonies will form a macroscopic metastasis, or macromet, visible to the naked eye at greater than 500 μm in diameter and usually consisting of thousands of cells (Luzzi *et al.* 1998, Grossniklaus 2013). Dormant micrometastases are thought to be tolerated by the host (**Figure 3b**) (Yang *et al.* 2010). However, micromet progression to macromets causes displacement or destruction of healthy liver tissue that ultimately leads to liver failure and death (**Figure 3c**).

Progression of metastasis in the liver consists of solitary cells forming small colonies called micrometastases (<50 μm), a subset of these growing to form intermediate metastases (50-200 μm), and even fewer continuing on to form life-threatening macrometastases (>200 μm).

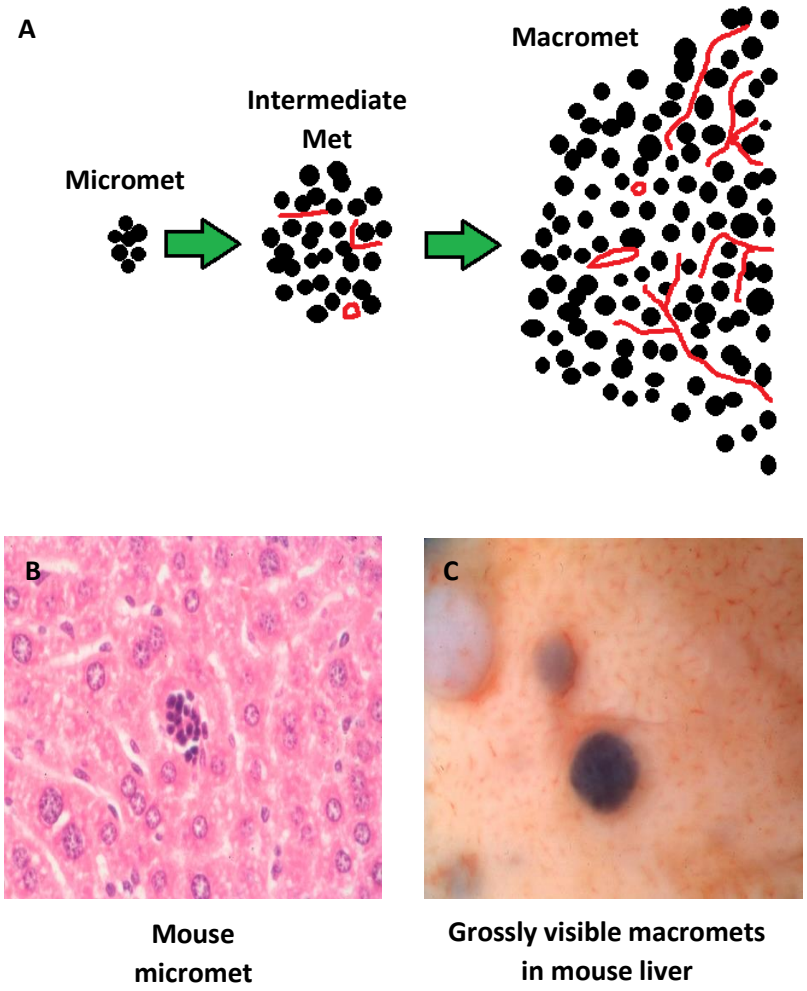

Figure 3 **Metastasis progression in the liver. A)** The majority of metastases found within the liver are micromets measuring up to 50 μm in diameter and consisting of about 4 to 16 cells. Some micromets can progress to become intermediate mets ranging from 50 to 200 μm in diameter. Intermediate mets are either avascular or have a low vascular density. A few intermediate mets may progress to form large macromets that measure 200 μm or more diameter. **B)** Micromet within a mouse liver is surrounded by hepatocytes. **C)** Macromets are

visible to the naked eye, often heavily vascularized, sometimes necrotic, and they lead to liver failure and death

1.3.4—Biology of the Metastatic Liver Microniche

Microscopic liver anatomy consists of repeating patterns of 6 blood vessels that form hexagonal apices that surround the hepatic lobule, not to be confused with the lobes of the liver (**Figure 4a**). These 6 blood vessels are termed the hepatic arterioles, and they supply oxygenated blood into the interior of the hepatic lobule. Adjacent to each hepatic arteriole are a portal venule and a bile duct, and together with the hepatic arterioles, these form the *portal triad*. At the center of the lobule is the central lobular vein which collects the deoxygenated blood and drains it via hepatic venules to the hepatic vein and eventually the inferior vena cava.

On its path from the hepatic arterioles toward the central lobular vein, blood passes through what are called sinusoidal spaces (**Figure 4a, inset**). These sinusoids are lined by endothelium and surrounded by hepatocytes, the main architectural cell in the liver, and hepatic stellate cells (HSC), the resident fibroblasts. The normal functions of hepatocytes include filtration and removal of harmful toxins, synthesis and storage of proteins and phospholipids and the production of bile. Meanwhile the functions of the hepatic stellate cells include production of extracellular matrix (ECM) proteins and growth factors. The resident macrophage of the liver, called the Kupffer cell, is found within the sinusoidal space (Bilzer *et al.* 2006). The Kupffer cell is responsible for phagocytosis of red blood cells, the production of cytokines, and regulation of the stress response. One of the primary cytokines produced by the Kupffer cell in times of stress is transforming growth factor beta

(TGF-beta) which activates HSCs to begin the wound healing response (De Bleser *et al.* 1997, Van den Eynden *et al.* 2013).

The growing tumor microniche consists of many different cell types (Vidal-Vanaclocha 2008). The hepatocyte is the largest (15-25 μm diameter) and most abundant (75%-85%) cell type in the liver, and its role is to facilitate carbohydrate and lipid biogenesis in addition to the breakdown of harmful substances. Endothelial cells are present in the metastatic microniche, in the form of mature, preexisting blood vessels that the tumor co-opts, in addition to immature endothelial cells that respond to low oxygen levels in the tumor, known as hypoxia, to form new vessels through a process known as angiogenesis. Smooth muscle lines the mature vasculature, and erythrocytes are found within. In addition, sinusoidal endothelial cells line the sinusoidal spaces in between hepatocytes. Another cell type present in the microniche is the hepatic stellate cell. This cell is a type of fibroblast which undergoes myofibroblastic differentiation during times of stress and produces growth factors and extracellular matrix proteins. Lastly, a variety of immune cells are present, including liver macrophages known as Kupffer cells. These cells reside in the sinusoidal space and act as the first responders to detect pathogens or diseased cells (Liaskou *et al.* 2012). Natural killer (NK) cells, a type of lymphocyte, are responsible for the elimination of uveal melanoma cells from sinusoidal spaces (Yang *et al.* 2004). Uveal melanoma with lower expression of major histocompatibility complex I (MHC) antigen are targeted by NK cells for lysis (Ma *et al.* 1995). Disruption of NK cells is directly correlated with increased

size of hepatic metastases from uveal melanoma (Ma *et al.* 1995). Metastatic melanoma cells interact with all of these cell types, either by cooperation or antagonism, as the colonies expand.

The metastatic liver microniche consists of many different cell types, including hepatocytes, endothelial cells, hepatic stellate cells, and immune cells, all of which interact with melanoma, both cooperatively and antagonistically.

1.3.5—Portal versus Lobular Pattern of Metastatic Growth

Two general patterns of metastatic growth of uveal melanoma have been observed (Grossniklaus 2013). One pattern of growth is the *portal pattern*, so named because tumor cells are found surrounding the portal triads on the perimeter of the hexagonal hepatic lobule (**Figure 4b**) (Grossniklaus 2013). Portal pattern metastases push nearby hepatocytes out of the way rather than grow into their space, a process called effacement. In this pattern, adjacent normal hepatocytes are found to be still viable and functional, but are compressed into a smaller area and separated from the tumor by a thin layer of reticulin (collagen type III) (Van den Eynden *et al.* 2013). A second pattern of growth of metastatic uveal melanoma is the *lobular pattern*, so named because tumor cells are found within the parenchyma of the hepatic lobule (**Figure 4c**). These lobular pattern metastases expand within the sinusoidal spaces, killing hepatocytes and eventually replacing them in a process known as invasion (Grossniklaus 2013). Patients with multiple liver metastases are usually found with predominantly one pattern of growth, either lobular or portal, although they may exhibit both patterns (Van den Eynden *et al.* 2013). These two patterns are also observed in patients with liver metastasis of colorectal cancer (Eefsen *et al.* 2012). Of the two patterns, it is thought that portal pattern metastases may grow at a faster rate than lobular pattern metastases, although neither pattern has been shown to cause a greater mortality rate.

Metastases in the liver display two patterns of growth: portal pattern metastases are found near the portal triad and push healthy tissue aside, while lobular pattern metastases are found in the parenchyma of the hepatic lobule and completely replace healthy tissue.

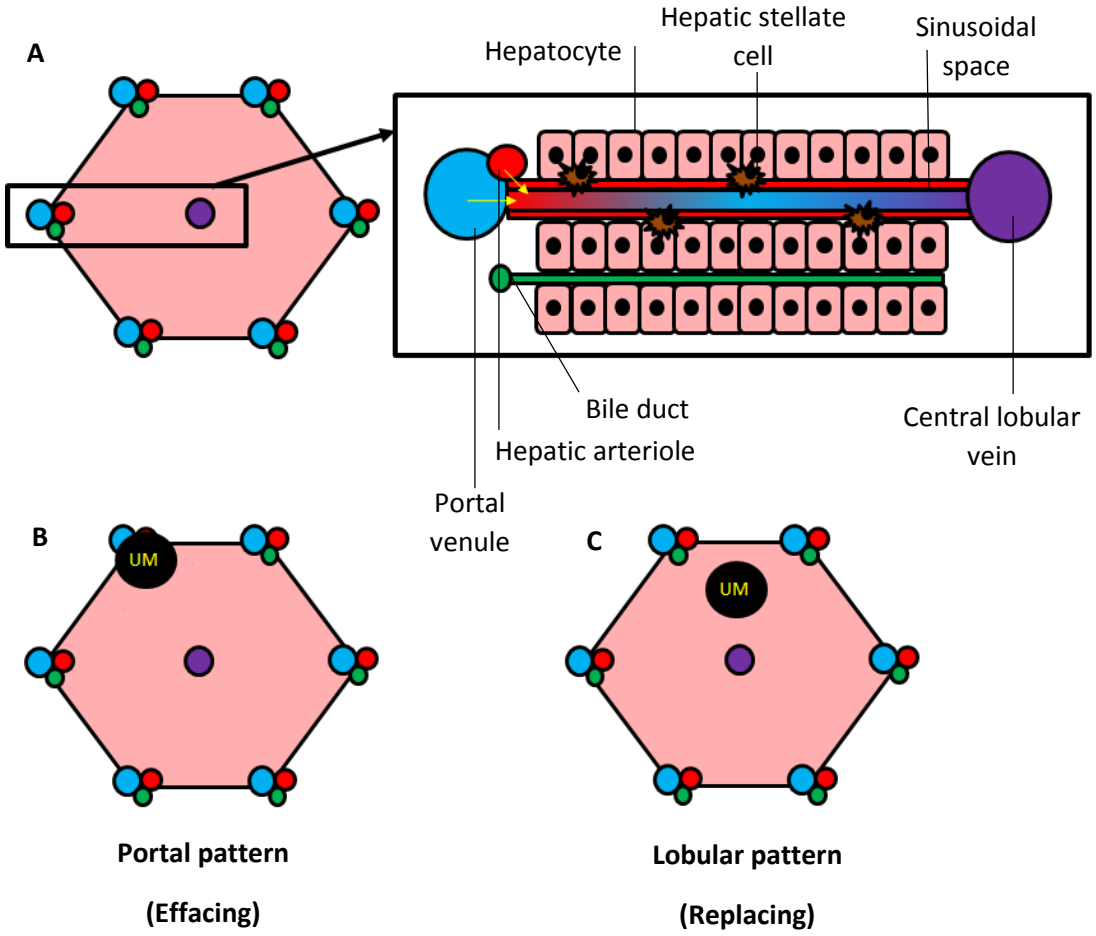

Figure 4 **Portal versus lobular pattern of metastatic growth. A)** A cross-section of a healthy hepatic lobule consisting of 6 regularly spaced hepatic arterioles (red), their accompanying portal venules (blue), and bile ducts (green). The black lines connecting them do not represent a biological structure and are simply drawn to portray the hexagonal pattern of the hepatic lobule. At the center of the lobule is a central lobular vein (purple) that collects and exports blood. The sinusoidal space (inset) is a drainage channel between the hepatic arterioles, portal venules, and the central lobular vein. Hepatocytes (pink) and hepatic stellate cells (brown) can be found adjacent to the sinusoidal spaces. **B)** *Portal pattern*

metastatic growth consists of melanoma cells that reside next to a portal venule. These metastases efface nearby healthy liver tissue, pushing the tissue aside. **C)** *Lobular pattern* metastatic growth consists of melanoma cells that reside in the parenchymal regions of the hepatic lobule. In this growth pattern, healthy tissue is completely replaced by melanoma cells

---

1.3.6—Mouse Models of Metastatic Uveal Melanoma

The common animal model for studying metastatic uveal melanoma is the mouse, due to the propensity of melanoma cells to metastasize from the eye to the liver in this animal. In order to ideally model uveal melanoma in a mouse, uveal melanoma cells of mouse origin would be cultured, counted, injected carefully into the uveal layer of a mouse eye, and allowed to metastasize. While uveal melanoma has spontaneously developed in mice, there have been no successful attempts to cultivate mouse uveal melanoma cells to make them available to the scientific community (Dithmar *et al.* 2000, Dithmar *et al.* 2000). Additionally, these uveal melanomas did not spontaneously metastasize. Mouse cutaneous melanoma cells such as the B16 line are often used in lieu of mouse uveal melanoma cells. B16 cells were first isolated from a skin lesion behind the ear of a mouse at Jackson Labs in the 1960s (Green 1968). Within several years, a clone was isolated for increased metastatic potential, termed B16-F10 (Fidler 1973). Another group isolated a B16 clone with high expression of c-met that preferentially metastasized to the liver, known as B16-LS9 (Rusciano *et al.* 1994). With this key cell type, scientists modeled uveal melanoma using a cutaneous melanoma cell type that was selected for its similar behavior to uveal melanoma (Dithmar *et al.* 2000, Yang *et al.* 2008). These B16-LS9 cells are injected into the posterior compartment of the eye, but because they are highly proliferative, the eye must be enucleated 1 week after injection in order to prevent cancer cell spread outside of the eye. By the time of enucleation, metastasis to the liver has already occurred, and these mice remain viable for up to 6 weeks after injection. Uveal and cutaneous melanoma have very

similar, but not identical, gene expression patterns (van den Bosch *et al.* 2010). Human uveal melanoma cells, when injected into C57BL/6 mice, are rejected by the mouse immune system and do not grow. To circumvent this problem, a method for modeling uveal melanoma cell metastasis is to inject human uveal melanoma cells into immune compromised mice (Heegaard *et al.* 2003). A limitation of this model is that the mouse immune system is not intact and the host immune response is not modeled. In addition to injection of cells into the uveal layer of the eye, some groups have undertaken an alternate method of injecting tumor cells directly into the liver itself (Barak *et al.* 2007, Folberg *et al.* 2007). However, this direct injection method does not model progression from the micromet to macromet stage, nor the recruitment of resident endothelial, stellate, or other cell types. Thus injection of mouse cutaneous melanoma cells into the mouse eye and injection of human uveal melanoma cells into the eye of immune compromised mice are both considered the standard methods for modeling metastatic uveal melanoma in mice. The 4 to 6 week timeframe of metastasis in the mouse model is accelerated compared to what occurs in humans with uveal melanoma. This is a strength in terms of efficiently obtaining data, but it may also be a weakness because biological processes differ due to the different timescales.

In order to model uveal melanoma in mice, melanoma cells are injected into the uveal layer of the eye. These cells are either of mouse cutaneous origin or of human uveal origin. Metastasis occurs within 1 week, but mice are observed 4 to 6 weeks before euthanization.

1.4—PROPERTIES REGULATING METASTATIC PROGRESSION: ANGIOGENESIS

1.4.1—Metastatic Tumor Hypoxia

Uveal melanoma cells that have extravasated into the liver and begun to proliferate into intermediate metastases may exhibit hypoxia, or low oxygen conditions, near the center of the colony (Lu *et al.* 2010). Low oxygen triggers the oxygen-sensitive domain of hypoxia-inducible factor 1 alpha (HIF-1α), causing this protein to dimerize with HIF-1β and become transcriptionally active within the nucleus (Das *et al.* 2007). HIF-1 promotes expression of vascular endothelial growth factor (VEGF) which is secreted by melanoma cells into the microenvironment where it binds to VEGF receptors on the surface of nearby immature endothelial cells (Hicklin *et al.* 2005). These endothelial cells activate, proliferate, and begin to migrate towards the VEGF gradient. Meanwhile, HIF-1 also promotes the expression of proteases such as matrix metalloproteinases 2 and 9 (MMP-2, MMP-9), which degrade extracellular matrix proteins, allowing the endothelial cells to invade hypoxic tissue where they fuse to form new vascular channels (Bergers *et al.* 2000, Hicklin *et al.* 2005). Hypoxia and upregulation of HIF-1 alone do not increase melanoma cell proliferation (el Filali *et al.* 2010). The hypoxic response promotes new blood vessel growth to bring oxygen and nutrients that then cause the tumors to grow larger (Medina *et al.* 2004). Without this blood supply, the growing metastasis may become necrotic (Minami *et al.* 2010). Uveal melanoma cell proliferation and increased cell density also cause upregulated VEGF production by melanoma cells (Grossniklaus lab, unpublished data).

Exposure to hypoxia causes several other changes within the metastasis, including an epithelial-to-mesenchymal transition (EMT) in uveal melanoma cells, increasing their propensity to invade nearby tissue (Victor *et al.* 2006, Shimojo *et al.* 2013). Inhibitors of the HIF-1 pathway also show anti-metastatic effects, such as quinoxaline di-N-oxide inducing apoptosis specifically in cells with high HIF-1 expression and inhibiting tumor volume in mice with breast cancer xenografts (Ghattass *et al.* 2014). High levels of HIF-1α expression in liver metastases has also been correlated with mutations in the phophoinositide-3-kinase alpha subunit (PIK3CA), which is involved in regulating VEGF signaling and endothelial cell activation (Shimomura *et al.* 2013). Overall, hypoxia is an important condition that promotes tumor growth in the presence of endothelial cells.

As metastatic tumors grow, they experience hypoxia, or low oxygen conditions. This leads to a release of pro-angiogenic factors such as vascular endothelial growth factor (VEGF) that attract immature endothelial cells to form new blood vessels.

1.4.2-Tumor Angiogenesis and the Angiogenic Switch

Angiogenesis is the formation of new blood vessels, which differs from vasculogenesis, or the formation of blood vessels during development. The mechanism of vasculogenesis is the regression, or pruning, of mesodermal tissue to leave behind vascular tracts. Conversely, angiogenesis involves the activation of

dormant and immature endothelial cells that differentiate and interlock with one another to form new channels. The importance of angiogenesis in tumor progression has long been apparent, and much effort has been made to investigate methods that abrogate this process and prolong survival. Tumors grown in avascular tissues grow slowly, whereas similar tumors transplanted into vascularized tissue grow much more quickly (Folkman 1990). Furthermore, cancer cell proliferation rates increase in the vicinity of blood vessels (Folkman 1990). Primary uveal melanoma tumors exhibit a documented pattern of branches, loops, arcs, and networks that is also seen in metastatic uveal melanoma of the liver, lung, and skin (Rummelt *et al.* 1998). The liver is a prime candidate end organ due to a voluminous blood supply and vascular channel density (Van den Eynden *et al.* 2013). Metastatic colonies may either co-opt preexisting vasculature or undergo neovascularization (Van den Eynden *et al.* 2013).

Metastatic colonies originate as avascular micrometastases (Grossniklaus 2013). These micromets have a tendency to remain dormant (Udagawa *et al.* 2002). While these have a relatively slow rate of growth, they have the potential to become vascularized and grow exponentially. The theoretical tipping point at which micromets proceed with angiogenesis is a balance between pro- and anti-angiogenic factors and is referred to as the angiogenic switch (**Figure 5**) (Folkman 2002). Anti-angiogenic factors include angiostatin, thrombospondin, and PEDF, while pro-angiogenic factors include VEGF, fibroblast growth factor (FGF), platelet-derived growth factor (PDGF), transforming growth factor (TGF-a and

TGF-b), angiopoietins, and matrix MMPs (Hanahan *et al.* 1996, Bergers *et al.* 2000, Filleur *et al.* 2005, Nyberg *et al.* 2005, Tassi *et al.* 2006, Ria *et al.* 2010).

Angiogenesis, the formation of new blood vessels, is a necessary event in the progression of metastasis because it provides oxygen and nutrients to the tumor. The angiogenic switch refers to the temporal point at which dormant metastases initiate angiogenesis and grow exponentially.

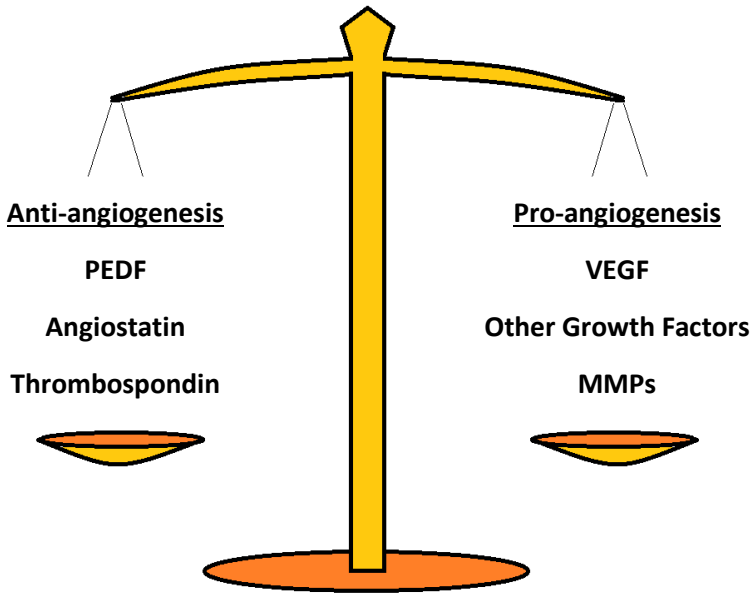

Figure 5 **The angiogenic switch.** The initiation of angiogenesis, or the formation of new blood vessels, is dependent upon a balance between anti-angiogenic factors such as pigment epithelium-derived factor, angiostatin, and thrombospondin versus pro-angiogenic factors such as VEGF and MMPs. When this balance tips in favor of the pro-angiogenic factors, either due to an abundance of pro-factors or a lack of anti-factors, or both, then the angiogenic switch is turned on

1.4.3—Factors Regulating Tumor Angiogenesis

VEGF is the master regulator of tumor angiogenesis and is essential for the survival and function of immature endothelial cells (McMahon 2000). VEGF can be secreted by melanoma cells, hepatocytes, hepatic stellate cells, and endothelial cells during hypoxia or stress (Claffey *et al.* 1996, Shimizu *et al.* 2005, Al-Nedawi *et al.* 2009, Zhao *et al.* 2012). In addition to these criteria, VEGF expression is also stimulated by PDGF and TGF-beta (Ferrara *et al.* 1997, Neufeld *et al.* 1999). VEGF is a dimeric protein that binds VEGF receptors (VEGF-R) on the cell surface. VEGF-Rs are receptor tyrosine kinases (RTK) that exist in either homodimeric or heterodimeric pairs which undergo auto-phosphorylation when activated by VEGF (Olsson *et al.* 2006). Stimulation of VEGF-R leads to activation of the phosphoinositide 3-kinase (PI3K) pathway and the mitogen activated protein kinase (MAPK) pathway, both of which lead to a plethora of transcriptional programming and cell functional regulation that are pro-angiogenic (Olsson *et al.* 2006). Metastatic cells in the liver undergo a loss of micrometastatic dormancy when transfected with VEGF, as seen in gastric carcinoma and osteogenic carcinoma (Udagawa *et al.* 2002). Growth factors that regulate many cell functions, such as FGF, are secreted by hepatic stellate cells that accumulate in the ECM and are released by the proteinase activity of MMPs (Steiling *et al.* 2004, Nyberg *et al.* 2005, Antoine *et al.* 2007, Tsai *et al.* 2011).

Angiostatin is a potent angiogenesis inhibitor formed as a fragment of the larger protein plasminogen (O'Reilly *et al.* 1994). This fragment was originally discovered

in the serum and urine of mice carrying Lewis lung carcinoma but not in control mice lacking a tumor, and later this protein was discovered to have both anti-angiogenic and anti-tumorigenic properties (O'Reilly *et al.* 1994, O'Reilly *et al.* 1994). Furthermore, angiostatin was specifically found to inhibit metastatic progression in a mouse model of melanoma (Dong *et al.* 1998). Given that patients with uveal melanoma experience an increased metastatic rate after removal of the primary tumor (Niederkorn 1984, Niederkorn 1984), it begs the question: is the primary tumor secreting angiostatin into the circulation and suppressing metastasis? While there have been several experiments manipulating angiostatin expression in cancer models with favorable results, this question remains unanswered (Yanagi *et al.* 2000, Xu *et al.* 2003). Angiostatin does, however, regulate the balance between VEGF and PEDF which may explain its role in controlling the angiogenic switch (Yang *et al.* 2006). Thrombospondin, the first naturally-occurring inhibitor of angiogenesis to be discovered, has also been hypothesized to suppress distant metastatic sites (Baenziger *et al.* 1971, Rofstad *et al.* 2001, Chijiwa *et al.* 2009). This protein accumulates in the ECM where it inhibits MMPs and regulates the distribution of VEGF (Rodriguez-Manzaneque *et al.* 2001).

Another endogenous inhibitor of angiogenesis is pigment epithelium-derived factor, or PEDF (Dawson *et al.* 1999). Unlike angiostatin or thrombospondin, PEDF is produced locally at the site of metastasis by nearby hepatocytes (Ho *et al.*

2010). PEDF protein reduces endothelial cell migration *in vitro* and vessel sprouting *in vivo* (Dawson *et al.* 1999).

The balance between anti-angiogenic factors, such as pigment epithelium-derived factor (PEDF), and pro-angiogenic factors, such as VEGF, is thought to regulate the angiogenic switch.

1.4.4—Vasculogenic Mimicry

Melanoma cells are able to form vascular-like channels on their own, a process known as vasculogenic mimicry (Maniotis *et al.* 1999). These tubular networks are comprised entirely of melanoma cells and may contain red blood cells, although they likely connect to true vascular channels. Immunohistochemical staining for endothelial cell marker CD31 revealed that the cells lining these channels within living tumors or within cell culture are void of CD31+ endothelial cells entirely (Maniotis *et al.* 1999). These channels are thought to be formed when the melanoma cells remodel the surrounding ECM by use of matrix metalloproteinases and signal to one another through the surface receptor laminin (Hendrix *et al.* 2003). The importance of this melanoma cell function is that blood may penetrate deep within an otherwise avascular tumor, providing oxygen and nutrients and preventing necrosis. Theoretically, this may also provide the tumor with resistance to anti-angiogenic treatments. However, prior studies have examined CD31 in melanoma tumors, a mature endothelial cell marker, but markers for melanoma and for immature blood vessels were not examined (Maniotis *et al.* 1999). The lack of CD31 led the researchers to conclude the cells were melanoma cells. However, CD31 is also absent in immature endothelial cells, such as those that would be forming new blood vessels within a melanoma tumor (Alessandri *et al.* 2001).

Vasculogenic mimicry occurs when melanoma cells create vascular channels themselves, in the absence of endothelial cells. This may provide tumor resistance to anti-angiogenic therapies. However, there is a question whether vasculogenic mimicry is a property of melanoma cells, some other cell type such as immature endothelial cells, or both.

1.5—PROPERTIES REGULATING METASTATIC PROGRESSION: STROMAGENESIS

1.5.1—Stromagenesis and the Hepatic Stellate Cell

Stromagenesis is a recently coined term to describe a key feature of cell biology: the ability of support cells to produce structural proteins and growth factors that play key roles in many microenvironments of the body (Ruiter *et al.* 2002). These support cells are commonly called stromal cells, a broad category of cell types that include fibroblasts, pericytes, the collagen-producing corneal stroma, and other cells. In the liver, the primary stromal cell is the hepatic stellate cell, a type of fibroblast (Vidal-Vanaclocha 2008). Under normal conditions, HSCs remain in an inactive state, residing in the sinusoidal spaces of the liver as quiescent fibroblasts. There, they store most of the body's vitamin A and have the ability to house lipid droplets filled with triglyceride for later metabolic use (Sato *et al.* 2003). When stressed, these HSCs become activated myofibrocytes. The cytoplasmic area of the HSC becomes reduced, and long star-like processes branch outward from the cell body (Sato *et al.* 2003). Once activated, the HSC produces smooth muscle actin (SMA) and MMPs to remodel the ECM, and increases production of ECM structural proteins such as collagen types I, III and IV and laminin, thus establishing a scaffold for tissue growth (Geerts 2001). Growth factors such as VEGF, TGF-beta, insulin-like growth factor (IGF), and members of the FGF family are also upregulated in activated hepatic stellate cells (Sato *et al.* 2003, Steiling *et al.* 2004, Sanz *et al.* 2005, Zhao *et al.* 2012).

Stromagenesis in the liver refers to the production of proteins that remodel the extracellular matrix along with growth factors that regulate proliferation and function of other cells in the niche. These proteins are produced primarily by the hepatic stellate cell, a type of fibroblast.

1.5.2—Metastatic Tumor Stromagenesis

In the metastatic microenvironment, hepatic stellate cells play a crucial role: the production of proteinases, structural proteins, and growth factors all aid in metastatic progression (**Figure 6**). Hepatic stellate cells are activated in part by TGF-beta produced by Kupffer cells, the resident macrophages of the liver, but can also be activated by hypoxic conditions (De Bleser *et al.* 1997, Das *et al.* 2007, Van den Eynden *et al.* 2013). The matrix metalloproteinases MMP-2 and MMP-9 are released, and these degrade preexisting ECM proteins (Van den Eynden *et al.* 2013). This allows for metastatic tumor invasion. The collagen produced by the HSCs provide a scaffolding for tumor cells to grow upon, and laminin in the ECM, produced by HSCs, regulates attachment during EMT and tissue invasion (Vidal-Vanaclocha 2008, Shimojo *et al.* 2013). Hepatic stellate cells further regulate their own function by production of collagenase, which breaks down collagen, and tissue inhibitors of metalloproteinases (TIMPs) which inactivate MMPs (Murphy *et al.* 2002). The scaffolding and growth factors associated with HSC extracellular matrix create a favorable environment not only for cancer cells but also for the

growth and maintenance of vascular endothelial cells that are necessary for metastatic tumor growth (Vidal-Vanaclocha 2008).

Tumor stromagenesis provides structural support for cancer cells and blood vessels to grow, and growth factors produced by hepatic stellate cells promote the growth and invasion of cancer cells and endothelial cells.

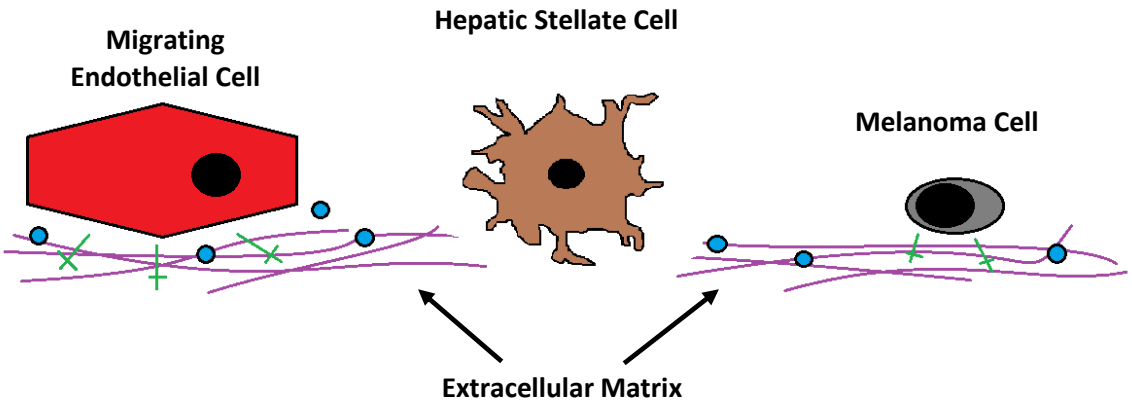

Figure 6 **Stromagenesis in the liver.** The hepatic stellate cell (brown, middle) is responsible for stromagenesis in the liver. The hepatic stellate cell produces ECM components, consisting of structural proteins such as collagen fiber networks (purple) and laminin (green) plus cytokines such as VEGF and FGF (blue circles). ECM provides support for migrating endothelial cells (red) and metastatic uveal melanoma cells (grey). The production of these structural proteins and cytokines is called *stromagenesis*

1.5.3—Factors Regulating Tumor Stromagenesis

While the activation of hepatic stellate cells by TGF-beta or hypoxia promotes metastatic progression, inhibition of HSC function is a potential treatment for metastasis (De Bleser *et al.* 1997, Das *et al.* 2007, Van den Eynden *et al.* 2013). This can be accomplished by targeting the proteins produced by the HSC, such as collagen or matrix metalloproteinases, or by inducing apoptosis in the HSC. One such inhibitor of HSC-produced collagen is N-(methylamino)isobutyric acid or MeAIB (Freeman *et al.* 2002). Oral administration of this non-metabolizable amino acid analog in rats successfully inhibited hepatic collagen production after induction of fibrosis with carbon tetrachloride treatment by inhibiting incorporation of proline.

One naturally occurring inhibitor of stromagenesis is PEDF. This protein, described previously as a naturally occurring inhibitor of angiogenesis, is produced by hepatocytes in the metastatic microenvironment. PEDF has a protective role in liver cirrhosis and induced fibrosis, and does so through a mechanism involving hepatic stellate cell apoptosis (Ho *et al.* 2010).

Activation of hepatic stellate cells that regulate liver stromagenesis is achieved through hypoxia or growth factors such as TGF-beta. Inhibition of these cells can be achieved through exogenous drugs or by naturally occurring factors such as PEDF.

1.6—PIGMENT EPITHELIUM-DERIVED FACTOR (PEDF)

1.6.1—History and Properties of PEDF

PEDF, previously described as an inhibitor of angiogenesis and stromagenesis, was originally discovered by Joyce Tombran-Tink and Lincoln Johnson in 1989 (**Figure 7**) (Tombran-Tink *et al.* 1989, Tombran-Tink *et al.* 1991). These authors were searching for factors produced by retinal pigment epithelium (RPE) that regulated retinoblastoma (Rb) cancer cell differentiation because differentiated cancer cells have decreased proliferation and invasion. Conditioned media from RPE induced neuritic outgrowths in Y79 retinoblastoma cells, a sign of differentiation (Tombran-Tink *et al.* 1989). Thus, PEDF is said to have a neurotrophic effect. These authors isolated a 50 kilodalton (kDa) protein from the RPE conditioned media that was responsible for Y79 differentiation (Tombran-Tink *et al.* 1991). In 1994, the gene for PEDF, which was previously named SERPINF1, was mapped to chromosome 17 in humans by using fluorescence *in situ* hybridization (Tombran-Tink *et al.* 1994). Since PEDF is a member of the serpin family of serine protease inhibitors, the first question asked about the function of PEDF was whether it behaved like other serpins and inhibited serine proteases such as trypsin. PEDF was found to lack serpin activity; furthermore, the serpin reactive domain was not responsible for the neurotrophic function of PEDF (Becerra *et al.* 1995).

In the 1990s, the presence of PEDF had been confirmed in low quantities in the interphotoreceptor space of mammalian eyes, where factors produced by the RPE

act upon the retina, and also in the vitreous (Wu *et al.* 1995, Wu *et al.* 1996). At the same time, the scientific community was searching for growth factors in the eye that may inhibit choroidal neovascularization (CNV). CNV is a process that occurs in multiple eye diseases and disorders, including age-related macular degeneration (Nowak *et al.* 2004). A study examining anti-angiogenic properties of fractionated retinoblastoma conditioned media uncovered a 50kDa protein with potent inhibition of endothelial cell migration (Dawson *et al.* 1999). Protein analysis revealed that this protein was PEDF. Later studies confirmed the protective role of PEDF in CNV in addition to a significant absence of PEDF in patients experiencing CNV (Mori *et al.* 2001, Spranger *et al.* 2001).

The crystal structure of PEDF was solved in 2001 (Simonovic *et al.* 2001). PEDF has asymmetric charge distribution, with the N-terminus populated by predominantly basic residues and the C-terminus predominantly acidic residues. Nearer to the N-terminus, PEDF contains an anti-angiogenic domain called the 34-mer, a neurotrophic domain called the 44-mer, and a putative nuclear localization sequence (NLS) (**Figure 7**) (Filleur *et al.* 2005, Anguissola *et al.* 2011). At the C-terminus, PEDF contains a non-functional serpin domain (Becerra *et al.* 1995).

PEDF is expressed in a wide variety of tissues in all vertebrates, and the hepatocytes of the liver are a major source of PEDF (Tombran-Tink *et al.* 2003, Ho *et al.* 2010). Expression of PEDF is upregulated by angiostatin, a cleavage product

of plasminogen (Gao *et al.* 2002, Yang *et al.* 2006). Hypoxia, however, downregulates PEDF at the protein level in melanoma (Notari *et al.* 2005, Fernandez-Barral *et al.* 2012). The promoter region of PEDF includes potential binding sites for the transcription factors hepatocyte nuclear factor 4 (HNF4), CCAAT/enhancer-binding protein homologous protein (CHOP), and upstream stimulatory factor (USF) (Xu *et al.* 2006). Matrix metalloproteinases MMP-2 and MMP-9, which are both upregulated in hypoxic conditions, degrade PEDF, suggesting a mechanism for shifting the balance of the angiogenic switch towards VEGF in times of hypoxia (Notari *et al.* 2005). The PEDF cleavage products after MMP degradation are biologically inactive in both angiogenesis assays and retinal survival assays (Notari *et al.* 2005).

PEDF is known to bind two receptors, one being adipose triglyceride lipase (ATGL) which regulates lipid hydrolysis, and the other being the laminin receptor (Notari *et al.* 2006, Bernard *et al.* 2009). Several downstream effects of PEDF signaling are known. PEDF initiates the FAS-FASL cascade that induces apoptosis in melanoma cells, endothelial cells, and the stromagenic hepatic stellate cells (Volpert *et al.* 2002, Garcia *et al.* 2004). PEDF induces PPAR-gamma expression which activates p53, a tumor suppressor (Ho *et al.* 2007). The NF-kB pathway is stimulated by PEDF, and this is responsible for controlling cell proliferation and survival (Tombran-Tink *et al.* 2003). And the anti-angiogenic protein thrombospondin is upregulated by PEDF (Guan *et al.* 2004). All of these features

implicate PEDF in many processes that may be important in metastatic progression.

PEDF is a secreted protein produced by many tissues including retinal pigment epithelium and liver hepatocytes. PEDF has anti-angiogenic and anti-stromagenic properties and also regulates lipid metabolism.

FACTSHEET	
Name	Pigment epithelium-derived factor
Gene name (human)	SERPINF1
Chromosome	17p13.3
Bases	15,616
Exons	11
Splice variants	9
Evolutionary origin	All vertebrates
Protein name (human)	PEDF
Amino acids	418
Size (Daltons)	46,312
Primary tissues	Retinal pigment epithelium, liver, kidney
Cell localization	Secreted into extracellular space
Primary functions	Apoptosis, anti-angiogenesis, anti-stromagenesis, anti-tumorigenesis, cell differentiation

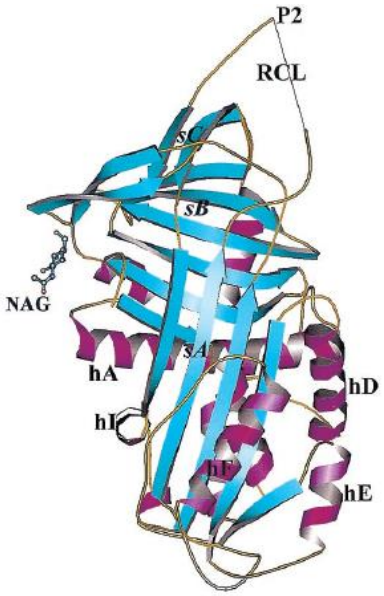

Pigment epithelium-derived factor (PEDF)

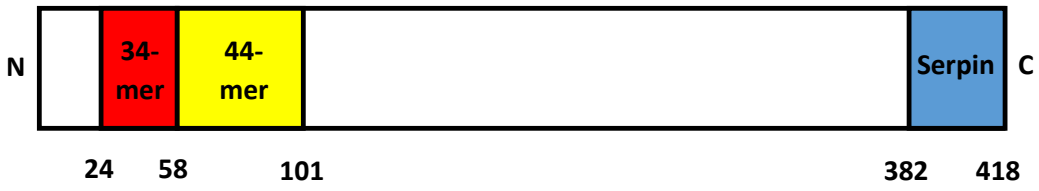

Figure 7 **Pigment epithelium-derived factor (PEDF).** The factsheet contains the pertinent gene and protein information along with localization and function regarding PEDF. Shown below is the crystal structure of PEDF with the following labels: helices (h), sheets (s), the inactive serpin reactive center loop (RCL) and its proline (p), and N-acetylglucosamine (NAG) (Simonovic *et al.* 2001) (Copyright 2001, National Academy of Sciences, USA). Shown below is the primary protein structure of the 418-amino acid PEDF including the anti-angiogenic 34-mer (red, amino acids 24-57) and the neurotrophic 44-mer (yellow, amino acids 58-101) near the N-terminus and the inactive serpin reactive center loop (blue, amino acids 382-418) near the C-terminus. A putative NLS exists within the 34-mer domain

1.6.2—The Role of PEDF in Angiogenesis

PEDF is one of the most potent inhibitors of angiogenesis (Takenaka *et al.* 2005). The functional epitope responsible for the anti-angiogenic properties of PEDF has been mapped to residues 24-57, and this epitope has been termed the 34-mer (Filleur *et al.* 2005). This 34-mer causes a significant increase in endothelial cell apoptosis, a reduction in endothelial cell migration *in vitro*, and a reduction in neovascular growth in the mouse cornea (Filleur *et al.* 2005).

PEDF, like thrombospondin, can initiate the FAS/FASL cascade and induce apoptosis in endothelial cells (Volpert *et al.* 2002). Specifically, FASL, the ligand for the FAS receptor, is activated by PEDF, while the FAS receptor is activated by VEGF (Bouck 2002, Volpert *et al.* 2002). PEDF also induces apoptosis in a FAS-independent mechanism, by activating p38 which leads to the cleavage of caspases 3, 8, and 9 (Chen *et al.* 2006).

Additional endothelial cell functions, including migration, are inhibited through a mechanism involving PEDF, VEGF, and VEGF receptors. PEDF can inhibit the expression of VEGF in both retinal capillary endothelial cells and Müller cells (Zhang *et al.* 2006). VEGF receptor 1, VEGF-R1, is cleaved when bound by PEDF, and the cleavage product accumulates in the cytoplasm, preventing VEGF signaling (Cai *et al.* 2006). Furthermore, PEDF competes with VEGF for the VEGF-binding site in VEGF-R2 (Zhang *et al.* 2006).

PEDF is a potent inhibitor of angiogenesis. It achieves this by downregulating VEGF, interfering with VEGF receptor signaling, and inducing apoptosis in vascular endothelial cells.

1.6.3—The Role of PEDF in Stromagenesis

Much less is known about the role of PEDF in stromagenesis. PEDF levels in patients with cirrhosis are significantly reduced (Matsumoto *et al.* 2004). Cirrhosis is a disease of the liver wherein extensive fibrosis occurs. The excessive connective tissue is generated due to the overactivity of hepatic stellate cells. This mechanism has been linked to ethanol exposure and upregulation of MMPs that degrade PEDF and allow for ECM remodeling in the liver (Chung *et al.* 2009). PEDF protein is protective against carbon tetrachloride-induced cirrhosis (Ho *et al.* 2010). Hepatic stellate cell activation, as measured by smooth muscle actin and required for fibrosis, was inhibited by PEDF (Ho *et al.* 2010). Furthermore, PEDF induces apoptosis in hepatic stellate cells (Ho *et al.* 2010). Together, these data suggest that PEDF may have multiple anti-tumor roles, not only inhibiting angiogenesis, but also inhibiting stromagenesis which is very important for metastatic progression.

PEDF inhibits hepatic stellate cell activation and induces apoptosis in these cells. Additionally, PEDF inhibits hepatic fibrosis. These anti-stromagenic functions of PEDF suggest there may be additional anti-tumor effects of PEDF other than its anti-angiogenic effects.

1.6.4—The Role of PEDF in Lipid Metabolism

PEDF regulates lipid metabolism through its receptor ATGL, also known as PEDF-R (Notari *et al.* 2006, Chung *et al.* 2008). ATGL is a membrane-bound receptor in various cell types including hepatocytes, but its cellular localization is under debate. One study suggests that ATGL is bound to the surface of the cell where it presumably interacts with free PEDF proteins in the ECM (Notari *et al.* 2006). Another study demonstrates that ATGL is localized to intracellular lipid droplets but provides no explanation for how PEDF enters the cell (Chung *et al.* 2008). Normally, ATGL catalyzes the hydrolysis of triglycerides into diglycerides and free fatty acids (Smirnova *et al.* 2006). PEDF regulates phospholipase A2 activity of ATGL within the cell (Notari *et al.* 2006). PEDF null mice exhibit an increased triglyceride buildup within hepatocytes, heavier body weight, and liver steatosis, or fatty liver (Chung *et al.* 2008). Lipid loaded hepatocytes activate hepatic stellate cells and cause them to produce tumorigenic factors, such as TGF-beta, MMPs, and TIMPs, providing another potential protective effect of PEDF in metastatic progression via regulation of lipid hydrolysis (Wobser *et al.* 2009).

PEDF regulates triglyceride breakdown in the liver through its receptor adipose triglyceride lipase (ATGL). Mice lacking PEDF develop fatty (steatotic) livers. The role of PEDF in lipid metabolism provides a potential link between PEDF, hepatic stellate cell activation, and metastatic progression.

1.6.5—PEDF and Tumor Biology

Ever since the original discovery that PEDF induces differentiation of retinoblastoma, there has been interest in PEDF as an anti-tumor protein (Tombran-Tink *et al.* 1989). Data have accumulated linking PEDF to regulation of angiogenesis, stromagenesis, steatosis, fibrosis, and apoptosis, all suggesting a universal protective role for PEDF in cancer (Tombran-Tink *et al.* 2003). Several studies have since been performed to test the role of PEDF in cancer and metastasis. Melanoma cells constructed to overexpress PEDF inhibited subcutaneous tumor growth and entirely prevented metastasis in mice (Garcia *et al.* 2004). Further studies demonstrated this anti-tumor effect in glioma, osteosarcoma, (Guan *et al.* 2004, Takenaka *et al.* 2005, Zolochevska *et al.* 2012). In ocular melanoma, constitutive overexpression of PEDF by melanoma cells inhibited growth of the primary tumor in the eye and decreased the number of metastases in the liver (Yang *et al.* 2010). However, these studies have examined exogenous or vector-expressed PEDF in tumor growth and metastasis, while no previous study has analyzed the role of host-derived PEDF in cancer metastasis.

Exogenous PEDF inhibits the growth and metastasis of various types of cancer. There has been no previous study examining the effects of host-derived (endogenous) PEDF on tumor growth and metastasis.

1.6.6—The PEDF Null Mouse

PEDF null mice were previously generated on a C57BL/6 background by a collaborator (Doll *et al.* 2003). Exons 3 through 6 of PEDF were replaced with an IRES-LacZ-Neo cassette. These mice are viable and fertile, but they exhibit prostate epithelial hyperplasia, fatty liver, and obesity in adulthood (Doll *et al.* 2003, Chung *et al.* 2008). The rate of retinal vascular growth is increased in PEDF null mice (Huang *et al.* 2008). Hepatocytes isolated from these mice respond favorably to exogenous PEDF which lowers the triglyceride load (Chung *et al.* 2008).

PEDF null mice show signs of fatty liver and obesity, along with prostate epithelial hyperplasia, but they are otherwise healthy and fertile.

1.7—INTRODUCTION SUMMARY

It is clear that PEDF has many protective functions in cancer biology. This protein inhibits angiogenesis, blocking the ability for tumors to obtain oxygen and nutrients. It inhibits stromagenesis, preventing hepatic stellate cells from building the structural proteins and growth factors that assist in metastatic progression. PEDF also regulates lipid metabolism which is linked to activation of stromagenesis.

The following studies were designed to investigate the role of host PEDF in ocular melanoma and metastasis progression in the liver, with an emphasis on angiogenesis, stromagenesis, and lipid metabolism.

Chapter 2:

Host pigment epithelium-derived factor (PEDF)

prevents progression of liver metastasis

in a mouse model of uveal melanoma

Key questions to be addressed in this section:

1. Does host PEDF affect the size of the primary ocular tumor?
2. Does host PEDF affect the number of metastases in the liver of mice that have been injected with melanoma in the eye?
3. Does host PEDF affect the size of metastases in the liver?
4. Does host PEDF affect the distribution of micrometastases, intermediate metastases, or macrometastases?
5. Does host PEDF affect the vascular density in the metastases or the surrounding liver tissue?
6. Does host PEDF affect the density of activated hepatic stellate cells in the metastases?
7. Does host PEDF affect the density of collagen within the metastases?

Published as Lattier, J.M., et al., *Host pigment epithelium-derived factor (PEDF) prevents progression of liver metastasis in a mouse model of uveal melanoma.* Clin Exp Metastasis, 2013.

References are provided at the end of this dissertation.

Host Pigment Epithelium-Derived Factor (PEDF) Prevents Progression of Liver Metastasis in a Mouse Model of Uveal Melanoma

John M. Lattier, BS[1], Hua Yang, MD, PhD[1], Susan Crawford, DO[2], Hans E. Grossniklaus, MD, MBA[1]

From the [1]Department of Ophthalmology, Emory University, Atlanta, GA, and the [2]Department of Pathology, University of St. Louis, St. Louis, MO

Correspondence to Dr. Hans E. Grossniklaus, BT428, Emory Eye Center, Atlanta, GA 30307, Tel 404-778-4616, Fax 404-778-4610, ophtheg@emory.edu

ACKNOWLEDGEMENTS

Supported in part by NIH R01CA176001 (HEG), P30EYE06360 (HEG), T32EY007092 (JML), and an unrestricted departmental grant from Research to Prevent Blindness, Inc., New York, NY

CONFLICT OF INTEREST

The authors declare that they have no conflict of interest.

2.1—ABSTRACT

Uveal melanoma (UM) has a 30% five-year mortality rate, primarily due to liver metastasis. Both angiogenesis and stromagenesis are important mechanisms for the progression of liver metastasis. Pigment epithelium-derived factor (PEDF), an anti-angiogenic and anti-stromagenic protein, is produced by hepatocytes. Exogenous PEDF suppresses metastasis progression; however, the effects of host-produced PEDF on metastasis progression are unknown.

We hypothesize that host PEDF inhibits liver metastasis progression through a mechanism involving angiogenesis and stromagenesis.

Mouse melanoma cells were injected into the posterior ocular compartment of PEDF-null mice and control mice. After one month, the number, size, and mean vascular density (MVD) of liver metastases were determined. The stromal component of hepatic stellate cells (HSCs) and the type III collagen they produce was evaluated by immunohistochemistry. Host PEDF inhibited the total area of liver metastasis and the frequency of macrometastases (diameter >200μm) but did not affect the total number of metastases. Mice expressing PEDF exhibited significantly lower MVD and less type III collagen production in metastases. An increase in activated HSCs was seen in the absence of PEDF, but this result was not statistically significant. In conclusion, host PEDF inhibits the progression of hepatic metastases in a mouse model of UM, and loss of PEDF is accompanied by an increase in tumor blood vessel density and type III collagen.

2.2—INTRODUCTION

Uveal melanoma (UM) originates in melanocytes in the choroid, ciliary body, or iris, collectively known as the uvea. In the United States, UM is the most common form of eye cancer in adults with 5.1 cases per million (Singh *et al.* 2011). Caucasians account for 98% of cases, with fair skin and light-colored eyes among the risk factors (Damato 2011, Singh *et al.* 2011). Data regarding ultraviolet light exposure as a risk factor for UM have been inconclusive (Swerdlow *et al.* 1995, Vajdic *et al.* 2002, Hurst *et al.* 2003). Familial UM is rare, accounting for only 0.6% of cases (Damato 2011, Singh *et al.* 2011). Treatment of UM has recently shifted away from enucleation (removal of the eye) towards irradiation and plaque radiotherapy, but the 5-year survival rate has remained unchanged at 80% over the last 40 years (Sato *et al.* 2008, Singh *et al.* 2011). This is because the cause of death in patients with metastatic UM is most commonly due to hepatic metastasis and liver failure, suggesting that metastasis occurs before treatment of the primary tumor (Sato *et al.* 2008). In humans, when UM metastasizes to the liver, it initially appears to form dormant, avascular metastases that are too small to be imaged (Blanco *et al.* 2012, Grossniklaus 2013). Gene expression profiling or multiplex ligation probe amplification can be used to predict which UM patients will develop aggressive metastases (Onken *et al.* 2004, Lake *et al.* 2012, Vaarwater *et al.* 2012).

The liver is the main site of metastasis in 80% of patients with UM who develop metastatic disease (Sato *et al.* 2008). One hypothesis as to why UM cells

predominantly metastasize to the liver is that passive, mechanical factors such as the location of the liver in the vascular path and the trapping of cells in the liver vasculature cause cancer cells to deposit in the liver (Vidal-Vanaclocha 2008). Another hypothesis is that UM surface receptors CXCR4 and c-Met mediate migration toward ligand gradients produced by the liver, namely stromal cell-derived factor (SDF) and hepatocyte growth factor (HGF) (Bakalian *et al.* 2008). Micrometastases (around 4 to 16 cells, diameter <50μm) may stay quiescent for years (Luzzi *et al.* 1998, Grossniklaus 2013). At some point, these micrometastatic colonies may enlarge to form intermediate metastases (diameter 50-500μm in humans, 50-200μm in mice) or larger still to form macrometastases (diameter >500μm in humans, >200μm in mice) (Grossniklaus 2013). What triggers activation from dormancy is unknown; however, there are several properties of the UM cell and of the host liver microenvironment that may potentiate metastatic progression.

Intrinsic properties of the UM cell, such as monosomy 3, correlate strongly with highly metastatic UM and mortality (Damato *et al.* 2007, Materin *et al.* 2011). Mutations in the deubiquitinating enzyme BRCA1-associated protein (BAP1) located on chromosome 3 are seen almost exclusively in patients with metastatic UM (Harbour *et al.* 2010). In addition, tumor cells upregulate factors that may enhance metastatic progression such as fibronectin 1, insulin receptor substrate 2 (IRS2), and matrix metalloproteinase 2 (MMP2) (Marshall *et al.* 2007). Metastatic

UM cells may also downregulate HLA antigen expression and evade the host immune response (Jager *et al.* 2002).

Extrinsic, or host, properties may also play an important role in suppressing or promoting metastatic tumor progression. Angiogenesis, or the formation of new blood vessels to supply the tumor with nutrients and oxygen, is necessary for metastases to grow larger than 2-3mm^3 (Bingle *et al.* 2002). As the metastases grow, tumor cells become hypoxic and release vascular endothelial growth factor (VEGF) into the tumor microenvironment, recruiting host vascular endothelial cells. Additionally, stromagenesis is an important and often overlooked component of metastatic progression (Beacham *et al.* 2005). Stromagenesis in the liver includes the activation of hepatic stellate cells (HSCs) into a migratory and proliferative state, in addition to the formation of extracellular matrix components such as type I and III collagen and the secretion of growth factors (Vidal-Vanaclocha 2008, Zong *et al.* 2012). The extracellular matrix provides a scaffold for blood vessel and tumor cell growth, meanwhile growth factors such as VEGF promote angiogenesis and metastatic progression (Vidal-Vanaclocha 2008).

A candidate host-produced factor, and one of the most potent inhibitors of angiogenesis and stromagenesis, is pigment epithelium-derived factor (PEDF). PEDF is a secreted protein that is produced by hepatocytes but downregulated in hypoxic cutaneous melanoma cells (Dawson *et al.* 1999, Orgaz *et al.* 2009, Ho *et al.* 2010, Fernandez-Barral *et al.* 2012). PEDF binds the receptors PNPLA2,

laminin receptor, and ATP synthase (Notari *et al.* 2006, Bernard *et al.* 2009, Notari *et al.* 2010). PEDF induces apoptosis of the endothelial cell, inhibiting angiogenesis, and this occurs through multiple pathways including Fas/FasL and cleavage of caspases 8 and 9 (Volpert *et al.* 2002, Chen *et al.* 2006). In addition, PEDF inhibits VEGF receptors 1 and 2 (Cai *et al.* 2006, Zhang *et al.* 2006). PEDF inhibits stromagenesis by causing apoptosis in HSCs and by causing the cytoskeleton of surviving HSCs to break down (Ho *et al.* 2010). Deficiency in PEDF leads to increased pancreatic cancer invasiveness, hyperplasia, and disease morphology in mice, while patients with pancreatic cancer have decreased levels of PEDF in serum and tumor cells (Grippo *et al.* 2012). PEDF is inhibited in hypoxic environments and degraded by matrix metalloproteinases MMP-2 and MMP-9 which are secreted by tumor cells and macrophages, suggesting that as metastases progress, they downregulate host PEDF (Notari *et al.* 2005, Allavena *et al.* 2008, Fernandez-Barral *et al.* 2012). The VEGF/PEDF ratio has been suggested as an angiogenic switch in UM metastasis (Hanahan *et al.* 1996, Yang *et al.* 2006). B16-LS9 melanoma cells that were transfected to overexpress PEDF and were injected into the eye of C57BL/6 mice exhibit decreased growth of primary tumor and decreased number of metastases in the liver, suggesting an anti-proliferative role of PEDF in cancer cells (Yang *et al.* 2010). However, there have been no studies to date that have analyzed the role of specifically host-produced PEDF in suppressing metastatic UM progression (Garcia *et al.* 2004, Yang *et al.* 2010).

The aim of this study is to uncover the role of an anti-angiogenic and anti-stromagenic factor produced by the host liver, PEDF, with regards to the progression of hepatic metastasis of UM. We used an established mouse model of UM in a strain of transgenic PEDF-null mice to examine properties of liver metastasis in the presence versus absence of host-produced PEDF.

2.3—METHODS

All experiments were performed in conduct with the Association for Research in Vision and Ophthalmology (ARVO) Statement for the Use of Animals in Ophthalmic and Visual Research and with Institutional Animal Care and Use Committee (IACUC) policies and procedures.

Cell culture

B16-LS9 mouse melanoma cells were cultured at 37°C and 5% CO_2. Cells were fed every 2-3 days in RPMI-1640 with 10% FBS, L-glutamine, HEPES, 1% non-essential amino acids, 1% sodium pyruvate, 1% MEM vitamin solution, and 1% penicillin-streptomycin. Before use in animal experiments, cells were trypsinized and suspended at $1.5x10^5/1.5\mu L$ in phosphate buffer solution. Separate cultures were lysed with radioimmunoprecipitation assay buffer for use in western blot (50μg protein blotted with AB-PEDF1 antibody by BioProducts of Maryland, 1/5000). Human PEDF protein was used as a positive control (BioProducts of Maryland, 4ng per lane), with an expected band 50-75 kDa, and actin was used as a loading control (Millipore MAB1501, 1/5000). B16-LS9 melanoma cells are a representative model of human melanoma due to their high levels of c-Met expression and their propensity to metastasize to the liver (Diaz *et al.* 1999, Dithmar *et al.* 2000).

Mouse model of uveal melanoma

PEDF-null mice were previously generated on a C57BL/6 background (Doll *et al.* 2003). These mice are viable and have no known development deficiencies aside from being slightly overweight and exhibiting fatty liver (Chung *et al.* 2008). Genotyping was confirmed by tail snip PCR analysis. Liver PEDF mRNA levels were determined by quantitative real-time polymerase chain reaction (n=4) of liver lysate collected in TRIzol reagent (Invitrogen Corp.). PEDF forward primer sequence was AAGGTCCCTGTGAACAAGC, and reverse primer sequence was GTCGTAGTAGAGAGCCCGGT. Protein expression was determined by immunohistochemistry of liver sections (n=3, antibody sc-16596 by Santa Cruz Biotechnology, Inc., 1/50) or western blot of 200μg liver lysates (n=3, antibody AB-PEDF1 by BioProducts of Maryland, 1/5000). Human PEDF protein was used as a positive control (BioProducts of Maryland, 4ng per lane), with an expected band 50-75 kDa, and actin was used as a loading control (Millipore MAB1501, 1/5000). Wild-type C57BL/6 mice were obtained from Charles River Labs; 7-week old female mice were anesthetized by intraperitoneal injection of 100mg/kg ketamine and 12mg/kg xylazine mixture in phosphate buffer solution. B16-LS9 cells were injected into the uveal layer of the right eye by first preparing a passageway using a 30 gauge needle then by injecting $1.5x10^5$/1.5μL cells into the passageway (Dithmar *et al.* 2000). Seven days post-injection, the right eye was enucleated, a method that precludes direct extraocular extension of the melanoma and promotes growth of liver metastases (Dithmar *et al.* 2000, Yang *et al.* 2008), and the eyes were stored in formalin. Twenty-eight days post-injection the mice

were euthanized and livers were collected and routinely processed for histologic examination. Formalin fixed paraffin embedded slides of eyes and livers were prepared for use in staining procedures. A 7μm thick hematoxylin and eosin (H&E) stained section through the center of the eye containing the pupil, optic nerve, and maximum thickness of the melanoma was utilized for determining intraocular tumor size (n=4). Three 7μm thick H&E stained sections through the centers of the livers of each mouse (n=5) were used to determine metastatic melanoma size and frequency per previous protocols (Yang *et al.* 2004). Unstained sections were used for histochemical and immunohistochemical staining. Eye and liver sections were obtained from the same set of mice.

Metastasis size and frequency assays

Formalin-fixed paraffin-embedded slides were stained with hematoxylin and eosin (H&E) and viewed using an Olympus DP-12 microscope (Tokyo, Japan). Three liver sections per mouse were measured, with five mice per genotype. The sizes of all metastases from a single liver section were summed to produce a total metastasis area value in μm^2 and this value was averaged across three sections per mouse. The total liver size was also measured, creating a ratio of metastasis size per liver size for normalization. Wild-type mouse metastasis area was set to 1.0 for comparison. Metastatic frequency was calculated by totaling the number of metastases of all sizes and normalizing by liver area. Additionally, the metastases were separated by size, where micrometastases have a diameter of less than $50\mu m^2$, intermediate metastases have a diameter of $50\text{-}200\mu m^2$, and macrometastases

have a diameter greater than 200μm^2, with sizes slightly different from the categorization in humans. These data are reported as a ratio per liver area, and all measurements were performed in triplicate sections that represented the liver as a whole (n=5).

Staining assays

Mean vascular density was determined through use of H&E staining or periodic acid-Schiff staining without hematoxylin. A cross section of a lumen lined with endothelial cells counted as one blood vessel, while tracts and branches were counted as separate vessels. The number of blood vessels per area was determined for both metastatic tissue and surrounding liver tissue (n=5) (Foss *et al.* 1996). HSCs were visualized by smooth muscle actin (SMA) immunostaining (Mako M0851, 1:160) and analyzed by ImageJ (Version 1.45s, National Institutes of Health, Bethesda, MD) on a scale of 0:black to 255:white. In order to estimate tumor stromal component, reticulin staining was performed for type III collagen within the metastases (n=5). Fibers were manually traced and quantified by ImageJ.

Statistical analysis

Comparison of the three groups (PEDF+/+, PEDF+/-, and PEDF-/- mice) for all assays was performed using one-way analysis of variance (ANOVA) with the Newman-Keuls post-test to determine statistical significance among pairs. When

comparing metastasis types among three groups, a two-way ANOVA with a Bonferroni post-test was utilized. We defined $p<0.05$ as denoting statistical significance for all assays and reported data with standard error of the mean. An unpaired t-test was used to analyze densitometry of the western blot.

2.4—RESULTS

Mouse model of uveal melanoma

To establish our mouse model of PEDF deficiency, we measured PEDF mRNA and protein levels in the livers of PEDF+/+ and PEDF-/- mice. PEDF+/+ mice express PEDF mRNA in the liver, whereas PEDF mRNA is absent from PEDF-/- mouse liver (**Figure 8**). Cycle threshold was reached after 21.7 cycles in PEDF+/+ mice and 33.7 cycles in PEDF-/- mice. Liver PEDF protein in PEDF+/+ and PEDF-/- mice was assayed by immunohistochemistry (**Figure 9a**) and western blot (**Figures 9b and 9c**). Both assays demonstrated an abundance of PEDF protein in the livers of PEDF+/+ mice but not in livers of PEDF-/- mice. B16-LS9 melanoma cells express PEDF in culture as expected (**Figure 10**). The eyes collected at day 7 showed that primary tumors were of equivalent size regardless of PEDF genotype (**Figure 11**). Thus we conclude that this is an appropriate model with which to study the role of liver-produced PEDF on UM metastasis.

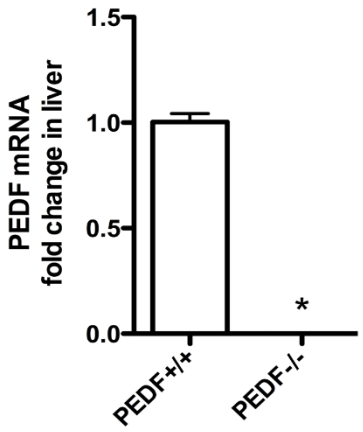

Figure 8 **PEDF mRNA is present in PEDF+/+ mice but absent in PEDF-/- mice.** Quantitative real-time PCR performed on mRNA collected from liver of PEDF+/+ versus PEDF-/- mice demonstrated that PEDF mRNA is present in PEDF+/+ mice but absent in PEDF-/- mice. PEDF+/+ mice exhibited cycle threshold values of 21.7, while PEDF-/- mice showed cycle threshold values of 33.7. Data are reported with standard error of the mean, n=4, *$p<0.05$ using one-way ANOVA with Newman-Keuls post-test

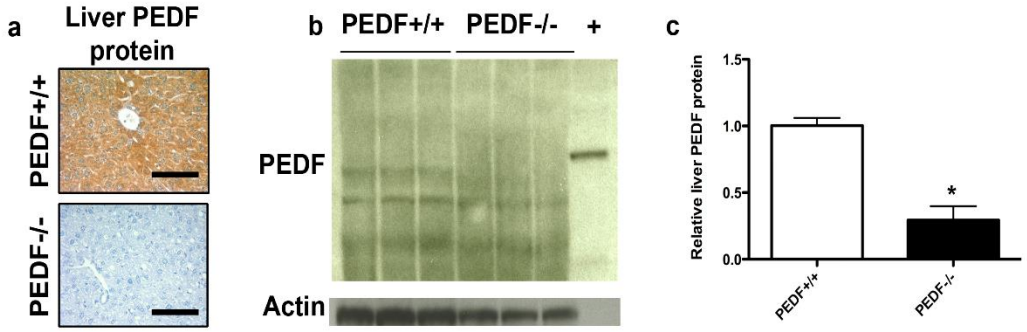

Figure 9 **PEDF protein is present in PEDF+/+ mice but is absent in PEDF-/- mice.** a) Immunohistochemical staining for PEDF protein in the livers of PEDF+/+ and PEDF-/- mice reveal the abundant expression of PEDF in PEDF+/+ mouse liver (n=3) and the absence of PEDF protein in PEDF-/- mouse liver (n=3). Black bar = 50μm. b) Western blot assay of 200μg liver lysate revealed a band between 50-75 kDa in PEDF+/+ mice (n=3) that was absent from PEDF-/- mice (n=3) which correlated with 4ng positive control recombinant PEDF protein. Actin was used as a loading control (Millipore MAB1501, 1/5000). c) Densitometry quantification of the western blot revealed that the PEDF band seen in PEDF+/+ liver lysate was significant. Data are reported with standard error of the mean, n=3, $p^*<0.05$ using unpaired t-test

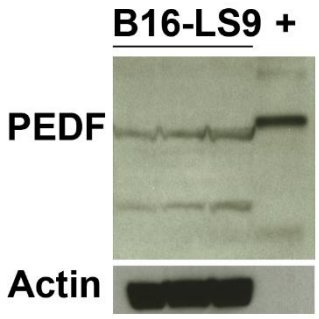

Figure 10 **B16-LS9 cells express PEDF protein.** Western blot assay of 50μg B16-LS9 cell culture lysate revealed the presence of PEDF protein as indicated by a band between 50-75 kDa which correlated with 4ng positive control recombinant PEDF protein. An additional, unknown band was detected around 25 kDa. Actin was used as a loading control

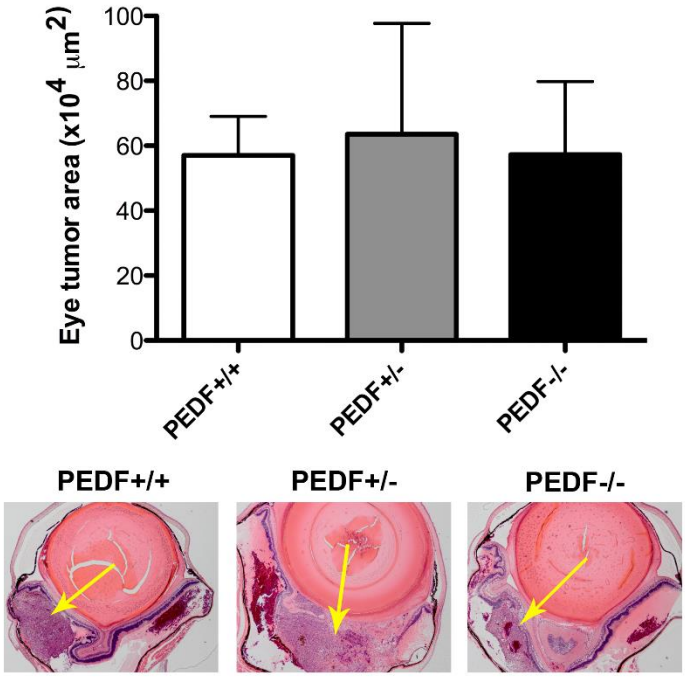

Figure 11 **Eye tumor size is not a function of mouse PEDF genotype.** PEDF+/+, PEDF+/-, and PEDF-/- mice were injected with B16-LS9 cells into the posterior compartment of the right eye. One week after injection, the right eye was enucleated, sectioned, and stained by H&E. Three sections were averaged per mouse and reported as total eye tumor area. H&E images of eye tumor from PEDF+/+, PEDF+/-, and PEDF-/- mice show the equivalence in primary tumor size across genotypes. A yellow arrow highlights the primary tumor located in the posterior compartment of the eye. No statistical difference was found between each genotype of mouse. Eye and liver sections were obtained from the same set of mice. Data are reported with standard error of the mean, n=4, *$p<0.05$ using one-way ANOVA with Newman-Keuls post-test

Metastasis size and frequency

PEDF+/- mice exhibited a 7.1 fold increase in metastasis area per liver section than PEDF+/+ mice, and PEDF-/- mice showed a 34.6 fold increase, both significantly greater than wild-type (**Figure 12**). There was no statistical difference in the total number of metastases per liver section across the three genotypes (**Figure 13a**). However, wild-type mouse livers contained predominantly micrometastases, PEDF+/- mice contained more intermediate metastases and several macrometastases, and PEDF-/- mice contained significantly more macrometastases than either wild-type or PEDF+/- mice (**Figure 13b**). These data clearly demonstrate that the loss of host PEDF leads to a significant increase in the size of the metastatic tumor.

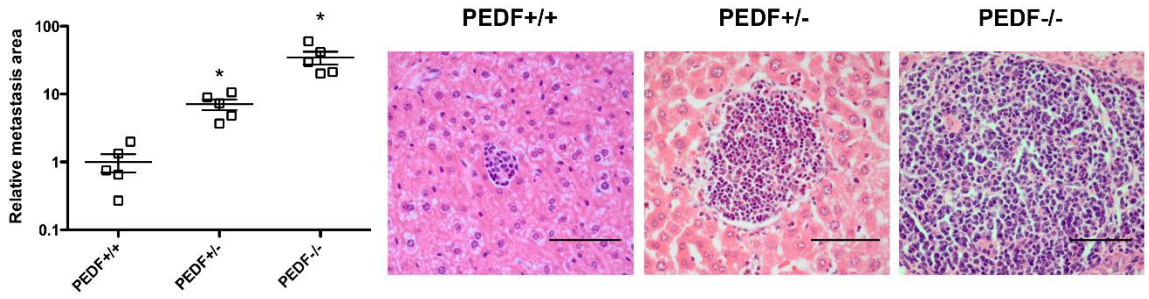

Figure 12 **Host PEDF inhibits total area of liver metastasis in a model of uveal melanoma.** PEDF+/+, PEDF+/-, and PEDF-/- mice were injected with B16-LS9 cells into the posterior compartment of the right eye and allowed to metastasize over one month. Total area of metastasis coverage was measured and normalized to the total area of the liver and reported as a relative value with wild-type set to 1. Values were displayed on a scatter plot with a $\log_{10}$ scale where each box represents the averaged values of one mouse, the long bar represents the mean, and the smaller bars represent standard error of the mean, n=5, *$p<0.05$ using one-way ANOVA with Newman-Keuls post-test. PEDF+/- mice experienced a 7.1 fold increase in the area of liver metastasis over wild-type, and PEDF-/- mice experienced a 34.6 fold increase. Representative H&E images show metastases from PEDF+/+, PEDF+/-, and PEDF-/- mice. Eye and liver sections were obtained from the same set of mice. Black bar = 50μm

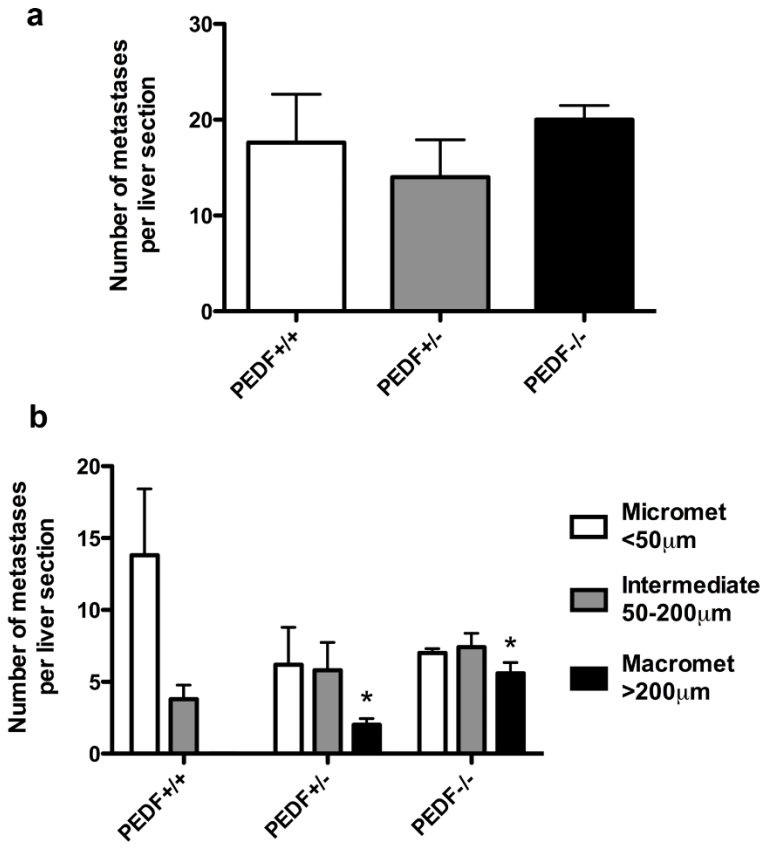

Figure 13 **The number of metastases is not a function of mouse PEDF genotype, but the number of macrometastases (diameter >200μm) increases in the absence of PEDF.** a) Total count of metastases per liver section was tallied without respect to the size of each metastasis. No statistical difference was found across mouse PEDF genotypes. Data are reported with standard error of the mean, n=5, *p<0.05 using one-way ANOVA with Newman-Keuls post-test. b) The size of each individual liver metastasis from PEDF+/+, PEDF+/-, and PEDF-/- mice was measured and categorized as a micromet (diameter <50μm), an intermediate met (diameter 50-200μm), or a macromet

(diameter greater than 200μm). PEDF+/+ mouse livers contained no macrometastases, while PEDF+/- and PEDF-/- mouse livers contained a progressively greater number of macrometastases. Data are reported with standard error of the mean, n=5, *$p<0.05$ using two-way ANOVA with Bonferroni post-test

Angiogenesis: mean vascular density

PEDF+/- mice showed a 7.3 fold increase in mean vascular density (MVD), or blood vessels per 40x high-powered field of magnification (40HPF), versus PEDF+/+ controls, and the MVD of PEDF-/- mice was 20.8 fold greater than wild-type, both significantly greater ($p<0.05$) (**Figure 14**). Additionally, both PEDF-/- and PEDF+/- mice had significantly greater MVD in metastases than surrounding liver tissue, while WT mice did not. MVD of non-metastatic liver tissue was equivalent across the three genotypes. These findings corroborate a well-known function of PEDF, suggesting that PEDF may inhibit angiogenesis, or the formation of new blood vessels, in the metastases in mouse liver, but not vasculogenesis, or the formation of blood vessels during embryonic development. However, increased vascular density is a common result of metastatic progression, thus the relationship to loss of host PEDF may only be indirect.

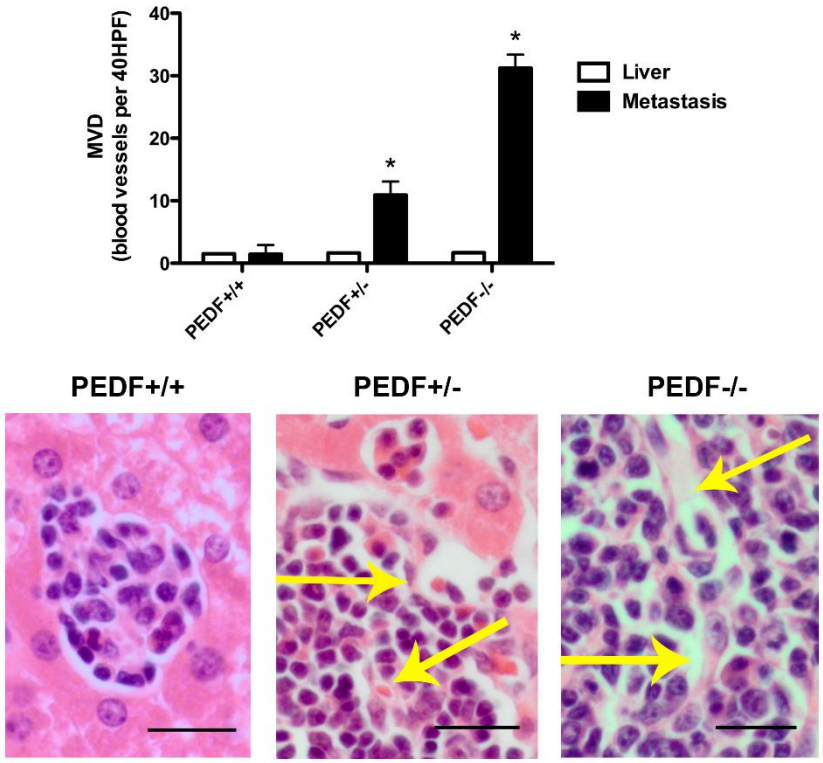

Figure 14 **Loss of PEDF is accompanied by greater vascular density within metastases.** The number of blood vessels was calculated per area for each metastasis and the surrounding liver tissue and extrapolated over a full 40x high-powered field of magnification (40HPF). PEDF+/- mice had a 7.3 fold increase in the mean vascular density over wild-type mice. PEDF-/- mice showed a 20.8 fold increase in mean vascular density over wild-type mice. MVD was significantly greater within metastases than in surrounding liver tissue in both PEDF+/- and PEDF-/- mice. PEDF did not affect the MVD of surrounding liver tissue across genotypes. Metastasis and liver tissue were stained using periodic acid-Schiff without hematoxylin in order to view and count blood vessels, and shown in H&E for visual purposes. Yellow arrows point to some but not all vascular channels.

Black bar = 20μm. Data are reported with standard error of the mean, n=5, *p<0.05 using one-way ANOVA with Newman-Keuls post-test

Stromagenesis: hepatic stellate cell and type III collagen immunohistochemistry

A trend toward greater activated HSC density was found only in PEDF-/- mice but not PEDF+/- mice; however, this was not significantly different among the three groups (**Figure 15**). There was however significantly less type III collagen, a marker for basement membrane production, in PEDF+/+ mice versus both PEDF+/- and PEDF-/- mice (**Figure 16**). Type III collagen was not seen in micrometastases but was prevalent in both intermediate and macrometastases. These data suggest that HSCs are activated in micrometastases even in the presence of PEDF, and only slightly more so in the absence of PEDF, but that their production of extracellular matrix is delayed until at least the intermediate metastasis phase.

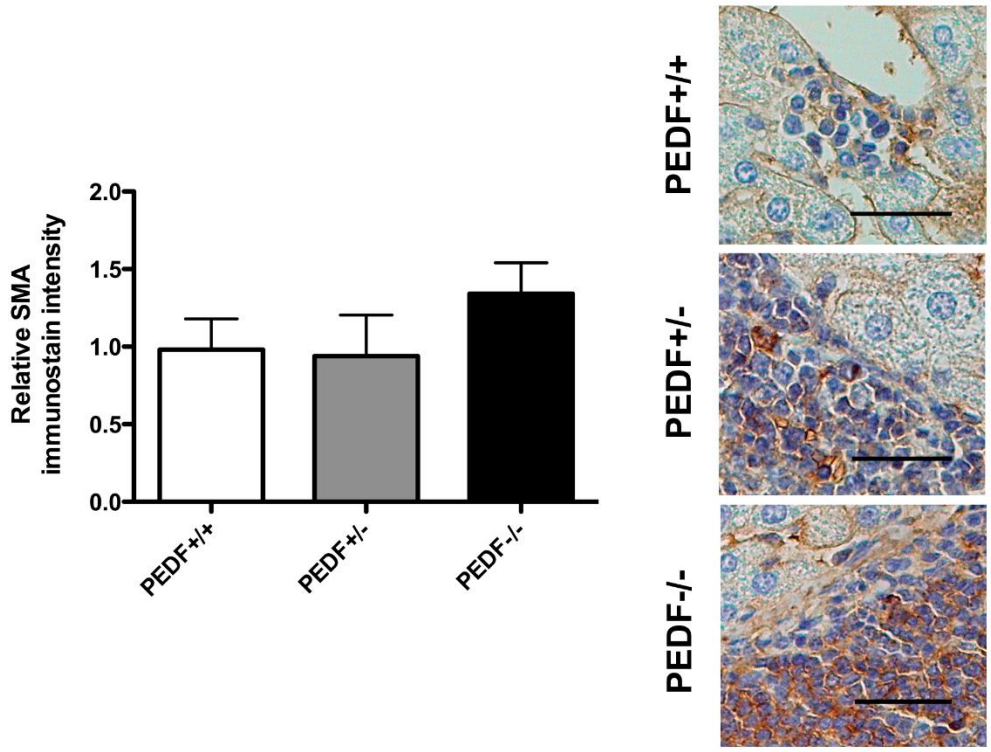

Figure 15 **Activated hepatic stellate cells were slightly more abundant in the absence of PEDF.** Smooth muscle actin (SMA) immunostain intensity, a marker for activated hepatic stellate cells (HSCs), was only slightly greater in PEDF-/- metastases versus PEDF+/- and PEDF-/-, although the trend was not significant. Livers were stained with an SMA antibody to view the abundance of activated HSCs within the metastases, and no statistical difference was seen across genotypes. Representative images show SMA immunohistochemistry (brown) in PEDF+/+, PEDF+/-, and PEDF-/- mice. Black bar = 25μm. Data are reported with standard error of the mean, n=5, *$p<0.05$ using one-way ANOVA with Newman-Keuls post-test

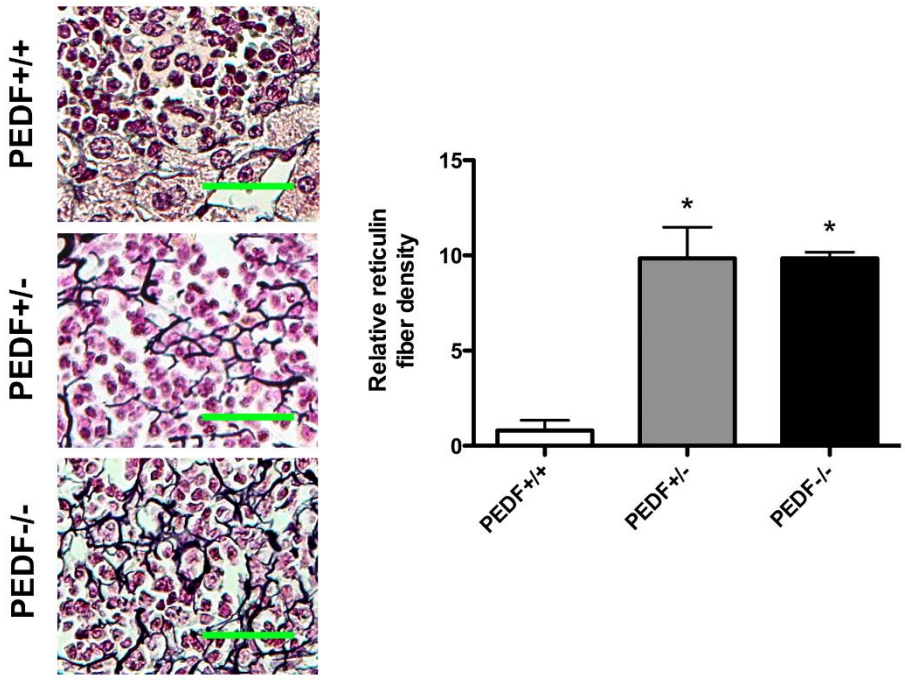

Figure 16 **Type III collagen, a stromal protein produced by hepatic stellate cells, was increased as host PEDF was lost.** Reticulin stains were performed on PEDF+/+, PEDF+/-, and PEDF-/- mouse livers in order to analyze type III collagen production. Both PEDF+/- and PEDF-/- mice showed significantly greater reticulin fiber density. Representative images show reticulin fiber staining (dark purple) in PEDF+/+, PEDF+/-, and PEDF-/- mice. Fibers were traced and their lengths were summed to calculate reticulin fiber density. Green bar = 25μm. Data are reported with standard error of the mean, n=5, *$p<0.05$ using one-way ANOVA with Newman-Keuls post-test

2.5—DISCUSSION

Stephen Paget proposed the *seed and soil* hypothesis in the late 1800s to explain why given forms of cancer are able to thrive in certain end organs (Paget 1889). He suggested that each type of cancer, the seed, is only able to metastasize to organs that resemble its original microenvironment, the soil. By this reasoning, the end organ must be expressing factors that potentiate or suppress the growth of the metastasizing cancer cells. Indeed, key mediators of angiogenesis such as vascular endothelial growth factor (VEGF) and hypoxia-inducible factors (HIFs) are involved in end organ angiogenesis and growth of metastatic cancer (Folkman 2002, Quintero *et al.* 2004, Crosby *et al.* 2011). Now we have shown that pigment epithelium-derived factor (PEDF) is also an important factor produced by the host that suppresses metastatic progression, and loss of PEDF is accompanied by an increase in angiogenesis and stromagenesis within the metastases.

PEDF produced and secreted by hepatocytes is thought to suppress metastasis in two ways. By interrupting the VEGF signaling cascade and inducing apoptosis in endothelial cells, PEDF suppresses the angiogenesis necessary for metastatic progression. By disrupting the cytoskeleton of HSCs and inducing their apoptosis, PEDF inhibits stromagenesis. In a hypothetical model, in healthy hepatic tissue the PEDF-VEGF ratio favors PEDF. VEGF is not being produced by tumor cells or HSCs, endothelial cell growth is not being recruited, and MMP-2 and MMP-9 are not being produced by melanoma cells or endothelial cells to degrade PEDF. However in the metastatic microenvironment, as the metastasis grows, it becomes

hypoxic. VEGF and MMPs are produced, leading to the downregulation of PEDF and the unimpeded formation of stroma and growth of blood vessels. This process of breaking down the balance between PEDF and hypoxia appears to occur over several years. However, in PEDF-/- mice, the PEDF-VEGF balance is lost, stromagenesis and angiogenesis are potentiated, and this hypothetically leads to enlargement of the metastases over the span of one month.

We used B16-LS9 melanoma cells, which metastasize from the eye to the liver, in our model. Despite the production of PEDF by B16-LS9 cells in the tumor microenvironment, our data clearly demonstrate that metastatic progression is increased when host-produced PEDF is knocked out. This effect is due to the increased presence of macrometastases of 200μm diameter or more. We have shown when host PEDF is lost the mean vascular density rises significantly, but only in metastatic tissue and not in liver tissue. This suggests that PEDF may play role in angiogenesis during metastasis but not vasculogenesis during development. Furthermore, we found that activated HSC density was slightly increased in PEDF-null mice, but this result was not statistically significant. This suggests that HSCs are activated at an early point in metastatic progression and only slightly responsive to PEDF *in vivo*. However, type III collagen normally produced by activated HSCs followed an interesting pattern where both copies of the PEDF gene must be present to prevent HSCs from producing massive amounts of stroma, and this is worthy of further inspection. The increased vascular density and type III collagen production may simply be a result of metastatic progression and thus only

indirectly related to loss of host PEDF. PEDF+/+ contain mostly micrometastases and low-end intermediate metastases, thus we are unable to accurately compare vascular density and type III collagen production in large metastases across the three genotypes.

We envision a two-step mechanism for the progression of UM metastasis involving first the activation of HSCs and production of stroma as a scaffold for blood vessel and tumor growth, followed by the induction of angiogenesis to feed the metastasis with nutrients and oxygen. Our data suggest that host PEDF inhibits metastatic progression via both of these mechanisms. Further investigation needs to be done regarding the role of fatty liver in the progression of metastasis, as PEDF-null mice have increased liver steatosis, and this may be another mechanism regulating metastasis size.

In conclusion, host-produced PEDF clearly has a distinct role in preventing the progression of liver metastases in a mouse model of UM. This is an excellent model to study UM, as the mice develop micrometastases, intermediate metastases, and macrometastases similar to patients with metastatic disease. These findings suggest that host-produced PEDF may be a therapeutic target for patients with metastatic UM.

Chapter 3:

Further Investigation of Angiogenesis in our Mouse Model of Metastatic Uveal Melanoma

Key questions to be addressed in this section:

1. How does metastatic uveal melanoma angiogenesis in PEDF null mice compare to wild type mice?
2. Does PEDF affect the number of immature vascular channels in intermediate mets?
3. Does PEDF affect the density of mature endothelial cells as revealed by CD31 immunohistochemistry?
4. Does PEDF affect the density of immature endothelial cells as revealed by CD105 immunohistochemistry?
5. Does PEDF affect the percentage of metastases displaying a portal pattern of growth versus the lobular pattern?
6. Does PEDF affect vascularization of the primary eye tumor? Could this explain the larger metastasis area in the PEDF null animals despite the evidence that the number of metastases are equivalent across genotypes?

3.1—Further Characterization of Angiogenesis: Rationale and Hypothesis

One of the primary findings of the published article in Chapter 2 was that loss of PEDF correlates with a greater vascular density within the metastases. However, this increase in vascular density is expected when metastases grow larger, such as they do in the PEDF null mice, thus it is difficult to establish a cause and effect relationship between PEDF and vascular density.

PEDF wild type mice did not form any macromets, but they do develop intermediate mets. The intermediate met (50-200μm diameter) represents a transitionary phase between micromets (<50μm diameter) and macromets (>200μm diameter). Thus, if I examine the vascularity of the intermediate metastases across the three genotypes, I may obtain information regarding the role of PEDF in angiogenesis in our mouse model of uveal melanoma. Three methods of counting angiogenesis in these intermediate metastases include visual inspection of H&E stained slides, CD31 (PECAM-1) immunostaining for mature endothelial cells, and CD105 (endoglin) immunostaining for immature endothelial cells, since metastases may contain both mature and immature blood vessels along with individual endothelial cells.

An observation was made during the counting of all metastases that the loss of PEDF correlated with a portal pattern of metastatic growth. This pattern consists

of melanoma cells collecting around the portal venule of the hepatic lobule in contrast to the lobular pattern of growth where cells collect in the interior of the lobule commonly seen in wild type metastases. I plan to quantify this finding and discuss its implications.

Lastly, it is possible that individual micrometastatic colonies in close proximity to one another may combine with one another to form a single macromet. If this occurs, the number of metastases would be reduced while the size of metastasis area increases. This must be considered when we reported that the number of metastases across the three genotypes is equivalent. Thus it is possible that more cells did in fact escape the primary tumor in PEDF null mice due to increased vascularization and later combined to form fewer, larger metastases in the liver. This could be a potential explanation for the increased number of large metastases we observed in PEDF het and null mice. In order to investigate this idea, I will examine the vascular density in the primary tumors in the eye.

I hypothesize that the intermediate metastases in wild type mice contain significantly fewer blood vessels than in the PEDF het and PEDF null mice.

I hypothesize that wild type mice will display a lobular pattern of metastatic growth while PEDF hets and PEDF null display a portal pattern of growth.

I hypothesize that the primary tumor in the eye of PEDF null mice has a greater vascular density that that of wild type mice.

3.2—Further Characterization of Angiogenesis: Methods

In order to investigate the blood vessel density of intermediate metastases in PEDF wild type, het, and null mice, I used 3 previously stained H&E sections from (n=5) mice for each of the 3 genotypes. An equal number of intermediate metastasis were analyzed across the 3 genotypes, and blood vessel density was determined by three methods. 1) I determined blood vessel count by visual inspection of H&E stained slides. 2) I performed immunohistochemistry (IHC) using anti-CD31 (Mako M0823, 1:180 dilution), a marker for mature endothelial cells also known as PECAM-1, with healthy liver tissue as a positive control. 3) I performed IHC using anti-CD105 (Santa Cruz, sc-20632, 1:50 dilution), a marker for immature endothelial cells also known as endoglin. The positive control for CD105 was mouse kidney tubules. CD31 immunohistochemistry was analyzed using ImageJ software (Version 1.39u, National Institutes of Health, Bethesda, MD), on a scale of 0:black to 255:white. CD105 immunohistochemistry was analyzed by visibly counting positively staining cell populations. To calculate statistical significance of $p<0.05$, one-way ANOVA was performed, with the Newman-Keuls post-test to determine statistical significance among pairs.

To determine the pattern of metastatic growth, I examined the H&E stained slides described previously and identified the location of portal venules. I recorded each metastasis—micromet, intermediate, and macromet—across 3 slides in (n=5) animals for each of the 3 genotypes, counting a metastasis as a portal pattern metastasis only if it is connected to the portal venule, while all other metastases

were located within the parenchyma of the hepatic lobule and considered to be lobular pattern metastases. To calculate statistical significance of $p<0.05$, one-way ANOVA was performed, with the Newman-Keuls post-test to determine statistical significance among pairs.

To determine the vascular density of primary eye tumors in PEDF wild type, het, and null animals, I used 3 slides across (n=4) animals for each of the 3 genotypes. Slides were previously H&E stained, and the number of blood vessels were counted by visual inspection. To calculate statistical significance of $p<0.05$, one-way ANOVA was performed, with the Newman-Keuls post-test to determine statistical significance among pairs.

3.3—Further Characterization of Angiogenesis: Results

Intermediate metastases, as defined by a diameter between 50 and 200 μm in mouse, exhibited a very low vascular density compared to macrometastases across all three genotypes, as expected. PEDF wild type mice average approximately 0.6 blood vessels per intermediate met, while PEDF hets average approximately 1.8, and PEDF nulls average about 2.7 (**Figure 17**). Intermediate metastases were all of similar size, and 3 were counted per mouse liver, or 9 per genotype, due to the limited number of intermediate metastases in the wild type mice. CD31 immunostaining in intermediate metastases revealed a significantly greater density of mature endothelial cells in PEDF null mice (**Figures 18a and 18b**). CD31 stained uniformly throughout the metastases. While this may suggest a uniform population of endothelial cells within the metastases, the CD31 antibody may also be cross-reacting with melanoma. CD31-positive channels were not distinguishable within the metastases but were abundant in the surrounding liver tissue.

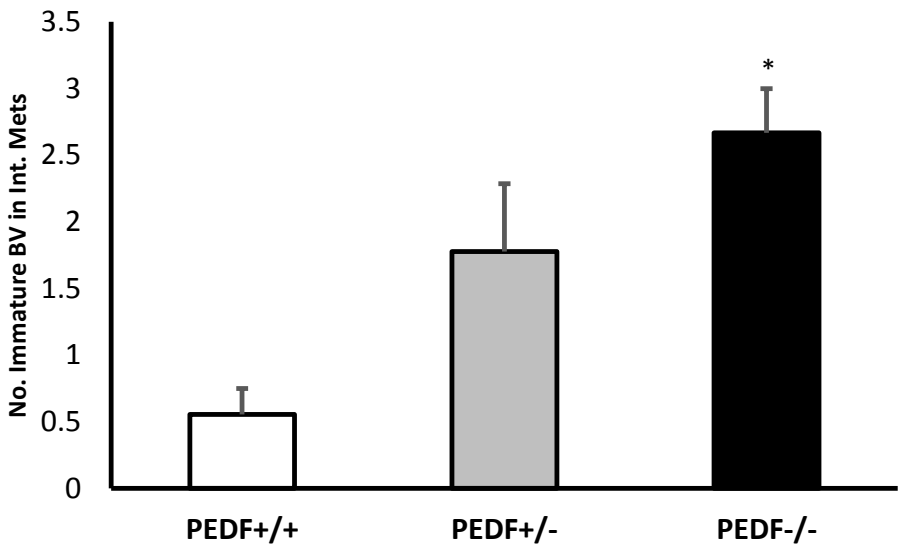

Fig. 17 **Host PEDF correlates with a lower number of blood vessels within intermediate metastases.** The number of immature blood vessels was counted in H&E stained slides and visible inspection of intermediate metastases. PEDF-/- mice exhibited a significantly greater number of immature blood vessels within the metastases versus PEDF+/+ controls. Data are reported with standard error of the mean, n=5, *$p<0.05$ using one-way ANOVA with Newman-Keuls post-test

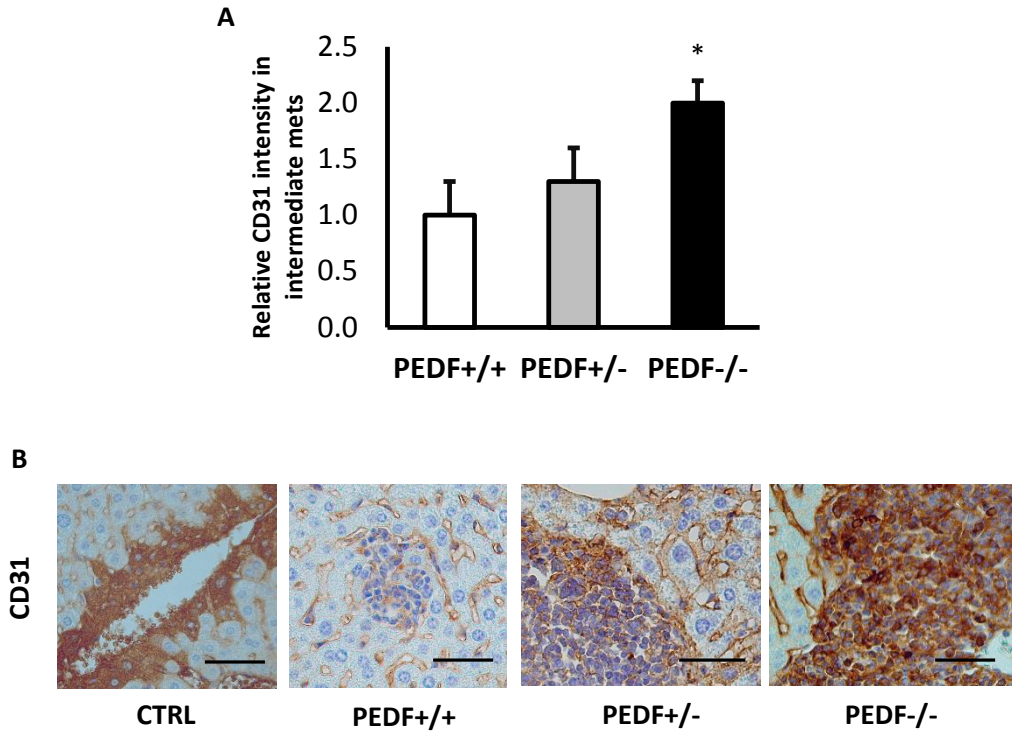

Fig. 18 **Host PEDF inhibits CD31 immunostain intensity, a marker for mature vascular endothelial cells, within intermediate metastases.** CD31 (PECAM-1) was measured within intermediate metastases in PEDF+/+, PEDF+/-, and PEDF-/- mice. **A)** PEDF null mice displayed a significantly greater expression of CD31. **B)** CD31 expression was found to be uniform throughout individual metastases, suggesting potential cross-reactivity with melanoma cells. Black bar = 20μm. Data are reported with standard error of the mean, n=5, *$p<0.05$ using one-way ANOVA with Newman-Keuls post-test

Meanwhile, CD105 immunostaining revealed a significant population of immature endothelial cells within PEDF het and null intermediate mets compared with wild type controls (**Figures 19a and 19c**). CD105 specifically measured individual cells, thus individual cells were counted and reported. CD105-positive channels were found within the intermediate metastases of both PEDF hets and null mice (**Figure 19b**).

The portal pattern of growth was much less common in the PEDF wild types, with 44% of metastases exhibiting a portal pattern in PEDF wild types versus about 80% of metastases exhibiting a portal pattern in PEDF hets and nulls (**Figure 20**). Conversely, 56% of PEDF wild type metastases demonstrated the lobular pattern of growth, while about 20% did so in the PEDF hets and nulls.

Lastly, I tested the hypothesis that the primary eye tumor in PEDF null mice had a greater vascular density than in PEDF wild types or hets. However, I found that there was no significant difference between the three genotypes, nor was there a trend, suggesting that the vascular density was equivalent in the eyes and the propensity for intravasation was similar (**Figure 21**).

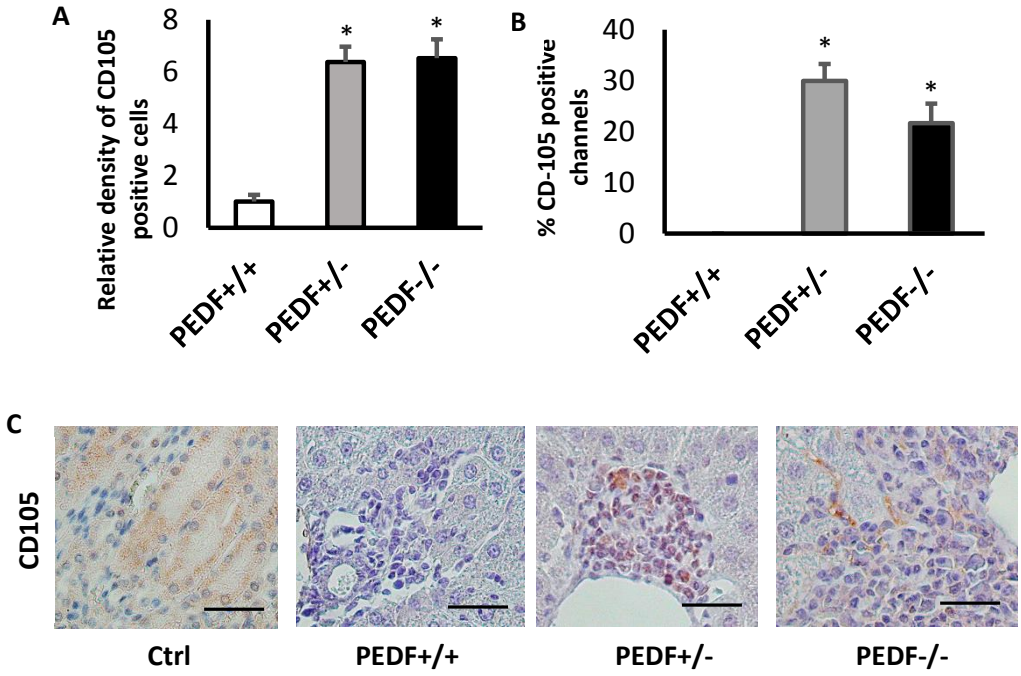

Fig. 19 **Host PEDF inhibits CD105 immunostain intensity, a marker for immature vascular endothelial cells, within intermediate metastases.** PEDF wild type mice showed **A)** a significantly lower population of CD105 positive cells within intermediate mets and **B)** a complete lack of CD105 positive vascular-like channels compared to PEDF hets and nulls. C) Control tissue (mouse kidney) stained positively for CD105, while PEDF+/- and PEDF-/- intermediate metastases showed individual cells staining CD105 positive in contrast to the more uniform CD31 staining seen previously. Black bar = 20μm. Data are reported with standard error of the mean, n=5, *$p<0.05$ using one-way ANOVA with Newman-Keuls post-test

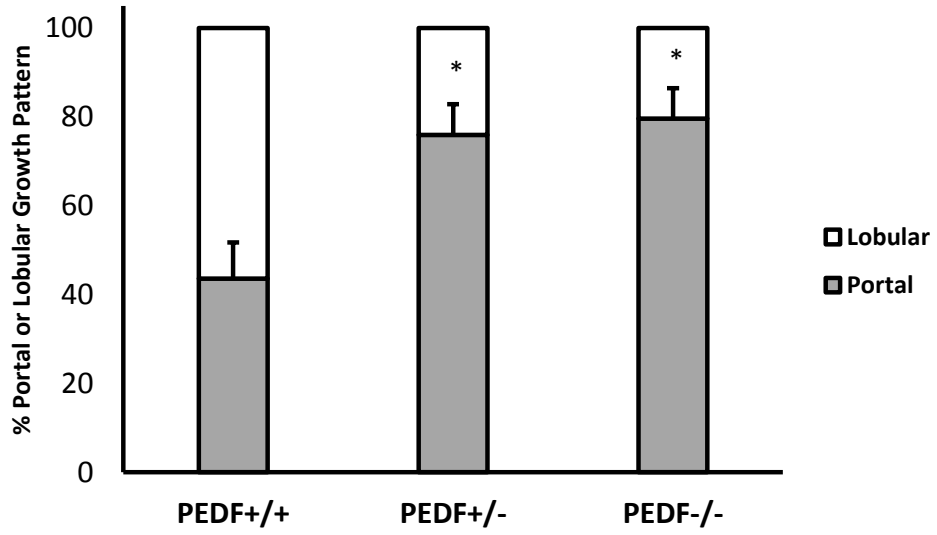

Fig. 20 **Host PEDF correlates with a lower percentage of portal pattern metastasis growth.** Metastases are either portal pattern (growing next to hepatic portal venules) or lobular pattern (growing in the parenchyma of the hepatic lobule). The percentage of portal pattern metastases is significantly lower in PEDF+/+ versus PEDF+/- and PEDF-/- mice. These data include micromets, intermediate, and macromets. Data are reported with standard error of the mean, n=5, *$p<0.05$ using one-way ANOVA with Newman-Keuls post-test

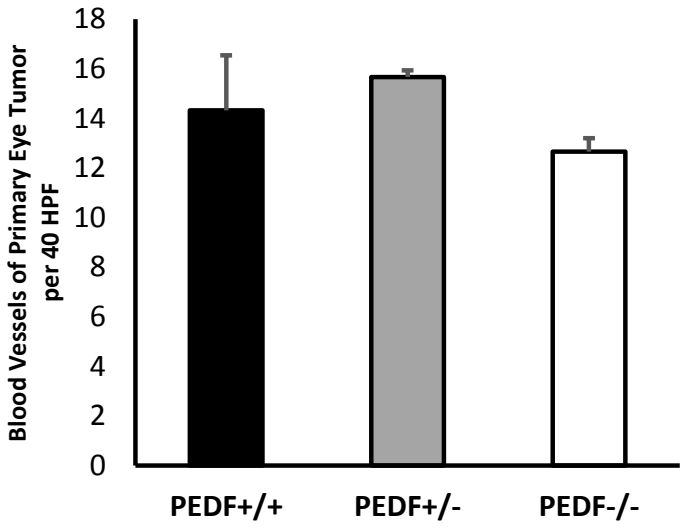

Fig. 21 **Host PEDF does not affect vascular density of the primary eye melanoma.** Vascular density of the primary eye tumor was measured by H&E staining and visible inspection. No significant difference was seen across the three genotypes. Data are reported with standard error of the mean, n=4, *p<0.05 using one-way ANOVA with Newman-Keuls post-test

The intermediate metastasis phase in wild type mice has significantly fewer blood vessels than in the PEDF het and PEDF null mice.

Wild type mice display a lobular pattern of metastatic growth while PEDF hets and PEDF null display a portal pattern of growth.

The primary tumor in the eye of PEDF null mice does not exhibit greater vascular density that that of wild type mice.

3.4—Further Characterization of Angiogenesis: Discussion

Here I have reported that the vascular density of intermediate metastases is increased in PEDF het and null mice versus wild types. This finding helps to separate and explicitly implicate PEDF as a primary factor in inhibiting angiogenesis in our mouse model of uveal melanoma. The increased vascular density of macrometastases only found in PEDF hets and nulls was no longer a factor, and the critique of the vascular density data in Chapter 2 has been addressed. Furthermore, the intermediate metastasis represents a transition between micromet and macromet. PEDF is shown here to have a specific role in transitioning metastases from avascular to vascular, thus contributing to the angiogenic switch.

Vasculogenic mimicry in metastatic melanoma is the formation of vascular channels within the tumor that are lined by CD-31 negative cells that are presumably melanoma. The presence of CD31 uniformly throughout the metastasis, but not at the edges of blood vessels, leads us to conclude that CD31 is cross-reacting with another cell type. CD31 is, in fact, expressed at times by melanoma cells where it regulates melanoma-melanoma and melanoma-endothelial cell contact (Lutzky *et al.* 2006). CD31 was not found to line the vascular channels in these intermediate mets. I hypothesized that those same tubes are CD105-positive (immature endothelium). CD105, however, did line a portion of the blood vessels in PEDF het and null mice. Still, some blood vessels were both

CD-31 negative and CD105-negative, leaving open the possibility that these are melanoma cells undergoing vasculogenic mimicry.

The finding that PEDF het and null mice exhibit primarily a portal pattern of growth suggests that PEDF plays a role in the localization of micrometastatic seeds once they reach the liver. Why this occurs is still unknown, given that the vascular density of the primary eye tumor is unaffected by PEDF and my hypothesis was thereby unsupported. This finding may explain why the metastases are considerably larger in PEDF null mice. Portal pattern metastases have a local supply of oxygenated blood in the form of the hepatic arteriole. Meanwhile, the lobular pattern metastases seen predominantly in wild type mice obtain their blood supply through the sinusoidal spaces. The lobular pattern of growth develops over a more prolonged period of time (Grossniklaus, unpublished). Thus in the 4 weeks that the mice are allowed to metastasize, the portal pattern mets would be expected to experience rapid growth compared to lobular pattern mets. In humans, metastasis is drawn out over the course of many years, and the lobular pattern is more common (Grossniklaus, unpublished).

The finding that intermediate metastases exhibited greater vascular density in PEDF null mice versus controls supported the hypothesis that PEDF regulates metastatic progression through inhibition of angiogenesis. The finding that PEDF het and null mice display a portal pattern of metastatic growth, while wild type mice display a lobular pattern of growth, may partially explain why metastases grow more rapidly in PEDF het and null mice.

Chapter 4:

Effects of Fatty Liver on Metastasis Progression

Key questions to be addressed in this section:

1. Is fatty liver responsible for the increased metastatic progression I see in the PEDF null mice?
2. Do mice on a high fat diet (60% calories from fat) exhibit liver steatosis?
3. Are these mice significantly overweight?
4. Do mice on a high fat diet develop more metastases or larger metastases compared to mice on a control diet (10% calories from fat)?

4.1—Fatty Liver & Metastasis: Rationale and Hypothesis

There are several possible explanations to explain why the PEDF null mice develop considerably larger liver metastases than control mice. Two possible explanations examined earlier were increased angiogenesis and enhanced stromagenesis in the PEDF nulls. Another possible explanation has to do with a third, lesser studied, function of PEDF—lipid hydrolysis. PEDF promotes the breakdown of triglycerides in the lipid droplets of hepatocytes. Without PEDF present, as in the PEDF null mice, lipid hydrolysis slows and triglycerides build up in the hepatocytes. PEDF null mice experience fatty liver, called steatosis, where lipid droplets are overloaded, and these mice often exhibit obesity. Since the liver is the primary site for uveal melanoma metastasis, I hypothesize that a lipid-loaded liver may be a factor in the increased metastatic progression of PEDF null mice. Lipid loaded hepatocytes have been shown to upregulate pro-tumorigenic factors that activate hepatic stellate cells, the cells responsible for providing cytokines and scaffolding that promote endothelial cell and metastatic uveal melanoma cell growth. In order to determine if a fatty liver promotes metastasis, I administered a high fat versus control diet to 3 month old C57BL/6 mice for 6 weeks before and after injection of melanoma cells into the eye and evaluated the number and size of metastases.

I hypothesize that a fatty liver promotes increased metastatic progression versus a non-fatty liver.

4.2—Fatty Liver & Metastasis: Methods

All experiments were performed in conduct with the Association for Research in Vision and Ophthalmology (ARVO) Statement for the Use of Animals in Ophthalmic and Visual Research and with Institutional Animal Care and Use Committee (IACUC) policies and procedures.

Three month old C57BL/6 wild type mice were fed a high fat diet (TestDiet 58Y1, DIO Rodent Purified Diet w/60% kcal from fat – blue) (n=12) versus a control diet (TestDiet, 58Y0, DIO Rodent Purified Diet w/10% kcal from fat – yellow) (n=12) (**Figure 22**). These mice were on their respective diets for 6 weeks prior to melanoma injection, designated weeks -6 to week 0, and regularly observed for signs of disease. Mice were ear tagged and weighed weekly. Data on mouse weights are reported as grams per week with standard error of the mean, and statistical analysis was performed by two-way ANOVA with a Bonferroni post-test, $p<0.05$. At week 0, all 24 mice were injected with $1.5x10^5/1.5\mu L$ B16-LS9 mouse cutaneous melanoma cells suspended in phosphate buffer solution. At week 1, all 24 mice were enucleated to ensure that melanoma growth did not overburden and escape the eye. At week 4, designated as endpoint 1 and representing the standard endpoint in our mouse model of uveal melanoma, half of the mice were euthanized humanely in a carbon dioxide chamber, and livers were immediately collected. At week 6, designated as endpoint 2 and representing a maximum endpoint in our model, the remaining mice were euthanized and livers were collected in the same manner.

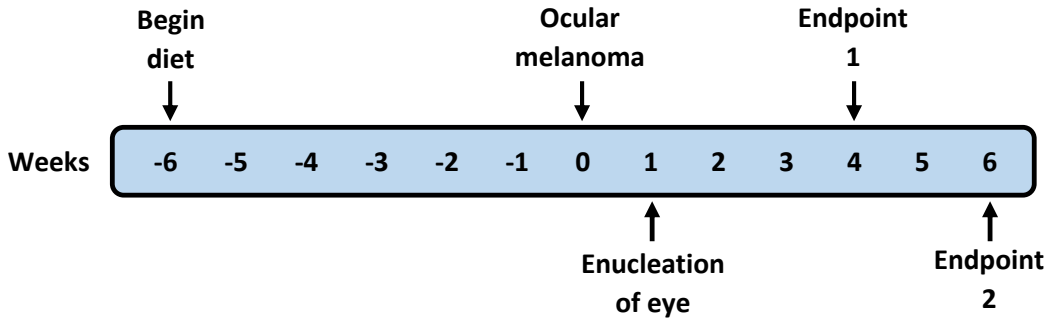

Figure 22 **Timeline of high fat or control diet in a mouse model of uveal melanoma.** Three month old C57BL/6 mice were fed either a high fat (60% calories from fat, n=12) or control diet (10% calories from fat, n=12) at t= -6 weeks. At t= 0 weeks, mice were injected with B16-LS9 mouse melanoma cells into their right eyes. The right eyes were enucleated at t= 1 week in order to prevent spread of tumor beyond the eye. At that point, metastasis had already occurred. Metastases were allowed to grow for 4 (endpoint 1, n=6) or 6 weeks (endpoint 2, n=6), at which time mice were euthanized. Mice were monitored daily and weighed weekly

Lipid droplet content (n=12) was determined by examination of H&E stained slides. Each lipid droplet stood out as a white spherical shape within the hepatocyte cytoplasm, and this was easily distinguished from irregularly-shaped white space due to artifactual tearing. Lipid droplets were measured by area, summed, and normalized to control diet = 1. Data on lipid droplet content are reported as relative lipid droplet area with standard error of the mean, and statistical analysis was performed by one-way ANOVA with a Newman-Keuls post-test, $p<0.05$.

Liver metastasis was measured by examination of H&E stained slides. Three liver sections per mouse were analyzed, with a total of 6 mice taken to week 4 and 6 mice taken to week 6 per diet. The metastases were tallied and subcategorized by size, where micrometastases have a diameter of less than 50μm^2, intermediate metastases have a diameter of 50-200μm^2, and macrometastases have a diameter greater than 200μm^2. Data on metastasis size are reported as number of metastases of each size category, with standard error of the mean, and statistical analysis was performed by two-way ANOVA with a Bonferroni post-test, $p<0.05$.

4.3—Fatty Liver & Metastasis: Results

Mice that consumed the high fat pellets became significantly heavier than their littermates on a control diet after only 2 weeks (**Figure 23**). Their body weights continued to increase linearly until week 0, which coincided with the injection of melanoma into their eyes, at which point the weight gain stopped and their weights generally stabilized. However, some mice continued to gain weight, while other mice, even those on the high fat diet, began to lose weight after melanoma injection, and this is evident in the increasing standard error bars in the later weeks of the assay. The livers of the mice were in fact steatotic, as evidenced by the increase lipid droplet area in the mice on a high fat diet (**Figure 24**). However, the mice on the high fat diet had no significant difference in the size distribution of liver metastases at weeks 4 or 6, nor was there a trend of any kind (**Figures 25a and 25b**).

My hypothesis that a fatty liver promotes metastatic progression was not supported. Thus the mechanism by which PEDF inhibited metastatic progression in the previous chapters is not due to fatty liver in these mice.

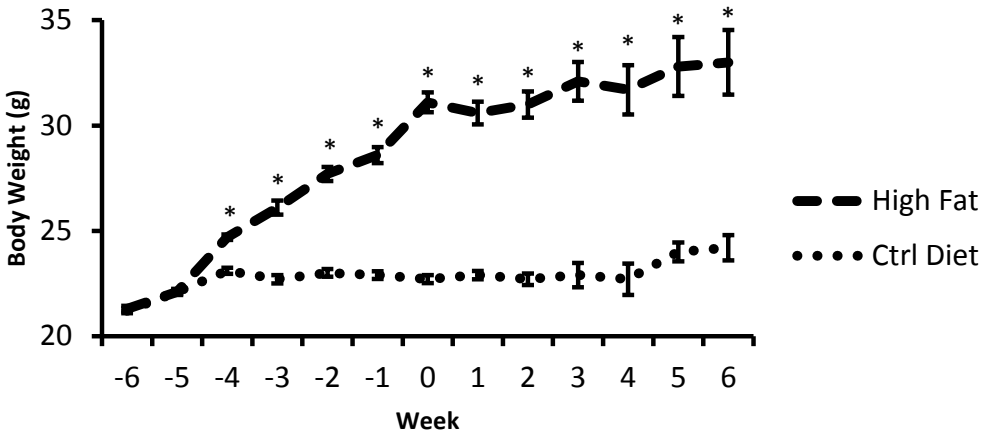

Fig. 23 **High fat diet, began at week -6, significantly increases mouse body weight after 2 weeks.** High fat (60% calories from fat, bold dashed line) and control diets (10% calories from fat, dotted line) were started at week -6. Mice were weighed weekly for 12 weeks. High fat mice were significantly heavier by week -4. Melanoma injection occurred at week 0 at which point the weight gain ceased. At week 1, mice were enucleated to prevent the spread of melanoma cells outside the eye. At week 4, half of the mice were euthanized for examination, and the other half were euthanized by week 6. Data are reported with standard error of the mean, n=12, *$p<0.05$ using two-way ANOVA with Bonferroni post-test

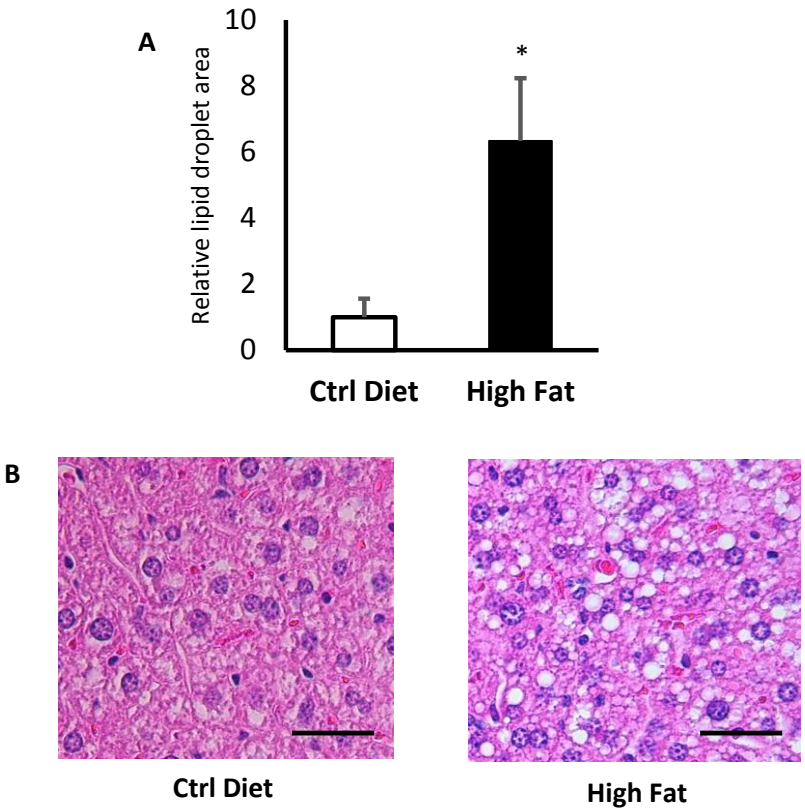

Fig. 24 **High fat diet significantly increases mouse hepatocyte lipid droplet content.** Mice were placed on a high fat diet for 4-6 weeks versus a control diet. Liver sections were collected and H&E stained. Lipid droplet area was measured and set relative to control=1. **A)** Mice on a high fat diet showed significantly greater lipid droplet area versus mice on a control diet. **B)** Lipid droplets appear as white spheres within the hepatocytes, and were distinguished from irregularly shaped artifact tearing. Black bar = 40μm. Data are reported with standard error of the mean, n=12, *$p<0.05$ using one-way ANOVA with Newman-Keuls post-test

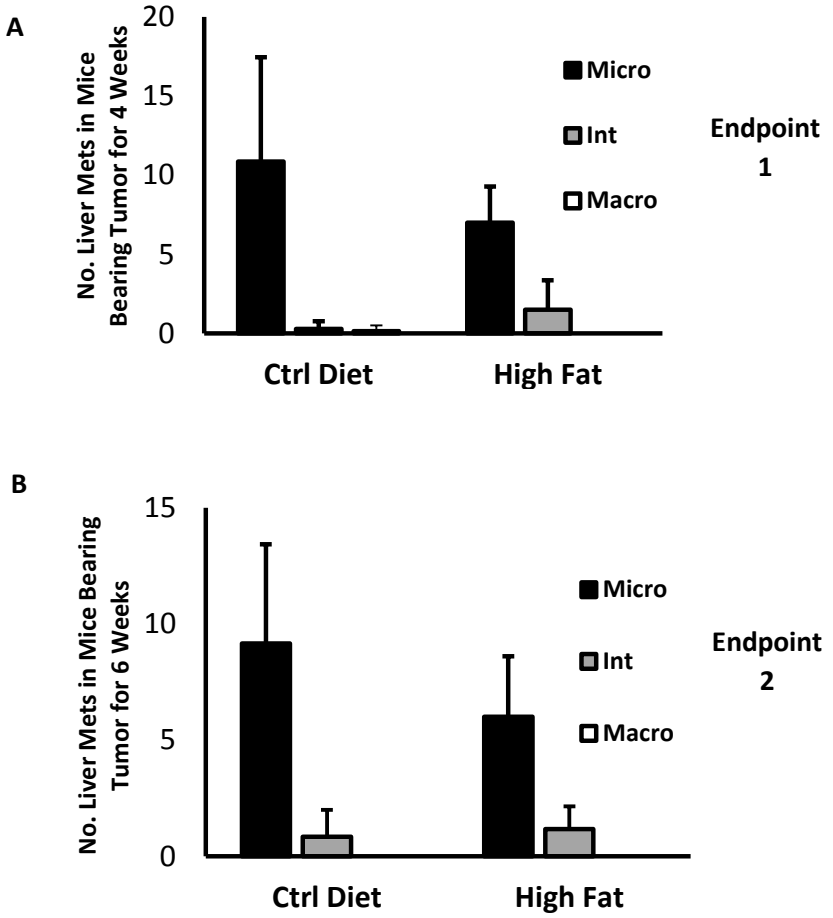

Fig. 25 **High fat diet does not increase the number or size of liver metastases in a mouse model of uveal melanoma.** Mice were placed on a high fat or control diet for 6 weeks prior to injection of melanoma in the eye, and maintained on this diet for **A)** 4 weeks (Endpoint 1) or **B)** 6 weeks (Endpoint 2). Livers were sectioned and stained with H&E. The number of metastases were counted and categorized as either micromets (micro, diameter <50μm^2), intermediate mets (int, diameter 50μm^2 to 200μm^2), or macromets (macro, diameter >200μm^2). After both 4 and 6 weeks of tumor bearing, the number and

size of liver metastasis was unaffected by a high fat diet. Data are reported with standard error of the mean, n=6 at 4 weeks and n=6 at 6 weeks

4.4—Fatty Liver & Metastasis: Discussion

My method for producing obese wild type C57BL/6 mice with fatty livers was successful, although my hypothesis was disproved. Fatty liver does not appear to be a factor that promotes liver metastasis in our mouse model of uveal melanoma, at least in the 4 to 6 week timeframe that our mouse model allows. These data do not support that lipid hydrolysis is a factor in uveal melanoma metastasis progression, but these experiments do not rule out the possibility of a joint contribution of PEDF loss and fatty liver contributing together to increase metastatic growth. PEDF KO mice used in the previous studies may have a different lipid composition than mice on a high fat diet, and this is a limitation of the current study. However, attention should be focused on the role of PEDF in inhibiting angiogenesis as a potential therapy for halting uveal melanoma metastasis progression in the liver, as supported by the first two studies in this dissertation.

Chapter 5:

Summary and Conclusions

5.1—Summary of Results

I have reported a novel finding that PEDF produced by the host liver inhibits metastatic progression in a mouse model of ocular melanoma. I used control C57BL/6 mice, along with mice that lacked one or both copies of PEDF, called PEDF hets and PEDF nulls respectively. I confirmed that PEDF wild type mice expressed PEDF mRNA and protein in the liver, but PEDF mRNA and protein were absent in the nulls. While PEDF did not affect the size or vascularity of the primary eye tumor, PEDF did indeed inhibit the size of the metastases in the liver. Specifically, the number of macromets in the PEDF nulls was elevated. Although the frequency of metastasis remained unaffected by PEDF.

In searching for the mechanism by which PEDF inhibited metastatic progression, I investigated angiogenesis, stromagenesis, and lipid hydrolysis, three of the main functions of PEDF with regard to metastasis. Vascular density was markedly increased in PEDF null metastases versus control, and the vascular density of healthy liver tissue was unaffected, thus serving as an internal control. Intermediate metastases, the largest size of metastasis displayed in all three genotypes, contained a greater number of immature blood vessels within PEDF null mice versus controls. This strengthens the hypothesis that PEDF regulates the transition between micromet and macromet by inhibiting angiogenesis as part of the angiogenic switch. PEDF null mice showed an increase in CD31 (mature endothelial marker) and CD105 (immature endothelial marker), although CD31 was thought to cross-react with melanoma cells. CD105, however, labeled individual immature endothelial cells within the intermediate metastases and

demonstrated that loss of PEDF correlates with an increase in immature endothelial cell density in the mets. This is important because previous studies only examined mature endothelial cells using anti-CD31 antibodies. The majority of PEDF null metastases were adjacent to portal venules, exhibiting a portal pattern of growth, whereas in wild type mice, the majority of mets exhibited a lobular pattern.

Hepatic stellate cells, which are responsible for stromagenesis and are normally inhibited by PEDF, were not found to be statistically increased in number in the PEDF null mice. However, the production of collagen fibers, which are produced in the liver by the hepatic stellate cell, was greatly elevated in PEDF hets and nulls.

Despite the fact that PEDF null mice develop a fatty liver that stresses hepatocytes and hepatic stellate cells and leads to the production of pro-stromagenic and pro-tumorigenic factors, fatty liver alone is insufficient to promote metastatic progression in our model.

5.2—Discussion of Results

The significance of this work is that I have demonstrated that the liver itself suppresses the growth of metastasis through PEDF, a protein native to the liver. This finding suggests that if host PEDF can be exploited, it may provide a route for therapy for patients who are at risk for developing hepatic metastases from uveal melanoma. In typical macrometastases, hypoxia upregulates VEGF, tipping the angiogenic switch in favor of angiogenesis. Hypoxia also upregulates MMPs which, in turn, degrade PEDF. Thus, I expect that PEDF will be absent, or present in low quantities, in fully formed macrometastases. However, prediction or early diagnosis of the metastatic disease may allow sufficient time for intervention and for PEDF to prevent progression of micrometastases to vascularized macrometastases.

I have shown that PEDF regulation of progression of liver metastasis in our mouse model of uveal melanoma functions through a mechanism involving angiogenesis. This was demonstrated by the increase in the number of vascular channels within the intermediate metastases of the PEDF null mice versus controls. The portal pattern of growth that I see in the PEDF nulls suggests that some unknown mechanism is regulating the localization of the micromet seeds, and once there, the PEDF null mets have access to oxygen and nutrients that expedite their growth in our uveal melanoma metastasis model. My data regarding the role of PEDF in regulating stromagenesis in the metastases indicated that PEDF suppresses hepatic stellate cell production of collagen type III, thus preventing a scaffold for

tumor progression. Lastly, I excluded fatty liver as a mechanism by which PEDF regulates metastatic progression in our model.

There are two patterns of metastatic growth—portal pattern and lobular pattern (**Figure 26**). In the portal pattern of growth found near portal triads, the tumor effaces or pushes back healthy cells such as hepatocytes. These metastases undergo angiogenesis, rapid expansion, and are inhibited by PEDF. The lobular pattern of growth found in the parenchyma of the hepatic lobule is a slower pattern of growth where melanoma cells replace hepatocytes entirely. This pattern is more common in nude mice, thus the immune cells found predominantly in the sinusoidal space are likely responsible for inhibition of lobular pattern growth (Grossniklaus, unpublished).

My hypothetical model of the two microniches of metastatic uveal melanoma growth in the liver is based on our findings (**Figure 27**). I hypothesize that uveal melanoma cells arrive in the liver via the portal venule from the spleen or the hepatic arteriole from the aorta. The cells arriving from the portal venule have less fluid force, thus they situate near the portal triad under the space of Mall. The space of Mall is an expandable space between portal triad endothelium and hepatocytes, and it is evident in the histological slides that melanoma cells accumulate in this space. The space between sinusoidal endothelium and hepatocytes is referred to as the space of Disse, although it is unclear from the histology whether melanoma cells reside there. The metastases growing in the space of Mall become angiogenic and stromagenic while they push or efface nearby tissue. My findings suggest that

PEDF may regulate whether these metastases grow larger. Meanwhile, cells arriving from the hepatic arteriole have greater fluid force and may accumulate further from the portal triad, within the sinusoidal spaces. The metastases growing in these spaces are possibly regulated by immune cells or other factors unrelated to PEDF.

In the clinic, a patient who presents with eye discomfort, vision loss, or is evaluated for a routine check-up, may be diagnosed with uveal melanoma, a life-threatening condition. In the event that this happens, the procedures to treat the primary tumor in the eye are very effective—radiation therapy, or in some cases, enucleation. However, these patients may have clinically undetectable micrometastases that may progress within 2 to 5 years. Gene expression profiling of the primary tumor is currently available to determine whether the melanoma is likely to have metastasized, despite the fact that micrometastases are undetectable. If a patient is determined to be a likely candidate for metastasis, current treatment options are limited. I hope this work provides a foundation for clinical trials involving PEDF and its potential to slow the progression of the micrometastases that have already occurred in many of these patients. Clinical trials may include gene therapy, targeting of inhibitors or activators of PEDF, or drugs that influence the expression or function of PEDF.

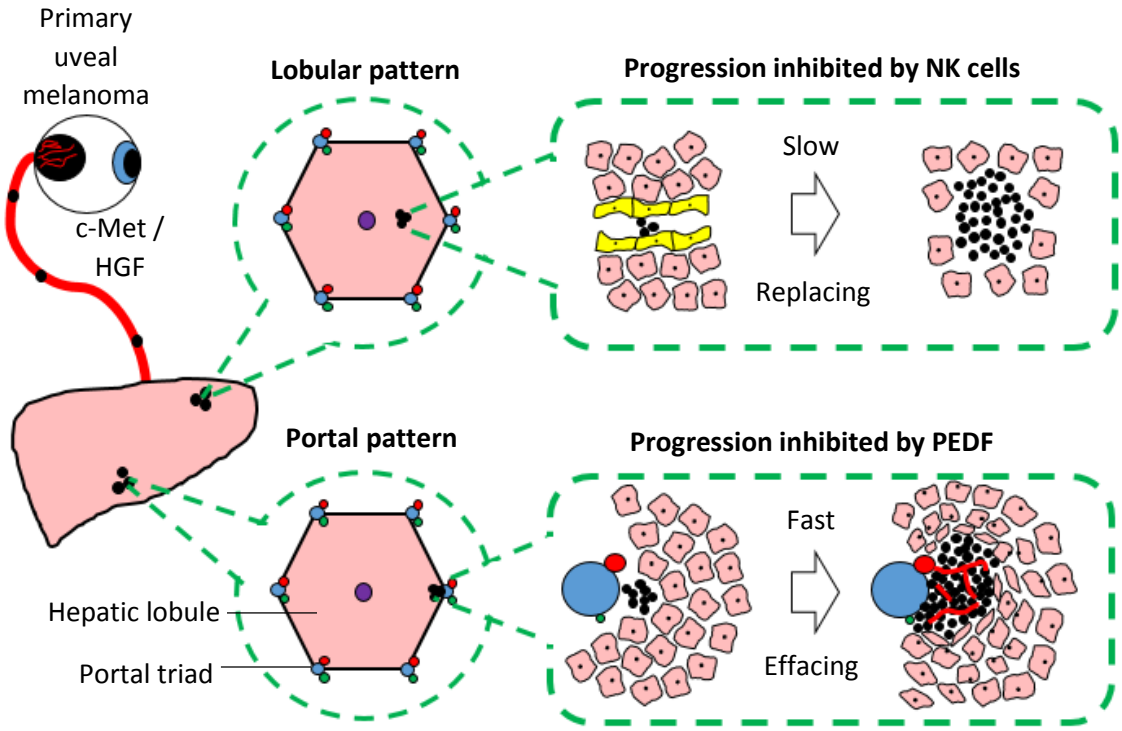

Fig. 26 **Model of the two patterns of metastatic growth in the liver.** Uveal melanoma cells (black) originating from the primary tumor in the eye travel through the circulatory system (red line). These cells are targeted to the liver due to a high level of c-Met expression, a surface receptor that binds HGF produced by the liver. Once melanoma cells reach the liver, we observe two patterns of metastatic growth depending on the location of melanoma cells within the *hepatic lobule* (hexagon). The *lobular pattern* begins with melanoma cells that are lodged in the sinusoidal spaces within the parenchyma of the hepatic lobule. These metastases grow slowly, and they replace nearby healthy tissue such as hepatocytes (pink) and sinusoidal endothelium (yellow). The *portal pattern* begins with melanoma cells that reside near the *portal triad* (portal venule, blue circle; hepatic

arteriole, red circle; and bile duct, green circle). These metastases grow more rapidly, exhibit increased vascularization, and efface nearby healthy cells such as hepatocytes. In our model, PEDF null mice have increased portal pattern growth and vascular density, suggesting PEDF inhibits this type of growth. The lobular pattern of growth is more common in immune compromised mice, suggesting that immune cells such as natural killer (NK) cells normally found in the sinusoidal spaces are responsible for inhibiting the lobular pattern of growth

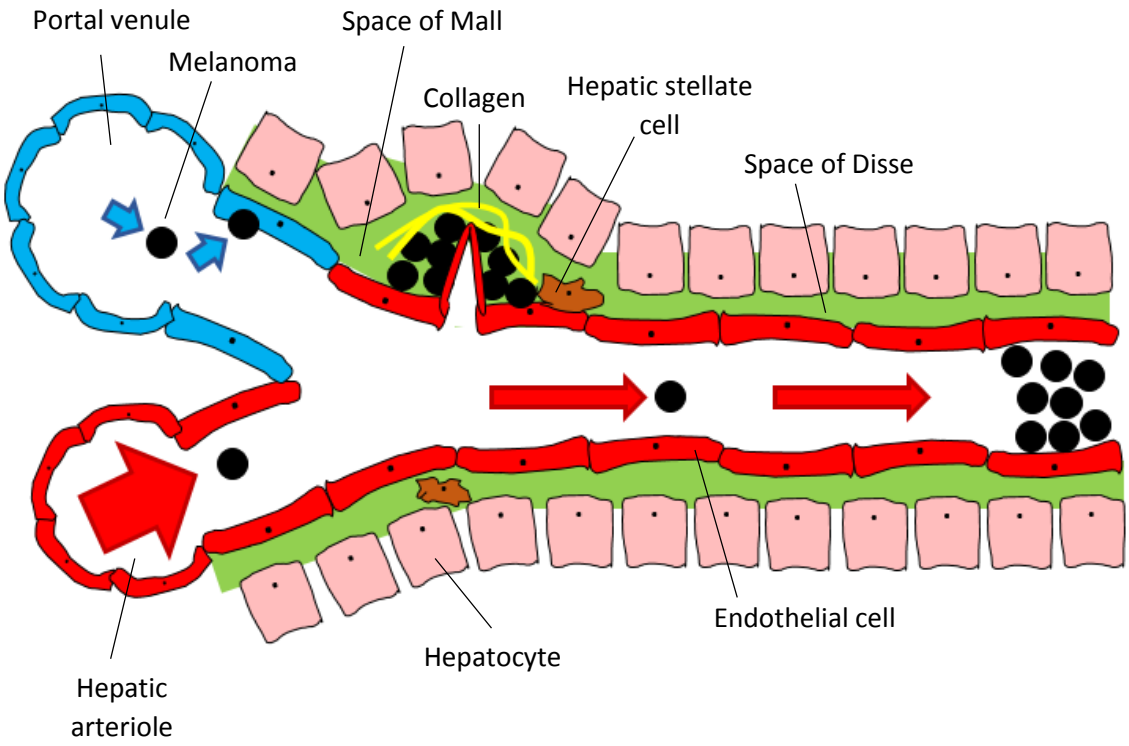

Fig. 27 **Hypothetical microniches of metastatic uveal melanoma in the liver.** I hypothesize that uveal melanoma cells arrive in the liver microniche via the portal venule or hepatic arteriole. Melanoma (black cells) arriving through the portal venule (blue arrows) experience less fluid force and accumulate near the portal triad in the space of Mall, an expandable space between endothelium (red cells) and hepatocytes (pink cells). In this microniche, metastases may encounter hepatic stellate cells (brown) and become angiogenic and stromagenic as they push or efface nearby tissue. PEDF regulates the size of metastases growing in this microniche. Cells arriving through the hepatic arteriole (red arrows) would experience greater fluid force and accumulate in the sinusoidal space. The space between sinusoidal endothelium and hepatocytes is the space of Disse, but metastases growing in this microniche grow within the sinusoidal space itself.

These metastases are likely regulated by immune cells or other factors unrelated to PEDF

5.3—Future Directions

There are several questions that remain regarding the role of PEDF in inhibiting metastatic uveal melanoma in the liver. First, it must be noted that our PEDF null mouse model provides an excellent and rapid way to examine macrometastases that would otherwise not be easily studied in wild type mice. Gene expression of many related factors such as MMPs, VEGF, additional growth factors, transcription factors, and cell surface proteins can be studied within the metastases by using laser-capture microdissection. MMPs are of special interest due to their capability to degrade PEDF, especially under hypoxic conditions. If MMPs are inhibited, PEDF function may be increased. These macrometastases also provide an excellent chance to perform electron microscopy and closely examine the three dimensional structure of metastatic microenvironment.

One drawback of this method is that I used cutaneous melanoma cells. No uveal melanoma cells of mouse origin are currently available. If mouse uveal melanoma cells become available, it would be prudent to obtain them and use them in our model to determine if the findings I see are reproducible using uveal melanoma cells rather than cutaneous melanoma cells.

Several other mechanisms need further inspection. One is the portal versus lobular pattern of growth. I do not know what causes this portal pattern in the PEDF null

mice, but it is also observed in patients (Grossniklaus, unpublished). A predominantly lobular pattern of growth was recently observed using the same protocol in nude mice injected with human uveal melanoma cell line Mel-290 (Grossniklaus, unpublished). It would be of interest to determine the similarities and differences between our two models that may affect growth patterns. One potential hypothesis is that anti-angiogenic molecules such as PEDF are responsible for inhibiting the portal pattern of growth while natural killer cells normally found in the sinusoidal space of the liver are responsible for inhibiting the lobular pattern of growth. This novel hypothesis that the liver microenvironment is responsible for metastatic growth patterns would explain why PEDF null mice exhibit a portal pattern while nude mice exhibit a lobular pattern.

Another set of mechanisms that have not been fully inspected in this model are proliferation and apoptosis. Since PEDF null mice have the same number of metastases but much larger metastases, we hypothesize that the cells are undergoing increased cell division or decreased apoptosis. This event may begin prior to angiogenesis. While the role of PEDF in apoptosis is known, it would be beneficial to find out the role of PEDF in regulating cell proliferation in these cells.

5.4—Conclusion

I have found that PEDF, a protein produced by the host liver and secreted into the liver microenvironment, inhibits the progression of metastasis in a mouse model of uveal melanoma. The loss of PEDF causes an increase in: 1) the percentage of metastases found adjacent to the portal triad (portal pattern), 2) vascularity in the intermediate metastasis phase, 3) production of collagen type III with a trend toward greater hepatic stellate cell density, both of which support the growth and invasion of tumor cells and endothelial cells, and 4) the total number of macrometastases. Overall, PEDF protects the host from the rapid expansion of portal pattern metastases. Thus, PEDF is a strong candidate for targeted therapy for metastasis of uveal melanoma.

REFERENCES

Abdel-Rahman, M. H., C. M. Cebulla, V. Verma, B. N. Christopher, W. E. Carson, 3rd, T. Olencki and F. H. Davidorf (2012). "Monosomy 3 status of uveal melanoma metastases is associated with rapidly progressive tumors and short survival." Exp Eye Res **100**: 26-31.

Al-Nedawi, K., B. Meehan, R. S. Kerbel, A. C. Allison and J. Rak (2009). "Endothelial expression of autocrine VEGF upon the uptake of tumor-derived microvesicles containing oncogenic EGFR." Proc Natl Acad Sci U S A **106**(10): 3794-3799.

Albert, D. (1998). "Histopathologic characteristics of uveal melanomas in eyes enucleated from the Collaborative Ocular Melanoma Study. COMS report no. 6." Am J Ophthalmol **125**(6): 745-766.

Albert, D. M., L. M. Ryan and E. C. Borden (1996). "Metastatic ocular and cutaneous melanoma: a comparison of patient characteristics and prognosis." Arch Ophthalmol **114**(1): 107-108.

Alessandri, G., M. Girelli, G. Taccagni, A. Colombo, R. Nicosia, A. Caruso, M. Baronio, S. Pagano, L. Cova and E. Parati (2001). "Human vasculogenesis ex vivo: embryonal aorta as a tool for isolation of endothelial cell progenitors." Lab Invest **81**(6): 875-885.

Allavena, P., A. Sica, G. Solinas, C. Porta and A. Mantovani (2008). "The inflammatory micro-environment in tumor progression: the role of tumor-associated macrophages." Crit Rev Oncol Hematol **66**(1): 1-9.

Anguissola, S., W. J. McCormack, M. A. Morrin, W. J. Higgins, D. M. Fox and D. M. Worrall (2011). "Pigment epithelium-derived factor (PEDF) interacts with transportin SR2, and active nuclear import is facilitated by a novel nuclear localization motif." PLoS One **6**(10): e26234.

Antoine, M., W. Wirz, C. G. Tag, A. M. Gressner, M. Marvituna, M. Wycislo, C. Hellerbrand and P. Kiefer (2007). "Expression and function of fibroblast growth factor (FGF) 9 in hepatic stellate cells and its role in toxic liver injury." Biochem Biophys Res Commun **361**(2): 335-341.

Baenziger, N. L., G. N. Brodie and P. W. Majerus (1971). "A thrombin-sensitive protein of human platelet membranes." Proc Natl Acad Sci U S A **68**(1): 240-243.

Bakalian, S., J. C. Marshall, P. Logan, D. Faingold, S. Maloney, S. Di Cesare, C. Martins, B. F. Fernandes and M. N. Burnier, Jr. (2008). "Molecular pathways mediating liver metastasis in patients with uveal melanoma." Clin Cancer Res **14**(4): 951-956.

Barak, V., S. Frenkel, K. Valyi-Nagy, L. Leach, M. A. Apushkin, A. Y. Lin, I. Kalickman, N. A. Baumann, J. Pe'er, A. J. Maniotis and R. Folberg (2007). "Using the direct-injection model of early uveal melanoma hepatic metastasis to identify TPS as a potentially useful serum biomarker." Invest Ophthalmol Vis Sci **48**(10): 4399-4402.

Beacham, D. A. and E. Cukierman (2005). "Stromagenesis: the changing face of fibroblastic microenvironments during tumor progression." Semin Cancer Biol **15**(5): 329-341.

Becerra, S. P., A. Sagasti, P. Spinella and V. Notario (1995). "Pigment epithelium-derived factor behaves like a noninhibitory serpin. Neurotrophic activity does not require the serpin reactive loop." J Biol Chem **270**(43): 25992-25999.

Bergers, G., R. Brekken, G. McMahon, T. H. Vu, T. Itoh, K. Tamaki, K. Tanzawa, P. Thorpe, S. Itohara, Z. Werb and D. Hanahan (2000). "Matrix metalloproteinase-9 triggers the angiogenic switch during carcinogenesis." Nat Cell Biol **2**(10): 737-744.

Bernard, A., J. Gao-Li, C. A. Franco, T. Bouceba, A. Huet and Z. Li (2009). "Laminin receptor involvement in the anti-angiogenic activity of pigment epithelium-derived factor." J Biol Chem **284**(16): 10480-10490.

Bilzer, M., F. Roggel and A. L. Gerbes (2006). "Role of Kupffer cells in host defense and liver disease." Liver Int **26**(10): 1175-1186.

Bingle, L., N. J. Brown and C. E. Lewis (2002). "The role of tumour-associated macrophages in tumour progression: implications for new anticancer therapies." J Pathol **196**(3): 254-265.

Blanco, P. L., L. A. Lim, C. Miyamoto and M. N. Burnier (2012). "Uveal melanoma dormancy: an acceptable clinical endpoint?" Melanoma Res **22**(5): 334-340.

Bouck, N. (2002). "PEDF: anti-angiogenic guardian of ocular function." Trends Mol Med **8**(7): 330-334.

Broaddus, E., A. Topham and A. D. Singh (2009). "Incidence of retinoblastoma in the USA: 1975-2004." Br J Ophthalmol **93**(1): 21-23.

Broaddus, E., A. Topham and A. D. Singh (2009). "Survival with retinoblastoma in the USA: 1975-2004." Br J Ophthalmol **93**(1): 24-27.

Cai, J., W. G. Jiang, M. B. Grant and M. Boulton (2006). "Pigment epithelium-derived factor inhibits angiogenesis via regulated intracellular proteolysis of vascular endothelial growth factor receptor 1." J Biol Chem **281**(6): 3604-3613.

Chang, S. H., L. A. Worley, M. D. Onken and J. W. Harbour (2008). "Prognostic biomarkers in uveal melanoma: evidence for a stem cell-like phenotype associated with metastasis." Melanoma Res **18**(3): 191-200.

Chen, L., S. S. Zhang, C. J. Barnstable and J. Tombran-Tink (2006). "PEDF induces apoptosis in human endothelial cells by activating p38 MAP kinase dependent cleavage of multiple caspases." Biochem Biophys Res Commun **348**(4): 1288-1295.

Chijiwa, T., Y. Abe, N. Ikoma, H. Yamazaki, H. Tsukamoto, H. Suemizu, K. Kawai, M. Wakui, C. Nishime, H. Matsumoto, M. Matsuyama, M. Mukai, Y. Ueyama and M. Nakamura (2009). "Thrombospondin 2 inhibits metastasis of human malignant melanoma through microenvironment-modification in NOD/SCID/gammaCnull (NOG) mice." Int J Oncol **34**(1): 5-13.

Chung, C., J. A. Doll, A. K. Gattu, C. Shugrue, M. Cornwell, P. Fitchev and S. E. Crawford (2008). "Anti-angiogenic pigment epithelium-derived factor regulates hepatocyte triglyceride content through adipose triglyceride lipase (ATGL)." J Hepatol **48**(3): 471-478.

Chung, C., C. Shugrue, A. Nagar, J. A. Doll, M. Cornwell, A. Gattu, T. Kolodecik, S. J. Pandol and F. Gorelick (2009). "Ethanol exposure depletes hepatic pigment epithelium-derived factor, a novel lipid regulator." Gastroenterology **136**(1): 331-340 e332.

Claffey, K. P., L. F. Brown, L. F. del Aguila, K. Tognazzi, K. T. Yeo, E. J. Manseau and H. F. Dvorak (1996). "Expression of vascular permeability factor/vascular endothelial growth factor by melanoma cells increases tumor growth, angiogenesis, and experimental metastasis." Cancer Res **56**(1): 172-181.

Crosby, M. B., H. Yang, W. Gao, L. Zhang and H. E. Grossniklaus (2011). "Serum vascular endothelial growth factor (VEGF) levels correlate with number and location of micrometastases in a murine model of uveal melanoma." Br J Ophthalmol **95**(1): 112-117.

Damato, B., C. Duke, S. E. Coupland, P. Hiscott, P. A. Smith, I. Campbell, A. Douglas and P. Howard (2007). "Cytogenetics of uveal melanoma: a 7-year clinical experience." Ophthalmology **114**(10): 1925-1931.

Damato, B., et al. (2011). "Uveal Melanoma--Where Are We Going?" US Ophthalmic Review **4**(1): 105-107.

Damato, E. M. and B. E. Damato (2012). "Detection and time to treatment of uveal melanoma in the United Kingdom: an evaluation of 2,384 patients." Ophthalmology **119**(8): 1582-1589.

Das, S. K. and D. M. Vasudevan (2007). "Essential factors associated with hepatic angiogenesis." Life Sci **81**(23-24): 1555-1564.

Dawson, D. W., O. V. Volpert, P. Gillis, S. E. Crawford, H. Xu, W. Benedict and N. P. Bouck (1999). "Pigment epithelium-derived factor: a potent inhibitor of angiogenesis." Science **285**(5425): 245-248.

De Bleser, P. J., T. Niki, V. Rogiers and A. Geerts (1997). "Transforming growth factor-beta gene expression in normal and fibrotic rat liver." J Hepatol **26**(4): 886-893.

Dey, A., D. Seshasayee, R. Noubade, D. M. French, J. Liu, M. S. Chaurushiya, D. S. Kirkpatrick, V. C. Pham, J. R. Lill, C. E. Bakalarski, J. Wu, L. Phu, P. Katavolos, L. M. LaFave, O. Abdel-Wahab, Z. Modrusan, S. Seshagiri, K. Dong, Z. Lin, M. Balazs, R. Suriben, K. Newton, S. Hymowitz, G. Garcia-Manero, F. Martin, R. L. Levine and V. M. Dixit (2012). "Loss of the tumor suppressor BAP1 causes myeloid transformation." Science **337**(6101): 1541-1546.

Diaz, C. E., D. Rusciano, S. Dithmar and H. E. Grossniklaus (1999). "B16LS9 melanoma cells spread to the liver from the murine ocular posterior compartment (PC)." Curr Eye Res **18**(2): 125-129.

Dithmar, S., D. M. Albert and H. E. Grossniklaus (2000). "Animal models of uveal melanoma." Melanoma Res **10**(3): 195-211.

Dithmar, S., D. Rusciano and H. E. Grossniklaus (2000). "A new technique for implantation of tissue culture melanoma cells in a murine model of metastatic ocular melanoma." Melanoma Res **10**(1): 2-8.

Doll, J. A., V. M. Stellmach, N. P. Bouck, A. R. Bergh, C. Lee, L. P. Abramson, M. L. Cornwell, M. R. Pins, J. Borensztajn and S. E. Crawford (2003). "Pigment epithelium-derived factor regulates the vasculature and mass of the prostate and pancreas." Nat Med **9**(6): 774-780.

Dong, Q., A. Shenker, J. Way, B. R. Haddad, K. Lin, M. R. Hughes, O. W. McBride, A. M. Spiegel and J. Battey (1995). "Molecular cloning of human G alpha q cDNA and chromosomal localization of the G alpha q gene (GNAQ) and a processed pseudogene." Genomics **30**(3): 470-475.

Dong, Z., J. Yoneda, R. Kumar and I. J. Fidler (1998). "Angiostatin-mediated suppression of cancer metastases by primary neoplasms engineered to produce granulocyte/macrophage colony-stimulating factor." J Exp Med **188**(4): 755-763.

Eagle, R. C., Jr. (2013). "The pathology of ocular cancer." Eye (Lond) **27**(2): 128-136.

Eefsen, R. L., G. G. Van den Eynden, G. Hoyer-Hansen, P. Brodt, O. D. Laerum, P. B. Vermeulen, I. J. Christensen, A. Wettergren, B. Federspiel, G. L. Willemoe, B. Vainer, K. Osterlind and M. Illemann (2012). "Histopathological growth pattern, proteolysis and angiogenesis in chemonaive patients resected for multiple colorectal liver metastases." J Oncol **2012**: 907971.

el Filali, M., G. S. Missotten, W. Maat, L. V. Ly, G. P. Luyten, P. A. van der Velden and M. J. Jager (2010). "Regulation of VEGF-A in uveal melanoma." Invest Ophthalmol Vis Sci **51**(5): 2329-2337.

Eskelin, S., S. Pyrhonen, P. Summanen, M. Hahka-Kemppinen and T. Kivela (2000). "Tumor doubling times in metastatic malignant melanoma of the uvea: tumor progression before and after treatment." Ophthalmology **107**(8): 1443-1449.

Fernandez-Barral, A., J. L. Orgaz, V. Gomez, L. del Peso, M. J. Calzada and B. Jimenez (2012). "Hypoxia negatively regulates antimetastatic PEDF in melanoma cells by a hypoxia inducible factor-independent, autophagy dependent mechanism." PLoS One **7**(3): e32989.

Ferrara, N. and T. Davis-Smyth (1997). "The biology of vascular endothelial growth factor." Endocr Rev **18**(1): 4-25.

Fidler, I. J. (1973). "Selection of successive tumour lines for metastasis." Nat New Biol **242**(118): 148-149.

Filleur, S., K. Volz, T. Nelius, Y. Mirochnik, H. Huang, T. A. Zaichuk, M. S. Aymerich, S. P. Becerra, R. Yap, D. Veliceasa, E. H. Shroff and O. V. Volpert (2005). "Two functional epitopes of pigment epithelial-derived factor block angiogenesis and induce differentiation in prostate cancer." Cancer Res **65**(12): 5144-5152.

Folberg, R., L. Leach, K. Valyi-Nagy, A. Y. Lin, M. A. Apushkin, Z. Ai, V. Barak, D. Majumdar, J. Pe'er and A. J. Maniotis (2007). "Modeling the behavior of uveal melanoma in the liver." Invest Ophthalmol Vis Sci **48**(7): 2967-2974.

Folkman, J. (1990). "What is the evidence that tumors are angiogenesis dependent?" J Natl Cancer Inst **82**(1): 4-6.

Folkman, J. (2002). "Role of angiogenesis in tumor growth and metastasis." Semin Oncol **29**(6 Suppl 16): 15-18.

Foss, A. J., R. A. Alexander, L. W. Jefferies, J. L. Hungerford, A. L. Harris and S. Lightman (1996). "Microvessel count predicts survival in uveal melanoma." Cancer Res **56**(13): 2900-2903.

Freeman, T. L., K. K. Kharbanda, D. J. Tuma and M. E. Mailliard (2002). "Inhibition of hepatic stellate cell collagen synthesis by N-(methylamino)isobutyric acid." Biochem Pharmacol **63**(4): 697-706.

Gallagher, R. P., J. M. Elwood, J. Rootman, J. J. Spinelli, G. B. Hill, W. J. Threlfall and J. M. Birdsell (1985). "Risk factors for ocular melanoma: Western Canada Melanoma Study." J Natl Cancer Inst **74**(4): 775-778.

Gao, G., Y. Li, S. Gee, A. Dudley, J. Fant, C. Crosson and J. X. Ma (2002). "Down-regulation of vascular endothelial growth factor and up-regulation of pigment epithelium-derived factor: a possible mechanism for the anti-angiogenic activity of plasminogen kringle 5." J Biol Chem **277**(11): 9492-9497.

Garcia, M., N. I. Fernandez-Garcia, V. Rivas, M. Carretero, M. J. Escamez, A. Gonzalez-Martin, E. E. Medrano, O. Volpert, J. L. Jorcano, B. Jimenez, F. Larcher and M. Del Rio (2004). "Inhibition of xenografted human melanoma growth and prevention of metastasis development by dual antiangiogenic/antitumor activities of pigment epithelium-derived factor." Cancer Res **64**(16): 5632-5642.

Geerts, A. (2001). "History, heterogeneity, developmental biology, and functions of quiescent hepatic stellate cells." Semin Liver Dis **21**(3): 311-335.

Ghattass, K., S. El-Sitt, K. Zibara, S. Rayes, M. J. Haddadin, M. El-Sabban and H. Gali-Muhtasib (2014). "The quinoxaline di-N-oxide DCQ blocks breast cancer metastasis in vitro and in vivo by targeting the hypoxia inducible factor-1 pathway." Mol Cancer **13**(1): 12.

Green, E. (1968). Handbook of genetically standardized JAX mice. Bar Harbor, ME, The Jackson Laboratory.

Grippo, P. J., P. S. Fitchev, D. J. Bentrem, L. G. Melstrom, S. Dangi-Garimella, S. B. Krantz, M. J. Heiferman, C. Chung, K. Adrian, M. L. Cornwell, J. B. Flesche, S. M. Rao, M. S. Talamonti, H. G. Munshi and S. E. Crawford (2012). "Concurrent PEDF deficiency and Kras mutation induce invasive pancreatic cancer and adipose-rich stroma in mice." Gut **61**(10): 1454-1464.

Grossniklaus, H. E. (1998). "Tumor vascularity and hematogenous metastasis in experimental murine intraocular melanoma." Trans Am Ophthalmol Soc **96**: 721-752.

Grossniklaus, H. E. (2013). "Progression of ocular melanoma metastasis to the liver: the 2012 Zimmerman lecture." JAMA Ophthalmol **131**(4): 462-469.

Guan, M., C. P. Pang, H. F. Yam, K. F. Cheung, W. W. Liu and Y. Lu (2004). "Inhibition of glioma invasion by overexpression of pigment epithelium-derived factor." Cancer Gene Ther **11**(5): 325-332.

Guenel, P., L. Laforest, D. Cyr, J. Fevotte, S. Sabroe, C. Dufour, J. M. Lutz and E. Lynge (2001). "Occupational risk factors, ultraviolet radiation, and ocular melanoma: a case-control study in France." Cancer Causes Control **12**(5): 451-459.

Hanahan, D. and J. Folkman (1996). "Patterns and emerging mechanisms of the angiogenic switch during tumorigenesis." Cell **86**(3): 353-364.

Harbour, J. W. (2014). "A prognostic test to predict the risk of metastasis in uveal melanoma based on a 15-gene expression profile." Methods Mol Biol **1102**: 427-440.

Harbour, J. W., M. D. Onken, E. D. Roberson, S. Duan, L. Cao, L. A. Worley, M. L. Council, K. A. Matatall, C. Helms and A. M. Bowcock (2010). "Frequent mutation of BAP1 in metastasizing uveal melanomas." Science **330**(6009): 1410-1413.

Heegaard, S., M. Spang-Thomsen and J. U. Prause (2003). "Establishment and characterization of human uveal malignant melanoma xenografts in nude mice." Melanoma Res **13**(3): 247-251.

Hendrix, M. J., E. A. Seftor, A. R. Hess and R. E. Seftor (2003). "Vasculogenic mimicry and tumour-cell plasticity: lessons from melanoma." Nat Rev Cancer **3**(6): 411-421.

Hendrix, M. J., E. A. Seftor, R. E. Seftor, D. A. Kirschmann, L. M. Gardner, H. C. Boldt, M. Meyer, J. Pe'er and R. Folberg (1998). "Regulation of uveal melanoma interconverted phenotype by hepatocyte growth factor/scatter factor (HGF/SF)." Am J Pathol **152**(4): 855-863.

Hicklin, D. J. and L. M. Ellis (2005). "Role of the vascular endothelial growth factor pathway in tumor growth and angiogenesis." J Clin Oncol **23**(5): 1011-1027.

Ho, T. C., S. L. Chen, S. C. Shih, J. Y. Wu, W. H. Han, H. C. Cheng, S. L. Yang and Y. P. Tsao (2010). "Pigment epithelium-derived factor is an intrinsic antifibrosis factor targeting hepatic stellate cells." Am J Pathol **177**(4): 1798-1811.

Ho, T. C., S. L. Chen, Y. C. Yang, C. L. Liao, H. C. Cheng and Y. P. Tsao (2007). "PEDF induces p53-mediated apoptosis through PPAR gamma signaling in human umbilical vein endothelial cells." Cardiovasc Res **76**(2): 213-223.

Holly, E. A., D. A. Aston, D. H. Char, J. J. Kristiansen and D. K. Ahn (1990). "Uveal melanoma in relation to ultraviolet light exposure and host factors." Cancer Res **50**(18): 5773-5777.

Hu, D. N., J. D. Simon and T. Sarna (2008). "Role of ocular melanin in ophthalmic physiology and pathology." Photochem Photobiol **84**(3): 639-644.

Hu, D. N., G. P. Yu, S. A. McCormick, S. Schneider and P. T. Finger (2005). "Population-based incidence of uveal melanoma in various races and ethnic groups." Am J Ophthalmol **140**(4): 612-617.

Huang, Q., S. Wang, C. M. Sorenson and N. Sheibani (2008). "PEDF-deficient mice exhibit an enhanced rate of retinal vascular expansion and are more sensitive to hyperoxia-mediated vessel obliteration." Exp Eye Res **87**(3): 226-241.

Hurst, E. A., J. W. Harbour and L. A. Cornelius (2003). "Ocular melanoma: a review and the relationship to cutaneous melanoma." Arch Dermatol **139**(8): 1067-1073.

Jager, M. J., H. M. Hurks, J. Levitskaya and R. Kiessling (2002). "HLA expression in uveal melanoma: there is no rule without some exception." Hum Immunol **63**(6): 444-451.

Jemal, A., M. Saraiya, P. Patel, S. S. Cherala, J. Barnholtz-Sloan, J. Kim, C. L. Wiggins and P. A. Wingo (2011). "Recent trends in cutaneous melanoma incidence and death rates in the United States, 1992-2006." J Am Acad Dermatol **65**(5 Suppl 1): S17-25 e11-13.

Jovanovic, P., M. Mihajlovic, J. Djordjevic-Jocic, S. Vlajkovic, S. Cekic and V. Stefanovic (2013). "Ocular melanoma: an overview of the current status." Int J Clin Exp Pathol **6**(7): 1230-1244.

Kujala, E., T. Makitie and T. Kivela (2003). "Very long-term prognosis of patients with malignant uveal melanoma." Invest Ophthalmol Vis Sci **44**(11): 4651-4659.

Lake, S. L., H. Kalirai, J. Dopierala, B. E. Damato and S. E. Coupland (2012). "Comparison of formalin-fixed and snap-frozen samples analyzed by multiplex ligation-dependent probe amplification for prognostic testing in uveal melanoma." Invest Ophthalmol Vis Sci **53**(6): 2647-2652.

Landreville, S., O. A. Agapova and J. W. Harbour (2008). "Emerging insights into the molecular pathogenesis of uveal melanoma." Future Oncol **4**(5): 629-636.

Lattier, J. M., H. Yang, S. Crawford and H. E. Grossniklaus (2013). "Host pigment epithelium-derived factor (PEDF) prevents progression of liver metastasis in a mouse model of uveal melanoma." Clin Exp Metastasis.

Lee, D. S., S. F. Anderson, E. M. Perez and J. C. Townsend (2001). "Amelanotic choroidal nevus and melanoma: cytology, tumor size, and pigmentation as prognostic indicators." Optom Vis Sci **78**(7): 483-491.

Liaskou, E., D. V. Wilson and Y. H. Oo (2012). "Innate immune cells in liver inflammation." Mediators Inflamm **2012**: 949157.

Lu, X. and Y. Kang (2010). "Hypoxia and hypoxia-inducible factors: master regulators of metastasis." Clin Cancer Res **16**(24): 5928-5935.

Lutzky, V. P., R. P. Carnevale, M. J. Alvarez, P. C. Maffia, S. I. Zittermann, O. L. Podhajcer, A. C. Issekutz and H. E. Chuluyan (2006). "Platelet-endothelial cell adhesion molecule-1 (CD31) recycles and induces cell growth inhibition on human tumor cell lines." J Cell Biochem **98**(5): 1334-1350.

Luzzi, K. J., I. C. MacDonald, E. E. Schmidt, N. Kerkvliet, V. L. Morris, A. F. Chambers and A. C. Groom (1998). "Multistep nature of metastatic inefficiency: dormancy of solitary cells after successful extravasation and limited survival of early micrometastases." Am J Pathol **153**(3): 865-873.

Ma, D., G. P. Luyten, T. M. Luider and J. Y. Niederkorn (1995). "Relationship between natural killer cell susceptibility and metastasis of human uveal melanoma cells in a murine model." Invest Ophthalmol Vis Sci **36**(2): 435-441.

Mallet, J. D., S. P. Gendron, M. C. Drigeard Desgarnier and P. J. Rochette (2013). "Implication of ultraviolet light in the etiology of uveal melanoma: A review." Photochem Photobiol.

Mallikarjuna, K., V. Pushparaj, J. Biswas and S. Krishnakumar (2007). "Expression of epidermal growth factor receptor, ezrin, hepatocyte growth factor, and c-Met in uveal melanoma: an immunohistochemical study." Curr Eye Res **32**(3): 281-290.

Maniotis, A. J., R. Folberg, A. Hess, E. A. Seftor, L. M. Gardner, J. Pe'er, J. M. Trent, P. S. Meltzer and M. J. Hendrix (1999). "Vascular channel formation by human melanoma cells in vivo and in vitro: vasculogenic mimicry." Am J Pathol **155**(3): 739-752.

Marshall, J. C., A. Nantel, P. Blanco, J. Ash, S. R. Cruess and M. N. Burnier, Jr. (2007). "Transcriptional profiling of human uveal melanoma from cell lines to intraocular tumors to metastasis." Clin Exp Metastasis **24**(5): 353-362.

Materin, M. A., M. Faries and H. M. Kluger (2011). "Molecular alternations in uveal melanoma." Curr Probl Cancer **35**(4): 211-224.

Matsumoto, K., H. Ishikawa, D. Nishimura, K. Hamasaki, K. Nakao and K. Eguchi (2004). "Antiangiogenic property of pigment epithelium-derived factor in hepatocellular carcinoma." Hepatology **40**(1): 252-259.

McMahon, G. (2000). "VEGF receptor signaling in tumor angiogenesis." Oncologist **5 Suppl 1**: 3-10.

Medina, J., A. G. Arroyo, F. Sanchez-Madrid and R. Moreno-Otero (2004). "Angiogenesis in chronic inflammatory liver disease." Hepatology **39**(5): 1185-1195.

Minami, Y. and M. Kudo (2010). "Hepatic malignancies: Correlation between sonographic findings and pathological features." World J Radiol **2**(7): 249-256.

Miyamoto, C., M. Balazsi, S. Bakalian, B. F. Fernandes and M. N. Burnier, Jr. (2012). "Uveal melanoma: Ocular and systemic disease." Saudi J Ophthalmol **26**(2): 145-149.

Mori, K., E. Duh, P. Gehlbach, A. Ando, K. Takahashi, J. Pearlman, K. Mori, H. S. Yang, D. J. Zack, D. Ettyreddy, D. E. Brough, L. L. Wei and P. A. Campochiaro (2001). "Pigment epithelium-derived factor inhibits retinal and choroidal neovascularization." J Cell Physiol **188**(2): 253-263.

Murphy, F. R., R. Issa, X. Zhou, S. Ratnarajah, H. Nagase, M. J. Arthur, C. Benyon and J. P. Iredale (2002). "Inhibition of apoptosis of activated hepatic stellate cells by tissue inhibitor of metalloproteinase-1 is mediated via effects on matrix metalloproteinase inhibition: implications for reversibility of liver fibrosis." J Biol Chem **277**(13): 11069-11076.

Nakao, S., A. Hafezi-Moghadam and T. Ishibashi (2012). "Lymphatics and lymphangiogenesis in the eye." J Ophthalmol **2012**: 783163.

Neufeld, G., T. Cohen, S. Gengrinovitch and Z. Poltorak (1999). "Vascular endothelial growth factor (VEGF) and its receptors." FASEB J **13**(1): 9-22.

Niederkorn, J. Y. (1984). "Enucleation-induced metastasis of intraocular melanomas in mice." Ophthalmology **91**(6): 692-700.

Niederkorn, J. Y. (1984). "Enucleation in consort with immunologic impairment promotes metastasis of intraocular melanomas in mice." Invest Ophthalmol Vis Sci **25**(9): 1080-1086.

Notari, L., N. Arakaki, D. Mueller, S. Meier, J. Amaral and S. P. Becerra (2010). "Pigment epithelium-derived factor binds to cell-surface F(1)-ATP synthase." FEBS J **277**(9): 2192-2205.

Notari, L., V. Baladron, J. D. Aroca-Aguilar, N. Balko, R. Heredia, C. Meyer, P. M. Notario, S. Saravanamuthu, M. L. Nueda, F. Sanchez-Sanchez, J. Escribano, J. Laborda and S. P. Becerra (2006). "Identification of a lipase-linked cell membrane receptor for pigment epithelium-derived factor." J Biol Chem **281**(49): 38022-38037.

Notari, L., A. Miller, A. Martinez, J. Amaral, M. Ju, G. Robinson, L. E. Smith and S. P. Becerra (2005). "Pigment epithelium-derived factor is a substrate for matrix metalloproteinase type 2 and type 9: implications for downregulation in hypoxia." Invest Ophthalmol Vis Sci **46**(8): 2736-2747.

Nowak, J. Z. and A. Wiktorowska-Owczarek (2004). "[Neovascularization in ocular tissues: mechanisms and role of proangiogenic and antiangiogenic factors]." Klin Oczna **106**(1-2): 90-97.

Nyberg, P., L. Xie and R. Kalluri (2005). "Endogenous inhibitors of angiogenesis." Cancer Res **65**(10): 3967-3979.

O'Reilly, M. S., L. Holmgren, Y. Shing, C. Chen, R. A. Rosenthal, Y. Cao, M. Moses, W. S. Lane, E. H. Sage and J. Folkman (1994). "Angiostatin: a circulating endothelial cell inhibitor that suppresses angiogenesis and tumor growth." Cold Spring Harb Symp Quant Biol **59**: 471-482.

O'Reilly, M. S., L. Holmgren, Y. Shing, C. Chen, R. A. Rosenthal, M. Moses, W. S. Lane, Y. Cao, E. H. Sage and J. Folkman (1994). "Angiostatin: a novel angiogenesis inhibitor that mediates the suppression of metastases by a Lewis lung carcinoma." Cell **79**(2): 315-328.

Olsson, A. K., A. Dimberg, J. Kreuger and L. Claesson-Welsh (2006). "VEGF receptor signalling - in control of vascular function." Nat Rev Mol Cell Biol **7**(5): 359-371.

Onken, M. D., L. A. Worley, R. M. Davila, D. H. Char and J. W. Harbour (2006). "Prognostic testing in uveal melanoma by transcriptomic profiling of fine needle biopsy specimens." J Mol Diagn **8**(5): 567-573.

Onken, M. D., L. A. Worley, J. P. Ehlers and J. W. Harbour (2004). "Gene expression profiling in uveal melanoma reveals two molecular classes and predicts metastatic death." Cancer Res **64**(20): 7205-7209.

Orgaz, J. L., O. Ladhani, K. S. Hoek, A. Fernandez-Barral, D. Mihic, O. Aguilera, E. A. Seftor, A. Bernad, J. L. Rodriguez-Peralto, M. J. Hendrix, O. V. Volpert and B. Jimenez (2009). "Loss of pigment epithelium-derived factor enables migration, invasion and metastatic spread of human melanoma." Oncogene **28**(47): 4147-4161.

Paget (1889). "The distribution of secondary growths in cancer of th breast." The Lancet **133**(3421).

Paget, G. (1889). "Remarks on a Case of Alternate Partial Anaesthesia." Br Med J **1**(1462): 1-3.

Pane, A. R. and L. W. Hirst (2000). "Ultraviolet light exposure as a risk factor for ocular melanoma in Queensland, Australia." Ophthalmic Epidemiol **7**(3): 159-167.

Pereira, P. R., A. N. Odashiro, L. A. Lim, C. Miyamoto, P. L. Blanco, M. Odashiro, S. Maloney, D. F. De Souza and M. N. Burnier, Jr. (2013). "Current and emerging treatment options for uveal melanoma." Clin Ophthalmol **7**: 1669-1682.

Pina, Y., C. M. Cebulla, T. G. Murray, A. Alegret, S. R. Dubovy, H. Boutrid, W. Feuer, L. Mutapcic and M. E. Jockovich (2009). "Blood vessel maturation in human uveal melanoma: spatial distribution of neovessels and mature vasculature." Ophthalmic Res **41**(3): 160-169.

Pollack, L. A., J. Li, Z. Berkowitz, H. K. Weir, X. C. Wu, U. A. Ajani, D. U. Ekwueme, C. Li and B. P. Pollack (2011). "Melanoma survival in the United States, 1992 to 2005." J Am Acad Dermatol **65**(5 Suppl 1): S78-86.

Prescher, G., N. Bornfeld, H. Hirche, B. Horsthemke, K. H. Jockel and R. Becher (1996). "Prognostic implications of monosomy 3 in uveal melanoma." Lancet **347**(9010): 1222-1225.

Quintero, M., N. Mackenzie and P. A. Brennan (2004). "Hypoxia-inducible factor 1 (HIF-1) in cancer." Eur J Surg Oncol **30**(5): 465-468.

Ria, R., A. Reale, A. Castrovilli, G. Mangialardi, F. Dammacco, D. Ribatti and A. Vacca (2010). "Angiogenesis and progression in human melanoma." Dermatol Res Pract **2010**: 185687.

Rodriguez-Manzaneque, J. C., T. F. Lane, M. A. Ortega, R. O. Hynes, J. Lawler and M. L. Iruela-Arispe (2001). "Thrombospondin-1 suppresses spontaneous tumor growth and inhibits activation of matrix metalloproteinase-9 and mobilization of vascular endothelial growth factor." Proc Natl Acad Sci U S A **98**(22): 12485-12490.

Rofstad, E. K. and B. A. Graff (2001). "Thrombospondin-1-mediated metastasis suppression by the primary tumor in human melanoma xenografts." J Invest Dermatol **117**(5): 1042-1049.

Ruiter, D., T. Bogenrieder, D. Elder and M. Herlyn (2002). "Melanoma-stroma interactions: structural and functional aspects." Lancet Oncol **3**(1): 35-43.

Rummelt, V., M. G. Mehaffey, R. J. Campbell, J. Pe'er, S. E. Bentler, R. F. Woolson, G. O. Naumann and R. Folberg (1998). "Microcirculation architecture of metastases from primary ciliary body and choroidal melanomas." Am J Ophthalmol **126**(2): 303-305.

Rusciano, D., P. Lorenzoni and M. Burger (1994). "Murine models of liver metastasis." Invasion Metastasis **14**(1-6): 349-361.

Sanz, S., J. B. Pucilowska, S. Liu, C. M. Rodriguez-Ortigosa, P. K. Lund, D. A. Brenner, C. R. Fuller, J. G. Simmons, A. Pardo, M. L. Martinez-Chantar, J. A. Fagin and J. Prieto (2005). "Expression of insulin-like growth factor I by activated hepatic stellate cells reduces fibrogenesis and enhances regeneration after liver injury." Gut **54**(1): 134-141.

Sato, M., S. Suzuki and H. Senoo (2003). "Hepatic stellate cells: unique characteristics in cell biology and phenotype." Cell Struct Funct **28**(2): 105-112.

Sato, T., F. Han and A. Yamamoto (2008). "The biology and management of uveal melanoma." Curr Oncol Rep **10**(5): 431-438.

Schwartz, L. H., R. Ferrand, P. Y. Boelle, C. Maylin, F. D'Hermies and J. Virmont (1997). "Lack of correlation between the location of choroidal melanoma and ultraviolet-radiation dose distribution." Radiat Res **147**(4): 451-456.

Seddon, J. M., E. S. Gragoudas, R. J. Glynn, K. M. Egan, D. M. Albert and P. H. Blitzer (1990). "Host factors, UV radiation, and risk of uveal melanoma. A case-control study." Arch Ophthalmol **108**(9): 1274-1280.

Shimizu, H., N. Mitsuhashi, M. Ohtsuka, H. Ito, F. Kimura, S. Ambiru, A. Togawa, H. Yoshidome, A. Kato and M. Miyazaki (2005). "Vascular endothelial growth factor and angiopoietins regulate sinusoidal regeneration and remodeling after partial hepatectomy in rats." World J Gastroenterol **11**(46): 7254-7260.

Shimojo, Y., M. Akimoto, T. Hisanaga, T. Tanaka, Y. Tajima, Y. Honma and K. Takenaga (2013). "Attenuation of reactive oxygen species by antioxidants suppresses hypoxia-induced epithelial-mesenchymal transition and metastasis of pancreatic cancer cells." Clin Exp Metastasis **30**(2): 143-154.

Shimomura, M., T. Hinoi, S. Kuroda, T. Adachi, Y. Kawaguchi, T. Sasada, Y. Takakura, H. Egi, M. Okajima, H. Tashiro, T. Nishizaka and H. Ohdan (2013). "Overexpression of hypoxia inducible factor-1 alpha is an independent risk factor for recurrence after curative resection of colorectal liver metastases." Ann Surg Oncol **20 Suppl 3**: S527-536.

Simonovic, M., P. G. Gettins and K. Volz (2001). "Crystal structure of human PEDF, a potent anti-angiogenic and neurite growth-promoting factor." Proc Natl Acad Sci U S A **98**(20): 11131-11135.

Singh, A. D. and E. C. Borden (2005). "Metastatic uveal melanoma." Ophthalmol Clin North Am **18**(1): 143-150, ix.

Singh, A. D., B. Damato, P. Howard and J. W. Harbour (2005). "Uveal melanoma: genetic aspects." Ophthalmol Clin North Am **18**(1): 85-97, viii.

Singh, A. D. and A. Topham (2003). "Survival rates with uveal melanoma in the United States: 1973-1997." Ophthalmology **110**(5): 962-965.

Singh, A. D., M. E. Turell and A. K. Topham (2011). "Uveal melanoma: trends in incidence, treatment, and survival." Ophthalmology **118**(9): 1881-1885.

Smirnova, E., E. B. Goldberg, K. S. Makarova, L. Lin, W. J. Brown and C. L. Jackson (2006). "ATGL has a key role in lipid droplet/adiposome degradation in mammalian cells." EMBO Rep **7**(1): 106-113.

Spranger, J., M. Osterhoff, M. Reimann, M. Mohlig, M. Ristow, M. K. Francis, V. Cristofalo, H. P. Hammes, G. Smith, M. Boulton and A. F. Pfeiffer (2001). "Loss of the antiangiogenic pigment epithelium-derived factor in patients with angiogenic eye disease." Diabetes **50**(12): 2641-2645.

Steiling, H., M. Muhlbauer, F. Bataille, J. Scholmerich, S. Werner and C. Hellerbrand (2004). "Activated hepatic stellate cells express keratinocyte growth factor in chronic liver disease." Am J Pathol **165**(4): 1233-1241.

Swerdlow, A. J., H. H. Storm and P. D. Sasieni (1995). "Risks of second primary malignancy in patients with cutaneous and ocular melanoma in Denmark, 1943-1989." Int J Cancer **61**(6): 773-779.

Takenaka, K., S. Yamagishi, Y. Jinnouchi, K. Nakamura, T. Matsui and T. Imaizumi (2005). "Pigment epithelium-derived factor (PEDF)-induced apoptosis and inhibition of vascular endothelial growth factor (VEGF) expression in MG63 human osteosarcoma cells." Life Sci **77**(25): 3231-3241.

Tassi, E. and A. Wellstein (2006). "The angiogenic switch molecule, secreted FGF-binding protein, an indicator of early stages of pancreatic and colorectal adenocarcinoma." Semin Oncol **33**(6 Suppl 11): S50-56.

Tolleson, W. H. (2005). "Human melanocyte biology, toxicology, and pathology." J Environ Sci Health C Environ Carcinog Ecotoxicol Rev **23**(2): 105-161.

Tombran-Tink, J. and C. J. Barnstable (2003). "PEDF: a multifaceted neurotrophic factor." Nat Rev Neurosci **4**(8): 628-636.

Tombran-Tink, J. and C. J. Barnstable (2003). "Therapeutic prospects for PEDF: more than a promising angiogenesis inhibitor." Trends Mol Med **9**(6): 244-250.

Tombran-Tink, J., G. G. Chader and L. V. Johnson (1991). "PEDF: a pigment epithelium-derived factor with potent neuronal differentiative activity." Exp Eye Res **53**(3): 411-414.

Tombran-Tink, J. and L. V. Johnson (1989). "Neuronal differentiation of retinoblastoma cells induced by medium conditioned by human RPE cells." Invest Ophthalmol Vis Sci **30**(8): 1700-1707.

Tombran-Tink, J., H. Pawar, A. Swaroop, I. Rodriguez and G. J. Chader (1994). "Localization of the gene for pigment epithelium-derived factor (PEDF) to chromosome 17p13.1 and expression in cultured human retinoblastoma cells." Genomics **19**(2): 266-272.

Tsai, S. M. and W. P. Wang (2011). "Expression and function of fibroblast growth factor (FGF) 7 during liver regeneration." Cell Physiol Biochem **27**(6): 641-652.

Tucker, M. A., J. A. Shields, P. Hartge, J. Augsburger, R. N. Hoover and J. F. Fraumeni, Jr. (1985). "Sunlight exposure as risk factor for intraocular malignant melanoma." N Engl J Med **313**(13): 789-792.

Udagawa, T., A. Fernandez, E. G. Achilles, J. Folkman and R. J. D'Amato (2002). "Persistence of microscopic human cancers in mice: alterations in the angiogenic balance accompanies loss of tumor dormancy." FASEB J **16**(11): 1361-1370.

Vaarwater, J., T. van den Bosch, H. W. Mensink, C. van Kempen, R. M. Verdijk, N. C. Naus, D. Paridaens, H. T. Bruggenwirth, E. Kilic and A. de Klein (2012). "Multiplex ligation-dependent probe amplification equals fluorescence in-situ hybridization for the identification of patients at risk for metastatic disease in uveal melanoma." Melanoma Res **22**(1): 30-37.

Vajdic, C. M., A. Kricker, M. Giblin, J. McKenzie, J. Aitken, G. G. Giles and B. K. Armstrong (2002). "Sun exposure predicts risk of ocular melanoma in Australia." Int J Cancer **101**(2): 175-182.

van den Bosch, T., E. Kilic, D. Paridaens and A. de Klein (2010). "Genetics of uveal melanoma and cutaneous melanoma: two of a kind?" Dermatol Res Pract **2010**: 360136.

Van den Eynden, G. G., A. W. Majeed, M. Illemann, P. B. Vermeulen, N. C. Bird, G. Hoyer-Hansen, R. L. Eefsen, A. R. Reynolds and P. Brodt (2013). "The multifaceted role of the microenvironment in liver metastasis: biology and clinical implications." Cancer Res **73**(7): 2031-2043.

Van Raamsdonk, C. D., V. Bezrookove, G. Green, J. Bauer, L. Gaugler, J. M. O'Brien, E. M. Simpson, G. S. Barsh and B. C. Bastian (2009). "Frequent somatic mutations of GNAQ in uveal melanoma and blue naevi." Nature **457**(7229): 599-602.

Van Raamsdonk, C. D., K. G. Griewank, M. B. Crosby, M. C. Garrido, S. Vemula, T. Wiesner, A. C. Obenauf, W. Wackernagel, G. Green, N. Bouvier, M. M. Sozen, G. Baimukanova, R. Roy, A. Heguy, I. Dolgalev, R. Khanin, K. Busam, M. R. Speicher, J. O'Brien and B. C. Bastian (2010). "Mutations in GNA11 in uveal melanoma." N Engl J Med **363**(23): 2191-2199.

van Zijl, F., G. Krupitza and W. Mikulits (2011). "Initial steps of metastasis: cell invasion and endothelial transmigration." Mutat Res **728**(1-2): 23-34.

Victor, N., A. Ivy, B. H. Jiang and F. H. Agani (2006). "Involvement of HIF-1 in invasion of Mum2B uveal melanoma cells." Clin Exp Metastasis **23**(1): 87-96.

Vidal-Vanaclocha, F. (2008). "The prometastatic microenvironment of the liver." Cancer Microenviron **1**(1): 113-129.

Volpert, O. V., T. Zaichuk, W. Zhou, F. Reiher, T. A. Ferguson, P. M. Stuart, M. Amin and N. P. Bouck (2002). "Inducer-stimulated Fas targets activated endothelium for destruction by anti-angiogenic thrombospondin-1 and pigment epithelium-derived factor." Nat Med **8**(4): 349-357.

Weis, E., C. P. Shah, M. Lajous, J. A. Shields and C. L. Shields (2006). "The association between host susceptibility factors and uveal melanoma: a meta-analysis." Arch Ophthalmol **124**(1): 54-60.

Wobser, H., C. Dorn, T. S. Weiss, T. Amann, C. Bollheimer, R. Buttner, J. Scholmerich and C. Hellerbrand (2009). "Lipid accumulation in hepatocytes induces fibrogenic activation of hepatic stellate cells." Cell Res **19**(8): 996-1005.

Woll, E., A. Bedikian and S. S. Legha (1999). "Uveal melanoma: natural history and treatment options for metastatic disease." Melanoma Res **9**(6): 575-581.

Woodward, J. K., S. R. Elshaw, A. K. Murray, C. E. Nichols, N. Cross, D. Laws, I. G. Rennie and K. Sisley (2002). "Stimulation and inhibition of uveal melanoma invasion by HGF, GRO, IL-1alpha and TGF-beta." Invest Ophthalmol Vis Sci **43**(10): 3144-3152.

Wu, Y. Q. and S. P. Becerra (1996). "Proteolytic activity directed toward pigment epithelium-derived factor in vitreous of bovine eyes. Implications of proteolytic processing." Invest Ophthalmol Vis Sci **37**(10): 1984-1993.

Wu, Y. Q., V. Notario, G. J. Chader and S. P. Becerra (1995). "Identification of pigment epithelium-derived factor in the interphotoreceptor matrix of bovine eyes." Protein Expr Purif **6**(4): 447-456.

Xu, R., X. Sun, L. Y. Tse, H. Li, P. C. Chan, S. Xu, W. Xiao, H. F. Kung, G. W. Krissansen and S. T. Fan (2003). "Long-term expression of angiostatin suppresses metastatic liver cancer in mice." Hepatology **37**(6): 1451-1460.

Xu, X., S. S. Zhang, C. J. Barnstable and J. Tombran-Tink (2006). "Molecular phylogeny of the antiangiogenic and neurotrophic serpin, pigment epithelium derived factor in vertebrates." BMC Genomics **7**: 248.

Yanagi, K., M. Onda and E. Uchida (2000). "Effect of angiostatin on liver metastasis of pancreatic cancer in hamsters." Jpn J Cancer Res **91**(7): 723-730.

Yang, H., C. Akor, S. Dithmar and H. E. Grossniklaus (2004). "Low dose adjuvant angiostatin decreases hepatic micrometastasis in murine ocular melanoma model." Mol Vis **10**: 987-995.

Yang, H., S. Dithmar and H. E. Grossniklaus (2004). "Interferon alpha 2b decreases hepatic micrometastasis in a murine model of ocular melanoma by activation of intrinsic hepatic natural killer cells." Invest Ophthalmol Vis Sci **45**(7): 2056-2064.

Yang, H., G. Fang, X. Huang, J. Yu, C. L. Hsieh and H. E. Grossniklaus (2008). "In-vivo xenograft murine human uveal melanoma model develops hepatic micrometastases." Melanoma Res **18**(2): 95-103.

Yang, H. and H. E. Grossniklaus (2010). "Constitutive overexpression of pigment epithelium-derived factor inhibition of ocular melanoma growth and metastasis." Invest Ophthalmol Vis Sci **51**(1): 28-34.

Yang, H., Z. Xu, P. M. Iuvone and H. E. Grossniklaus (2006). "Angiostatin decreases cell migration and vascular endothelium growth factor (VEGF) to pigment epithelium derived factor (PEDF) RNA ratio in vitro and in a murine ocular melanoma model." Mol Vis **12**: 511-517.

Zbytek, B., J. A. Carlson, J. Granese, J. Ross, M. C. Mihm, Jr. and A. Slominski (2008). "Current concepts of metastasis in melanoma." Expert Rev Dermatol **3**(5): 569-585.

Zhang, S. X., J. J. Wang, G. Gao, K. Parke and J. X. Ma (2006). "Pigment epithelium-derived factor downregulates vascular endothelial growth factor (VEGF) expression and inhibits VEGF-VEGF receptor 2 binding in diabetic retinopathy." J Mol Endocrinol **37**(1): 1-12.

Zhao, Y., Y. Wang, Q. Wang, Z. Liu, Q. Liu and X. Deng (2012). "Hepatic stellate cells produce vascular endothelial growth factor via phospho-p44/42 mitogen-activated protein kinase/cyclooxygenase-2 pathway." Mol Cell Biochem **359**(1-2): 217-223.

Zlotnik, A., A. M. Burkhardt and B. Homey (2011). "Homeostatic chemokine receptors and organ-specific metastasis." Nat Rev Immunol **11**(9): 597-606.

Zloto, O., J. Pe'er and S. Frenkel (2013). "Gender differences in clinical presentation and prognosis of uveal melanoma." Invest Ophthalmol Vis Sci **54**(1): 652-656.

Zolochevska, O., G. Yu, J. M. Gimble and M. L. Figueiredo (2012). "Pigment epithelial-derived factor and melanoma differentiation associated gene-7 cytokine gene therapies delivered by adipose-derived stromal/mesenchymal stem cells are effective in reducing prostate cancer cell growth." Stem Cells Dev **21**(7): 1112-1123.

Zong, L., Y. Qu, M. Y. Xu, Y. W. Dong and L. G. Lu (2012). "18alpha-glycyrrhetinic acid down-regulates expression of type I and III collagen via TGF-Beta1/Smad signaling pathway in human and rat hepatic stellate cells." Int J Med Sci **9**(5): 370-379.